AD-A020 945

HOLOGRAPHIC LENS FOR PILOT'S HEAD-UP DISPLAY

A. Au, A. Graube, et al

Hughes Research Laboratories

Prepared for:

Naval Air Development Center

1 February 1976

NADC-75293-30

058163

27

HOLOGRAPHIC LENS FOR PILOT'S HEAD-UP DISPLAY PHASE 3

A. AU, A. GRAUBE, AND L. G. COOK

HUGHES RESEARCH LABORATORIES
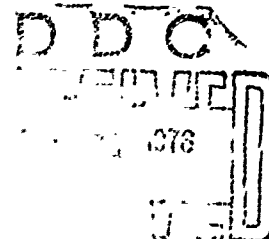3011 MALIBU CANYON ROAD
MALIBU, CA 90265

FEBRUARY 1976

CONTRACT N62269-75-C-0299
FINAL TECHNICAL REPORT
FOR PERIOD 18 MARCH 1975 TO 17 SEPTEMBER 1975

DDC

REPORT DOCUMENTATION PAGE		READ INSTRUCTIONS BEFORE COMPLETING FORM
1. REPORT NUMBER ~~NC2269-75-C-0299~~ -VADC - 75293-30	2 GOVT ACCESSION NO.	3 RECIPIENT'S CATALOG NUMBER
4. TITLE (and Subtitle) HOLOGRAPHIC LENS FOR PILOT'S HEAD-UP DISPLAY-PHASE III		5 TYPE OF REPORT & PERIOD COVERED Final Technical Report 16 Mar - 17 Sept 1975
		6 PERFORMING ORG REPORT NUMBER
7 AUTHOR(s) A. Au, A. Graube, and L. G. Cook		8 CONTRACT OR GRANT NUMBER(s) N62269-75-C-0299
9 PERFORMING ORGANIZATION NAME AND ADDRESS Hughes Research Laboratories 3011 Malibu Canyon Road Malibu, CA 90265		10 PROGRAM ELEMENT PROJECT TASK AREA & WORK UNIT NUMBERS
11 CONTROLLING OFFICE NAME AND ADDRESS Naval Air Development Center Warminster, PA 18974		12 REPORT DATE 1 February 1976
		13 NUMBER OF PAGES 107
14 MONITORING AGENCY NAME & ADDRESS (if different from Controlling Office)		15 SECURITY CLASS (of this report) Unclassified
		15a DECLASSIFICATION DOWNGRADING SCHEDULE

16 DISTRIBUTION STATEMENT (of this Report)

Approved for Public Release. Distribution Unlimited.

17 DISTRIBUTION STATEMENT (of the abstract entered in Block 20, if different from Report)

18 SUPPLEMENTARY NOTES

19 KEY WORDS (Continue on reverse side if necessary and identify by block number)

Head-Up Display, Full-Scale Hologram, Dye-Sentitized Dichromated Gelatin, Reflection Hologram Collimator/Combiner, T90-N8-21.9 Transmission Hologram

20 ABSTRACT (Continue on reverse side if necessary and identify by block number)

This report describes work on the fabrication of the full-scale holographic lens for a wide field of view (FOV) head-up display (HUD) system. The basic system parameters are a $25°$ FOV, a 25 in. eye relief, and a 3 in. high by 5 in. wide exit pupil. Processing equipments and techniques were fabricated and developed for recording the 16 in. diameter holographic element on 18 in. x 18 in. dye-sensitized

DD $_{1\ JAN\ 73}^{FORM}$ 1473   EDITION OF 1 NOV 65 IS OBSOLETE

dichromated gelatin works include a design study of reflec-
tion hologram collimator/combiner and the fabrication and
test of a T90-N8-21.9 transmission hologram lens.

The dynamically-stabilized recording apparatus for the full-
scale transmission hologram lens was designed and assembled
in Phase 2, Contract N62269-74-C-0642, Holographic Lens for
Pilot's Head-Up Display. The construction beam optical sys-
tem, based on the "continuous lens" approach, is symmetric
with a 50° off-axis angle. Four plate preparation techniques
were evaluated with small aperture hologram exposures. The
preferred technique, adapted to large area DSDCG preparation,
has good light sensitivity (~80% diffraction efficiency with
300 to 400 mJ/cm^2 exposure) and does not need special baking
and annealing processes. Fringe stability was maintained
during the 2.25 hr exposure period of the full-scale DSDCG
hologram lens. The optimum reconstruction geometry at 632.8
nm is 48.82° symmetric with a focal length of 14.97 in. At
the center of the lens, 42% diffraction efficiency was mea-
sured with 1 to 2% scatter.

A design study of reflection hologram collimator/combiner is
completed. This study was restricted to symmetric reflection
holographic elements with the "continuous lens" concept on
flat substrates. A baseline hologram of 43° off axis with a
focal length of 14.9 in. was selected based on parametric
study of field curvatures, tilts, and aberrations. Optical
system design optimization resulted in a 7 element relay lens
system with a folding mirror. Pupil errors were held to less
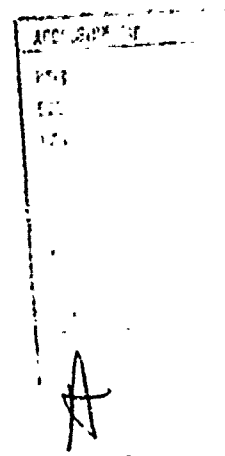than 5 mrad over a 25° FOV from a 3 in. x 5 in. racetrack
exit pupil.

The T90-N8-21.9 in. lens is an 8 in. diamter transmission
hologram lens fabricated on 8 in. x 10 in. Kodak 120-01 sil-
ver halide emulsion and bromine vapor bleached. Reconstruc-
tion geometry of the 21.9 in. focal length lens is 90° off
axis, 8° asymmetric. Single binocular vision can be main-
tained at the eye relief distance of 34.5 in. For a nominal
63 mm separated pair of eyes centered at the exit pupil, bi-
nocular FOV is 4.16° and -3.49° vertical, 14.56° horizontal.

TABLE OF CONTENTS

3

LIST OF ILLUSTRATIONS

PREFACE

This final report covers the work accomplished during the
period 18 March 1975 through 17 September 1975 under Contract
N62269-75-C-0299, "Holographic Lens for Pilot's Head-Up Display
(Phase 3)." This work was supported by the Naval Air Systems
Command under the sponsorship of Mr. George Isaparas and Mr.
William B. King. The program is under the technical direction of
Mr. Ed Rickner, Mr. Ken Priest, and Mr. Harold Green of the
Naval Air Development Center, Warminster, Pennsylvania.

The work was accomplished by the Exploratory Studies Depart-
ment of the Hughes Research Laboratories, Division of the Hughes
Aircraft Company, under the direction of Dr. Donald H. Close.
The technical work was performed by Mr. Anson Au. Mr. Andrejs
Graube optimized material characteristics and processing tech-
niques. Mr. Cesar C. DeAnda performed many of the experiments
and provided able assistance in fabricating the large aperture
hologram lens. Mr. Lawrence D. Allum provided further technical
support in fabricatir the processing equipment. The design
study of reflection HHUD systems was performed by Dr. Roger J.
Withrington and Mr. Lacy G. Cook, of the Electro-Optics Depart-
ment. Mr. Gaylord F. Moss acted as consultant to the program
and provided valuable assistance in the conduct of all major
tasks.

Preceding page blank

I. Introduction and Summary

1. INTRODUCTION

This final technical report contains detailed discussions of
the Phase 3 NADC program tasks, objectives, approaches and
results toward developing a Holographic Lens for Pilot's
Head-Up Display.

This is the final technical report on Contract N62269-75-C-
0299, Phase 3 of the Naval Air Development Center (NADC)
program to develop a Holographic Lens for Pilot's Head-Up
Display (HUD). The work covered by this report was performed
at Hughes Research Laboratories, Malibu, California during
the period 18 March 1975 to 17 September 1975.

The NADC program is to develop a HUD system meeting the optical
system parameters and performance goals as stated in the NADC
"Specification for Hologram Lens System."[1] The basic system
parameters are a 25^0 field of view (FOV), an exit pupil size
of 3" high by 5" wide, and an eye relief of ?5 in. In Phase 1
program,[2] preliminary system design and recording material
optimization led to a demonstration of high quality holographic
HUD imaging with a half-size transmission hologram configura-
tion with an off-axis angle of 40^0. In Phase 2 program,[3] we
designed and fabricated a dynamically-stabilized recording
system with symmetric 50^0 off-axis construction beams for
exposing the full-scale transmission hologram.

In this Phase 3 program, the specific subject of this report,
we fabricated the full-scale transmission holographic lens in
dye-sensitized dichromated gelatin (DSDCG). Processing equip-
ments were fabricated and processing techniques developed.
The full-scale hologram is recorded in DSDCG derived from
photographic gelatin films on 18" x 18" x 0.25" thick glass
substrate. The hologram aperture is approximately 16" in
diameter covering a 25^0 FOV from any point within a 3" x 5"
exit pupil at an eye relief of 25". Table I outlines the Task,
Objectives, Approach, and Results of the Phase 3 program.

The results of two other tasks are also described in this
report. A design study of flat reflection hologram collimator/
combiner for use in head-up display was completed. A 90^0
off-axis, 8^0 asymmetric, transmission hologram lens was fabri-
cated in bleached silver halide emulsion. The focal length
of this 8" diameter holographic element is 21.9".

TABLE 1

TASK	OBJECTIVE	APPROACH	RESULTS	LOCATION
1. Krypton ion laser procurement and test	Procure and test a krypton ion laser with an etalon for optimal coherence length and output power at 647.1 NM	Monitor power and mode stability; interferometrically measure coherence length at the 21 NM output	Stable operation of the Spectra Physics Krypton ion laser and etalon provided 400 mw of single frequency 647.1 NM power. Coherence length was measured to greater than 1.5 meters.	Section II
2. DSDCG processing techniques development	Develop holographic processing techniques for developing DSDCG holograms recorded in photographic gelatin films on 18"x18"x 1/4" thick glass substrate	Optimize processing techniques with small aperture holograms in DSDCG; adapt processing techniques to full-scale DSDCG hologram processing	Uniform DSDCG processing techniques for 18"x18" Kodak 649F plates were developed and used in fabricating the full-scale hologram	Section III
3. DSDCG hologram processing equipment fabrication	Fabricate full-scale hologram processing equipment for full range processing of large area DSDCG emulsion	Fabricate processing equipments, drying chamber and agitation tank as per design in Phase 2 program	Processing equipments, with minor modifications, were constructed and used as anticipated in Phase 2 Program	Section IV
4. Full-scale transmission hologram fabrication and test	Fabricate and test a full-scale transmission hologram at 647.1 NM	Fabricate the full-scale hologram in DSDCG emulsion at 647.1 NM with the dynamically stabilized recording apparatus; use processing equipment and optimized processing techniques; evaluate chief ray efficiency and scatter	Stable 2.25 hours exposure of the full-scale hologram lens was successful. Peak chief ray efficiency measured at 632.8 NM was 42% with 1-2% scatter	Section V
5. Reflection hologram collimator combiner design study	Perform detailed design study of systems using reflection hologram collimator/combiner elements with emphasis on 25° FOV with flat hologram substrates	Parametric study of hologram configurations; computer-based optimization of a HHUD optical design; evaluate pupil errors in the final system configuration	Less than 5 mrad pupil errors over a 25° FOV from a 3"x5" racetrack exit pupil was achieved in the final reflection HHUD design	Section VI
6. T90-N6-21.9 transmission hologram lens fabrication and test	Fabricate and test a 90° off-axis, 8" asymmetric, transmission hologram lens with a focal length of 21.9"	Fabricate T90-N6-21.9 lens in silver halide emulsion (Kodak 120-01 plates) and bromine bleach; evaluate efficiency and scatter	A 8" diameter T90-N6-21.9 hologram lens was fabricated. Good display imagery was seen in a laboratory display set-up with image input at the intermediate image plane	Section VII

I.   Introduction and Summary

2.   SPECIFIED SYSTEM PARAMETERS AND PERFORMANCE GOALS

> The optical characteristics specified by the NADC "Specification for the Hologram Lens System" are a 25° field of view, a 25 in. eye relief, a 3 in. high by 5 in. wide exit pupil, and high quality imagery.

The basic system characteristics as specified by the NADC "Specification for Hologram Lens System" are summarized in Table 2 along with the performance goals. Major parameters are a 25° circular FOV, a 25 in. eye relief, and an operating wavelength of 632.8 nm (HeNe Laser). An acousto-optical laser scanning system provides the input to the display system on a 4 in. by 4 in. diffusing screen. In order to provide a 25° FOV from this source, the system focal length must be

$$f_o = \frac{4 \text{ in.}}{2 \tan 12.5^O} = 9.0 \text{ in.}$$

Considering the 25 in. eye relief, 3 in. high by 5 in wide exit pupil, and the vertical tilt of the hologram element, the size of the hologram element is approximatley 16 in. diameter. Only the thin film, low weight nature of hologram optical elements makes it feasible to consider such a large HUD lens size.

The "continuous lens" design approach,[4] invented at Hughes Research Laboratories by Mr. Gaylord Moss, provides high optical efficiency across the angular FOV, and has uniform correctable aberrations. This design approach was used in providing the construction beam optical system in the dynamically-stabilized recording apparatus used to expose the full-scale lens. The full-scale transmission hologram lens, fabricated in DSDCG, provides 25° field of view display imagery at a 25 in. eye relief. The hologram focal length, f_H, is 14.97 in.

12

TABLE 2

25° Field of View System

Given Parameters

Field of View   25° circular

Eye Relief   25 in.

Exit Pupil Size   3 in. high x 5 in. wide

Operating Wavelength   632.8 nm (monochromatic)

Calculated Parameters

Hologram Size   16 in. x 16 in.

System Focal Length   9.0 in.

Hologram Focal Length   14.97 in.

Performance Goals

Optical Efficiency   80% min

Resolution   1.0 mrad

Accuracy   1.0 mrad, central 12°
                         2.0 mrad, to 25°

Binocular Disparity

Vertical   Less than 1.0 mrad

Horizontal divergent   Less than 1.0 mrad

Horizontal convergent   Less than 2.5 mrad

13

I.   Introduction and Summary

3.   SUMMARY OF FULL-SCALE HOLOGRAM DEVELOPMENT (TASKS 1, 2, 3, and 4)

> The full-scale hologram was successfully recorded at 647.1 nm
> on dye-sensitized dichromate gelatin emulsion derived from 18 in.
> square Kodak 649F photographic plates.

The full-scale transmission hologram is a 48.82° off-axis, sym-
metric transmission hologram lens with a focal length of
14.97 in. This display geometry is the optimization of a 50°
off-axis, symmetric construction geometry for 632.8 nm operating
wavelength. A dynamically stabilized recording apparatus pro-
vided adequate stability during the 2.25 hours required to
expose the continuous hologram lens in DSDCG.

The recording wavelength was the 647.1 nm spectral line of a
Spectra Physics krypton ion laser. Single frequency power of
400 mW was obtained with a fuse silica etalon. Power and mode
stability was tested and improved with an insulating enclosure.
Coherence length was interferometrically measured to be greater
than 1.5 meters. The output power of the krypton ion laser
provided approximately 280 mJ/cm^2 of exposing energy (per hour)
at the center of the hologram lens.

Four holographic plate preparation techniques were evaluated
based on small aperture holographic exposures made in a stable
recording setup. Methylene green was chosen as the sensitizing
dye due to its red light absorption in gelatin layers and ex-
posure sensitivity. High diffraction efficiencies of greater
than 80% with less than 5% scatter were achieved with two of
the processing techniques requiring 300 mJ/cm^2 and 500 mJ/cm^2
exposure. Detailed description of the preparation techniques
can be found in Section III, Subsection B, Topic 1.

The hologram plate preparation techniques developed with small
plates were, with slight modification, successfully applied to
full scale hologram fabrication on 18 in. square DSDCG plates.
Dichromate concentration was lowered to .4 - .5 molar to
prevent crystallization on the emulsion surface. Methylene
green concentration of 7 to 10 mg/ml of dichromate was used.
The sensitized DSDCG plates were dried in a humidity-controlled
chamber. Following exposure, the full-scale hologram was
processed in nitrogen burst agitation tanks. A twenty minutes
swelling wash was followed by graduated 25%, 50%, 75%, and
100% isopropanol wash. The processed hologram is allowed to
dry in a humidity-free nitrogen atmosphere. A 1/8 in. thick
cover glass is sealed with Epotek 305 over the gelatin film to
provide moisture and abrasion protection.

14

I.   Introduction and Summary

4.   SUMMARY OF FULL-SCALE HOLOGRAM TEST

> The display geometry (48.82° off-axis, symmetric transmission) of the full-scale DSDCG hologram lens has an intermediate image tilt of 14° at 14.97 inches focal length.

The display geometry (48.82° off-axis, symmetric transmission), as well as the focal length (14.97 in.), at 632.8 nm of the full-scale DSDCG hologram lens was experimentally confirmed. Computer outputs show an intermediate image plane tilt of 14° toward being parallel with the hologram lens is necessary for aberration uncorrected imaging with the 4" square diffusing screen of the acousto-optical laser scanner. The diffusing screen is adequate to provide 25° FOV imagery to the exit pupil, 25 in. eye relief from the lens.

Peak chief ray efficiency of 42% was measured with 1-2% scatter. Linear variation between exposure and efficiency is evidenced along the vertical and horizontal dimensions of the hologram aperture. The uniformity of the construction beams can be improved by expanding the beams further at the expense of longer exposure times. Also higher efficiency would result from fine tuning the exposure energy to correspond to modifications in sensitizing solution concentrations for full-scale hologram processing.

Good display imagery was seen with the full-scale DSDCG hologram lens. Intermodulation effects of weak secondary holographic recording from reflected light off construction optics and hardware cause slight loss in resolution and contrast. The hologram aperture size (approximately 16 in. diameter) is adequate to provide 25° FOV imagery to any point within the 3 in. high by 5 in. wide exit pupil. However, due to the 12 μm thickness of Kodak 649F gelatin emulsion, low angular diffraction bandwidth causes the vignetting of some extreme field points of the 25° FOV from the edges of the exit pupil. Improved angular bandwidth can be attained with thinner films like the 6 μm 120-01 gelatin emulsion. The full field of view is visible from a large portion of the exit pupil.

The achievements in this Phase 3 program are a step forward towards developing flyable holographic head-up displays. Major points of this Phase 3 program are

(a)   Large area processing uniformity was accomplished.

(b)   Long exposure times are feasible with a dynamically stabilized recording system.

16

Preceding page blank

(c) Greater than 80% diffraction efficiency has been achieved in small aperture DSDCG exposures. Similar efficiency can be obtained in large aperture exposures by fine tuning.

(d) Thinner emulsions are needed for a wider angular bandwidth, or the FOV and/or exit pupil must be reduced.

(e) Careful reflection shielding of construction optic and hardware is needed to eliminate secondary holograms.

I.   Introduction and Summary

5.   SUMMARY OF REFLECTION HOLOGRAM COLLIMATOR/COMBINER DESIGN
      STUDY

The final configuration of the reflection HHUD optical design
meets the basic system parameters of the NADC specification and
achieves less than 5 mrad pupil error over a 25° FOV from any
point within 3" high by 5" wide racetrack pupil.

The final configuration of the HHUD optical design includes
(a) a 43° off-axis, symmetric reflection hologram collimator/
combiner with a focal length of 14.9 in., (b) a curved folding
mirror to reduce the relay lens size and improve packaging,
(c) a relay lens system to achieve less than 5 mrad pupil
error with input imagery from the 4 in. diffusing screen of an
acousto-optical laser scanner.

The major objective of the reflective HHUD optical design study
is to establish the limits on the use of flat reflective holo-
graphic optical element in a head-up display. The basic system
parameters, as specified by the NADC "Specification for Hologram
Lens System," are a 25° circular FOV, a 3" high by 5" wide
exit pupil, and a 25" eye relief. This design study was restricted
to symmetric reflection holograms constructed with the con-
tinuous lens design concept.

The first phase of the study was a general parametric study of
field tilts, field curvatures, and coma as a function of focal
length and off-axis angle. Only hologram focal lengths between
10-16 inches were considered. Relay lens requirements out-
side of this range become very fast or very large in diameter.
Off-axis angles were restricted to the range of 20-80 degrees.
Major conclusions of this parametric study are

        (a)   Focal surface tilts of off-axis holograms increase
              with increasing off-axis angle and are nearly in-
              dependent of focal length.

        (b)   Disparity in field curvatures is minimized for
              focal lengths of 14" to 16" and off-axis angles
              $40^\circ - 60^\circ$.

        (c)   Coma, the dominant aberration, is minimized for
              small off-axis angles and large focal lengths.

Graphical data of the parametric study are included in Section
VI. Based on this study, the off-axis angle and focal length
of the reflection hologram is chosen for which the relay lens
system design optimization, the second phase of the study is
performed.

18

The long focal length, 14.9 in., implies overly large relay
lens. A folding mirror reduced the size of the relay elements
from 7.5 to 5 inches approximate diameter and reduced the
relay lens to hologram distance from 36.9 in. to 29.9 in.

The preliminary relay lens design was a derivative of a Cooke
triplet. Paraxial characteristics of the system are 1.66
magnification, 5.64" focal length, and horizontal/vertical
f-numbers of 1.13/1.88. The object size, input to the display
system, is 4". Automatic design optimization was accomplished
by the Hughes Aircraft Company in-house optical design com-
puter program.

Pupil errors, collimation and binocular disparity, are 1 to
2 mrad over most of the 25° FOV and much of the 3" x 5" wide
rectangular pupil. Computer output data of pupil errors
from various pupil locations for various field points are
graphically plotted in Section VI. Pupil errors are less
than 5 mrad within a 3" x 5" racetrack pupil. Larger pupil
errors at the corners of the rectangular pupil are believed
to be a limitation of the relay lens design form.

This HHUD design evolved with no specific cockpit geometry
in mind. It is a one point design and must be considered as
such.

I.   Introduction and Summary

6.   SUMMARY OF T90-N8-21.9 TRANSMISSION HOLOGRAM LENS

The T90-N8-21.9 transmission hologram, fabricated on bleached
silver halide emulsion, displays laser symbology from the
diffusing screen of an acousto-optical laser scanner at a
21.9 in. focal length in a 90° off-axis configuration.

The T90-N8-21.9 transmission hologram lens is a 90° off-axis,
8° asymmetric hologram lens with a focal length of 21.9".
The operating wavelength is 632.8 nm. The hologram aperture
is 8" in diameter recorded on Kodak 120-01 silver halide
emulsion and bromine bleached. Abrasion and moisture protec-
tion is provided by sealing the hologram lens with Epotek
305 to a .25" glass substrate cut to specified dimensions.
This substrate can be mounted in an AIMIS demonstrator to
display laser symbology from the diffusing screen of an
acousto-optical laser scanner.

Single binocular viewing can be maintained at an eye relief
of 34.5 in. For eyes nominally 63 mm apart, the hologram
aperture is adequate for +4.16°/-3.49° vertical FOV and
±4.56° horizontal FOV.

Display imagery can be seen with the diffusing screen input
at the intermediate image plane. This aberration-minimized
plane has a 27° tilt towards being parallel to the holo-
gram lens. Vertical and horizontal dimensions of +1.23"/-1.13"
and ±1.75", respectively, are required to fill the binocular
FOV. Uncorrected astigmatism across the field will cause
residual aberration in the display imagery.

A peak chief ray efficiency of 11% with 8% scatter was mea-
sured at 632.8 nm. These values are similar to the half-
scale demonstration hologram lens fabricated in Phase 1
program. This low efficiency is characteristic of instability
in the construction system. Despite this low efficiency, the
T90-N8-21.9 transmission hologram lens will adequately demon-
strate the complex lens function of holographic lens and will
display laser symbology in the AIMIS demonstrator. High
quality display imagery was seen with a laboratory setup
using diffused 632.8 nm illumination of a photographic slide
at the intermediate image plane.

I.   Introduction

7.   REFLECTION AND TRANSMISSION HOLOGRAPHIC COLLIMATOR/COMBINER ELEMENTS

Both reflection and transmission holographic collimator/combiner elements
as part of a head-up display can provide large field of view at long eye
relief with high display brightness and excellent external visibility.
Transmission elements are impractical in high ambient light situations,
due to the presence of distracting spectral flares.

Holographic collimator/combiner elements as part of a head-up display
can provide:

   (1)   Large field of view at long eye relief with no increase in
          weight due to the thin film nature of hologram optics.

   (2)   Improved display brightness and external visibility due to the
          wavelength dependence of optical efficiency in hologram optics.

A concise parametric analysis of reflection and transmission holographic
collimator/combiner elements for head-up displays can be found in refer-
ence 2, the Phase 1 final technical report. The fundamental character-
istics of reflection and transmission holographic elements are similar:

   (1)   High optical efficiency requires point source construction
          beams (continuous lens design) with minimal asymmetry.

   (2)   Spheroidal focal surfaces, for vertical and horizontal ray
          fans, have unique curvatures and tilts.

   (3)   Distortions are anamorphic and keystone.

   (4)   Aberrations are primarily coma with spherical aberration.

   (5)   Binocular disparity and collimation errors increase with
          off-axis angle.

Transmission holograms typically have smaller aberrations and pupil
errors than corresponding reflection holograms of similar geometry.
Fabrication of transmission holographic elements, although a complex
task, is less difficult than fabrication of reflection holograms.
However, transmission holograms are not well suited for application in
high ambient light environment. The orientation of recorded fringe
structure results in strong dispersion of ambient light. The spectral
flare from diffracted sunlight can be of great discomfort to the viewer.
Transmission elements can be applied in controlled lighting situations
where proper shielding can be achieved. Another application of trans-
mission hologram lenses, currently being investigated at HRL, is in
night vision goggles.

Reflection holograms retain the low weight and wavelength selective
nature of hologram optics without objectionable spectral flare. There-
fore, reflection collimator/combiner elements can provide wide FOV with
high image brightness in head-up displays. However, the fabrication of
reflection holographic elements requires material optimization for
sensitivity and thickness uniformity, extreme control in the stability
of the recording wavefront and hologram substrate, and optimization of
process and sealing techniques to 'freeze' the emulsion thickness for
the proper operating wavelength.

At Hughes we have the capability and experience required for a unified
design of holographic and conventional optical systems. State-of-the-
art fabrication techniques were developed in the successful fabrication
of large aperture transmission collimator/combiner elements. Further
optimization of these techniques is necessary for application to the
fabrication of reflection collimator/combiner elements.

II.   Krypton Ion Laser - Procurement and Test

1.   SPECTRA PHYSICS MODEL 165-01 KRYPTON ION LASER

> A Spectra Physics krypton ion laser with a fused silica etalon
> was procured to provide high, single frequency 647.1 nm out-
> put power with adequate coherence length.

The Spectra Physics Model 165-01 krypton ion laser was procured
due to its high continuous power output at 647.1 nm, a spectral
line near the operating wavelength 632.8 nm. The manufacturer's
specifications are:

Single transverse mode power (TEM$_{oo}$)	500 mW at 647.1 nm
Power stability	+.5% over 10 hrs with power stab- ilizer on
Input power requirement	190 to 225 V, 3-phase, 35 amps per line
Cooling water requirement	2.2 gal/min at 25 psi (minimum)

The laser cooling system is depicted in Fig. 1. The components
in the system were selected to meet the cooling requirements
with minimal pulsating water pressure. The regenerative tur-
bine pump provides three gallons per minute of flow at 30 psi
to the laser system.

A Model 589 single frequency, solid fused silica etalon was
also procured in anticipation of the need for extended coher-
ence length. For the 50° symmetric transmission construction
geometry, the coherence length required is 22.23 cm. The
theoretical spacing between adjacent optical frequencies for
the model 165 laser is 143 MHz ($\Delta f = c/2L$ where c is the
velocity of light and L = 1.05 m, the cavity length). With
a Doppler gain bandwidth greater than 5,000 MHz, more than
20 frequencies can oscillate simultaneously. For a 1.05 m
long laser oscillating in 20 modes, the theoretical coherence
length is conservatively approximated by

$$L_H \doteq .293 (\frac{2L}{N}) = .293 \frac{c}{\Delta f_o}$$

where L = cavity length, N = number of modes, c = speed of
light, and f_o = Doppler line width.

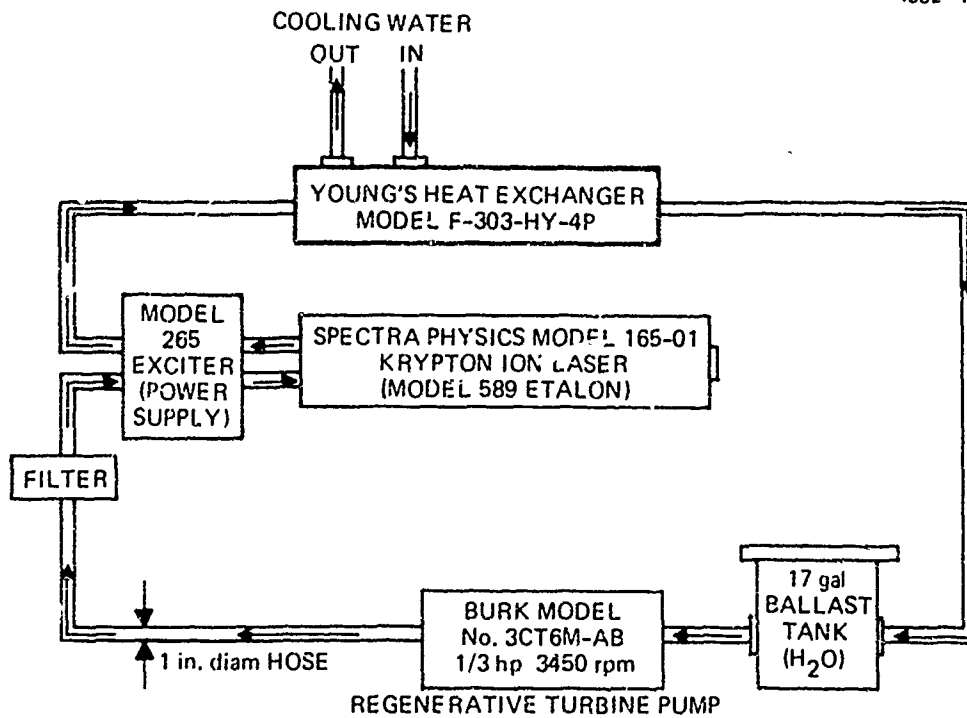$$L_H \doteq 3.08 \text{ cm for L = 1.05 m and N = 20.}$$

22

Fig. 1. The laser cooling system meets the requirement of the laser system with a 3 gal/min flow at 30 psi.

23

II.   Krypton Ion Laser - Procurement and Test

2.   LASER TEST SET-UP

> The laser test setup monitors power and mode stability and
> interferometrically measures the coherence length of the 647.1
> nm output of the krypton ion laser.

Power stability, mode stability and coherence length are evalu-
ated by the laser test setup pictured in Fig. 2. The laser
under test is the Model 165-01 Spectra Physics krypton ion
laser operating at 647.1 nm. This is the laser source for
the full-scale hologram recording apparatus designed and
constructed in Phase 2 program.

The output of the photodiode monitors power stability on a strip
chart recorder. A primary cause of power instability in the
krypton ion laser is contamination of the laser optics by dust
and foreign particles. Delays in this program were primarily
due to this laser power stability problem. The initial laser
tube was defective and cracked. The replacement tube degraded
due to outgassing from some rubber and anodized components of
the laser. Consequently, the laser system was returned to the
manufacturer for chemical cleaning of optics and mounts. A
third tube was installed, and some laser optics and an etalon
were replaced.

An etalon can be considered as a filter which inhibits laser
oscillation at all but one frequency or mode. The frequency
or mode selected from the laser cavity modes within the laser
gain profile is dependent on the optical length of the etalon
cavity. Therefore a dimensional instability due to temper-
ature variations can cause mode hops or instability. These
mode instabilities can be seen visually with the spectrum
analyzer. Power instability usually accompanies mode hops
due to difference in laser gain of various modes.

Coherence length is measured interferometrically[5] with the
Michelson interferometer in the test setup.   Coherence length,
ΔL_H, is equal to $c\tau_H$ (c = speed of light; τ_H = transit time
difference) such that the degree of coherence $|\mu_T(\tau)|$ is
equal to $1/\sqrt{2}$. This degree of coherence is related to the
fringe visibility by

$$V = \frac{2|\mu_T(\tau)|\sqrt{R}\cos\Omega}{R+1}$$

where R = beam ratio
      Ω = angle between
          polarization vector.

By keeping the beam ratio R = 1 and the polarization vector of the two beams unidirectionally parallel (Ω = 0), the fringe visibility reduces to V = $|\mu_T(\tau)|$.

In the test setup. the fringe intensity at the detector is dependent on the intensity, relative phase difference, and degree of coherence between the two beams. By keeping the beam intensities constant with a ratio of one, the maximum and minimum fringe intensities are measured as their relative phase difference is varied by the piezoelectric translator. Fringe visibility is calculated (V = $\frac{I_{max} - I_{min}}{I_{max} + I_{min}}$) and plotted versus ΔL. Coherence length is the ΔL at which visibility falls to .707 of maximum visibility.
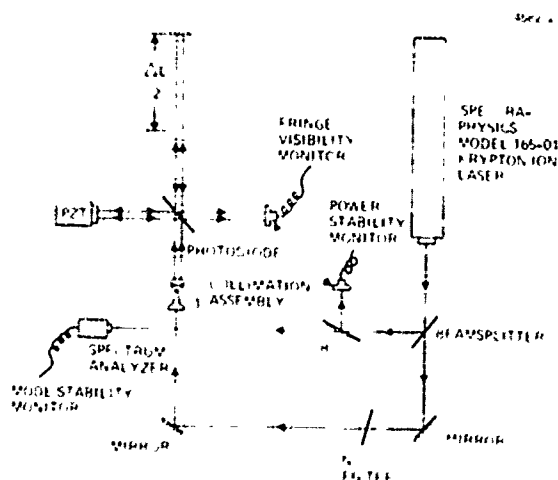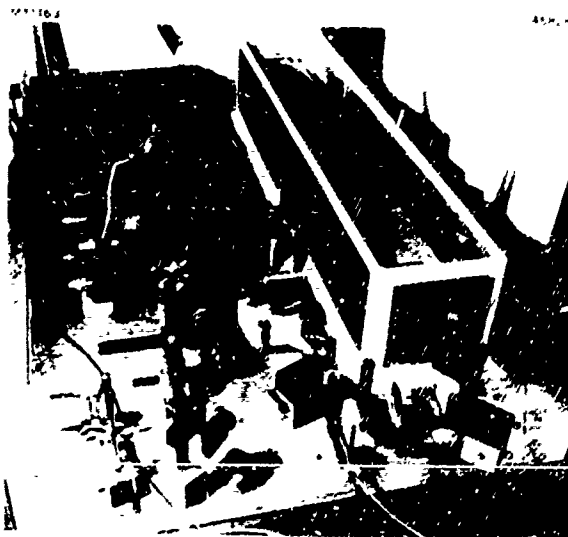

Fig. 2.
The coherence length is ΔL_H for which the fringe visibility measured is 0.707 of maximum visibility at ΔL = 0.

II.   Krypton Ion Laser - Procurement and Test

3.   LASER TEST RESULTS

Adequate power and mode stability was achieved with 400-
450 mW of single frequency 647.1 nm output power. Greater
than 1.5 meter coherence length was measured.

The krypton ion laser, operating at 647.1 nm TEM_{00} mode with
one watt of power, has a coherence length of only 3.5 cm. The
graph of experimental data for fringe visibility versus path
length difference, Fig. 3, shows a decrease to zero visibility
at 10 cm path length difference. Although high power output
is available in this TEM_{00} mode, the limited coherence length
is inadequate for full-scale hologram exposures.

Single frequency operation at 647.1 nm was obtained with the
Model 589 etalon in the krypton ion laser. The coherence
length was experimentally measured to be greater than 1.5
meters, the limit of the test setup.   Experimental data are
plotted in Fig. 4. The photograph from the spectrum analyzer
output shows the single longitudinal mode of the laser.

Due to the high conversion efficiency of the etalon, 600 mW
of single frequency power at 647.1 nm is available with the
laser system drawing 35 amps of current. However, due to the
high sensitivity of the etalon to ambient air temperature,
mode hops can cause the output power to vary unless the etalon
is constantly readjusted to keep the optical path within the
cavity constant.

An improvement in mode stability was consequently achieved by
shielding the laser with insulation material and operating
the laser in a light control mode. The enclosure composed of
particle board is lined with aluminum foil and rubber sheet.
The insulation keeps the temperature relatively constant near
the operating temperature of the laser cavity. In the light
control mode, the laser system compensates for power variations
due to mode hops by modulating the input current to the laser.
Consequently, the laser must operate below 35 amps, the satur-
ation current level.

Optimal operating conditions for the Model 165-01 krypton laser
were found to be 400-450 mW of single frequency 647.1 nm power.
The laser operates at 30 amps in light control. After the
temperature within the insulating enclosure has stabilized,
power output was observed to be stable for over 24 hours.
Mode hopping typically occurred every hour, although under
extreme conditions 4 - 5 hour mode stability was achieved.

26

Mode and power stability will probably be much improved when
a temperature controlled etalon or a more dimensional stable
etalon, like the air-spaced etalon available for the 450 nm -
520 nm spectral range, is commercially available. However, the
power and mode stability and coherence length of the krypton
ion laser with etalon are adequate for full-scale hologram
exposures. Optics in the full-scale hologram recording appara-
tus, designed and constructed in Phase 2 program, were aligned
with this krypton ion laser.
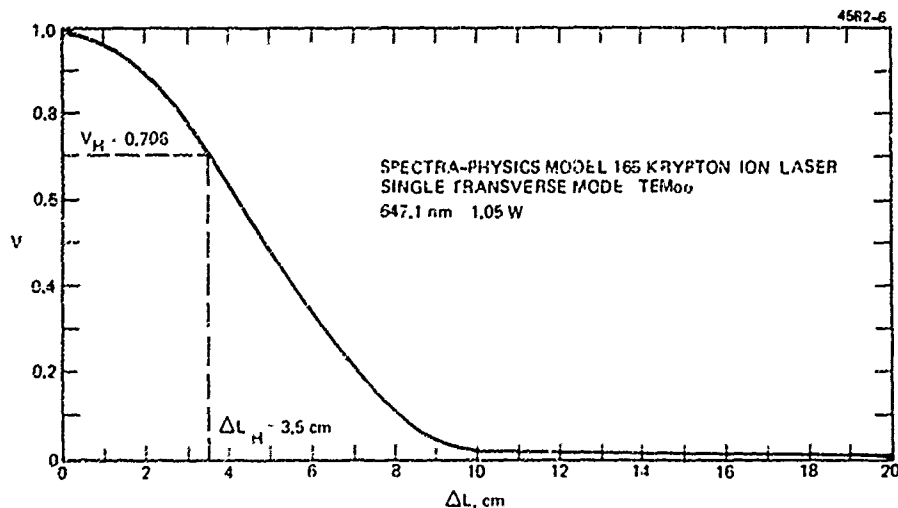

Fig. 3.   Coherence length for TEM_{OO} is 3.5 cm, the
          path length difference at which fringe
          visibility is 0.707 of maximum.
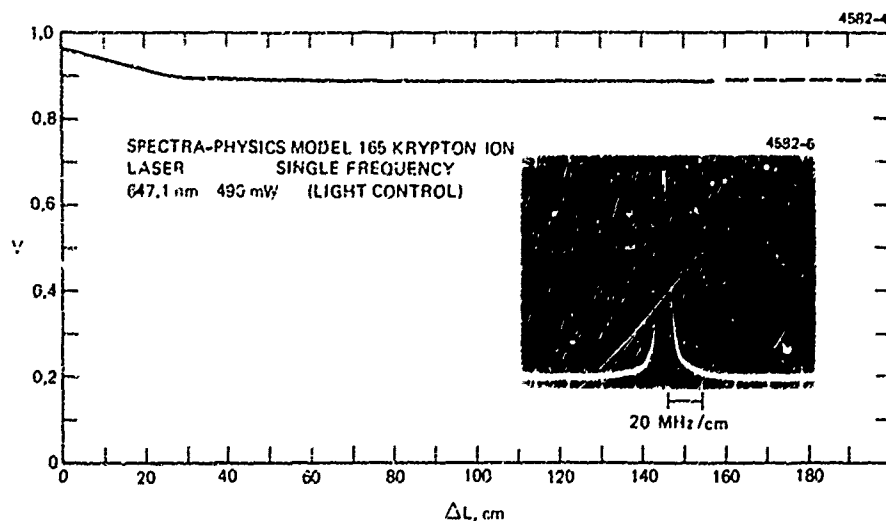

Fig. 4.   Measured single frequency coherence length
          of greater than 1.5 m is adequate for full-
          scale hologram exposures.

27

III.   DSDCG Hologram Processing Techniques Development

A.   Methylene Green Dye

1.   SPECTRAL SENSITIZERS

Dyes which are effective spectral sensitizers for dichromated
gelatin generally show poor compatability with dichromate ions.

The solubility of a substance is influenced by the presence
of other solutes in aqueous solution. In the preparation of
dye sensitized dichromated gelatin (DSDCG) sensitizing solu-
tion, a problem is encountered in providing sufficient solu-
bility for the necessary actinic chemical species.[6] We have
found that many spectrally sensitizing dyes are capable of
rendering DSDCG red sensitive, but the dyes precipitate out
in dichromate solutions.

Although some dyes possess the characteristics of water solu-
bility, red light absorption, and excellent compatibility with
dichromate in solution, these dyes are typically poor spectral
sensitizers for DSDCG. For example, vat green 11 (Color Index
No. 59850) has a solubility product in dichromate solution
exceeding 10^{-3} moles^2/liter^2, but its quantum efficiency for
index modulation production is very low. Gelatin layers sen-
sitized with this dye have excellent red light absorption, but
extremely long exposures are required to record even weak
holograms.

The thiazine dyes are particularly effective DSDCG sensitizers,
but their compatibility with the dichromate ion in solution
is very low. The relationship between thiazine dyes and
dichromate ions at the point of precipitation can be closely
approximated by a solubility product relationship, typically
having values of about 10^{-4} mole^2/liter^2. Although the solu-
bility of these dyes can be somewhat improved by the addition
of a chelating agent, such as triethanolamine, or by a sur-
factant, such as Kodak Photoflow, the solubility is still very
small. As a result, when gelatin layers are sensitized in
these solutions, little red light absorption is gained,
necessitating very long holographic exposures.

A more dichromate-compatible dye family is the triphenylmethane
group, showing very good solubility characteristics, while
maintaining fair sensitivity to red light. When these dyes
are used in DSDCG, exposures of about 2000 mJ/cm^2 at 632.8 nm
are required for efficient hologram production.[6] Some gain
in sensitivity can be gained by using a mixture of dyes. Such
a mixture can contain an efficient triphenylmethane dye, for

28

example, acid fast violet, to increase the apparent quantum efficiency.

As a general rule, it can be stated that sensitive dyes in the DSDCG system are readily attacked by dichromate ions. Although some steps can be taken to minimize the attack, its elimination does not appear possible.

III.   DSDCG Hologram Processing Techniques Development

A.   Methylene Green Dye

2.   SOLUBILITY IN DICHROMATE SOLUTION

> The solubility of methylene green dye is determined by the amount of dye added and the concentration of dichromate present.

Although the thiazine dyes have large quantum efficiencies for converting absorbed red light into holographic index modulation, their solubility in dichromate solution is generally very low. Gelatin layers sensitized with these dyes are usually ineffective since they absorb only a small fraction of incident radiation.

The notable exception to this thiazine dye family precipitation behavior is methylene green. This dye is identical in structure to the familiar methylene blue dye, except for a nitro group in the 1-position. Apparently, this nitro group is very effective in appreciably raising the dye's solubility product, while maintaining the high level of sensitivity typically displayed by thiazine dyes. Because of these favorable characteristics, methylene green was selected as the spectral sensitizer for DSDCG.

When methylene green dye and dichromate are placed together in solution, increasing dye additions do not always produce proportionately increasing concentrations of dye in solution, as shown in Fig. 5. It would be expected that, if no other effects were taking place other than dissolution, the optical density of a dye would increase linearly with the amount of dye added until a saturated dye solution would be attained. The curvilinear plot in Fig. 5 implies that a reaction is taking place between the dye and dichromate ions.

Because of this probable dye oxidation, which is particularly rapid at large dye concentrations, the estimation of true methylene green solubility in dichromate solution is particularly difficult. However, it is possible to estimate the practical maximum dye solubility that would be present in a DSDCG sensitizing solution, namely 30.0 milligrams/cm^3 of solution, or 0.082 molar. From the lower portion of this curve the real molar extinction coefficient can be estimated. It is estimated that if a 12 micron thick gelatin film expands six-fold in a sensitizing solution containing 0.082 molar methylene green, and if the gelatin does not chemically bind the dye, an optical density of 0.40 will be obtained in the dye layer. This means that an ample 60% of the active incident radiation will be absorbed in the film during a holographic exposure.
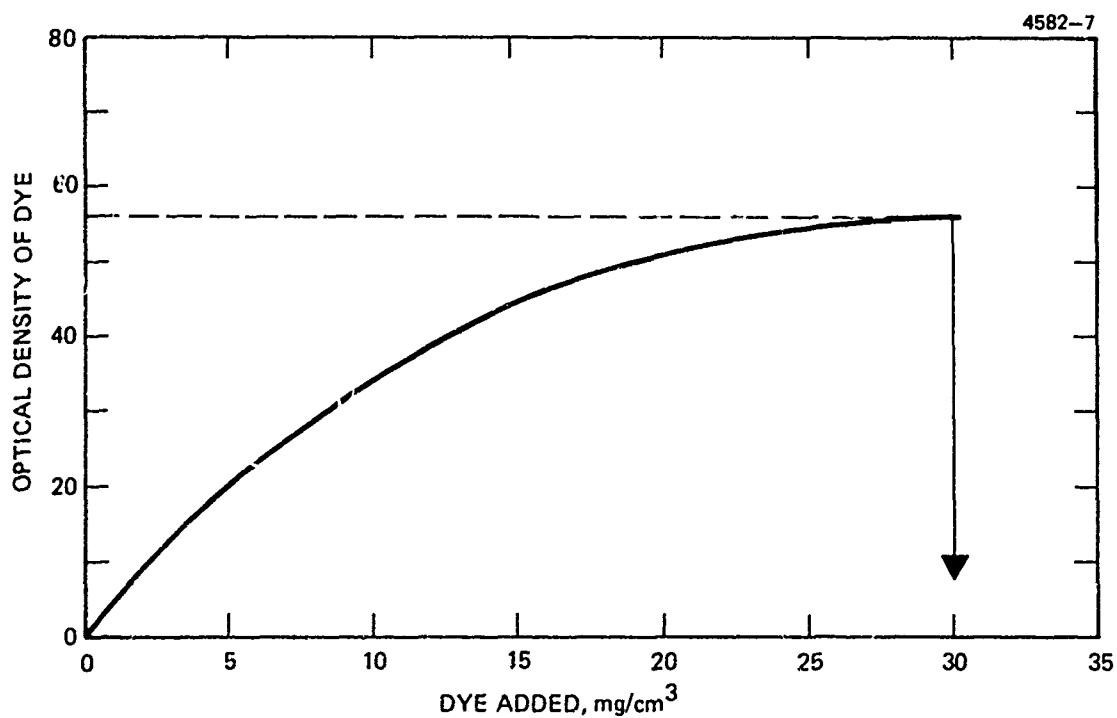
30

Fig. 5.   Optical density developed at 632.8 nm in 1 cm path
length as a function of the amount of methylene green
dye added to a 1 molar ammonium dichromate solution.

31

III.   DSDCG Hologram Processing Techniques Development

A.   Methylene Green Dye

3.   SENSITIZING PREPARATION SOLUTION

The sensitizing solution attains maximum optical density after
two minutes of mixing and must then be filtered free of pre-
cipitate and excess dye.

Since the optical density of the dye sensitized dichromated
gelatin (DSDCG) sensitizing solution does not increase linearly
with the amount of methylene green dye added, as shown in Fig.
5, it is apparent that the colored dye species must be removed
from solution, possibly as a result of an oxidation by the
dichromate ion. This loss of optical density in the sensitizing
solution is important in DSDCG in that it also influences the
density that will be inbibed into the gelatin layer. We con-
ducted an experiment to study the loss of the red light absor-
bancy in the preparation of the sensitizng solution and in the
keeping qualities of the solution once it was prepared.

When methylene green dye is manually mixed into a dichromate
solution, it has a tendency to clump together without dissolving.
With additional mixing, however, the dye does begin to dissolve
reluctantly, finally reaching a maximum color.

Figure 6 shows that the largest optical density is reached with
two minutes of agitation. Following the maximum density, the
color again becomes lighter before reaching a steady state in
about eighteen minutes. The dye solution samples were filtered
through medium filter paper before each density measurement
to exclude any precipitate from giving a larger apparent density.

We do not have an explanation for the decrease in density from
its maximum, but it appears that as the dye is being mixed into
the solution, an opposing process begins to take place that
removes or changes the dye molecules. It is postulated that a
steady state is not reached at 52 optical density because the
undissolved dye reacts with the products of the dissolved dye
oxidation, forming copious precipitate. This secondary reaction,
it is thought, quickly removes the oxidation products from the
solution, shifting the chemical equilibrium toward increased
oxidation. The practical consequence of this investigation for
DSDCG is that with moderate mixing rates, optimum and maximum
dye solubility is reached in about two minutes when by filtra-
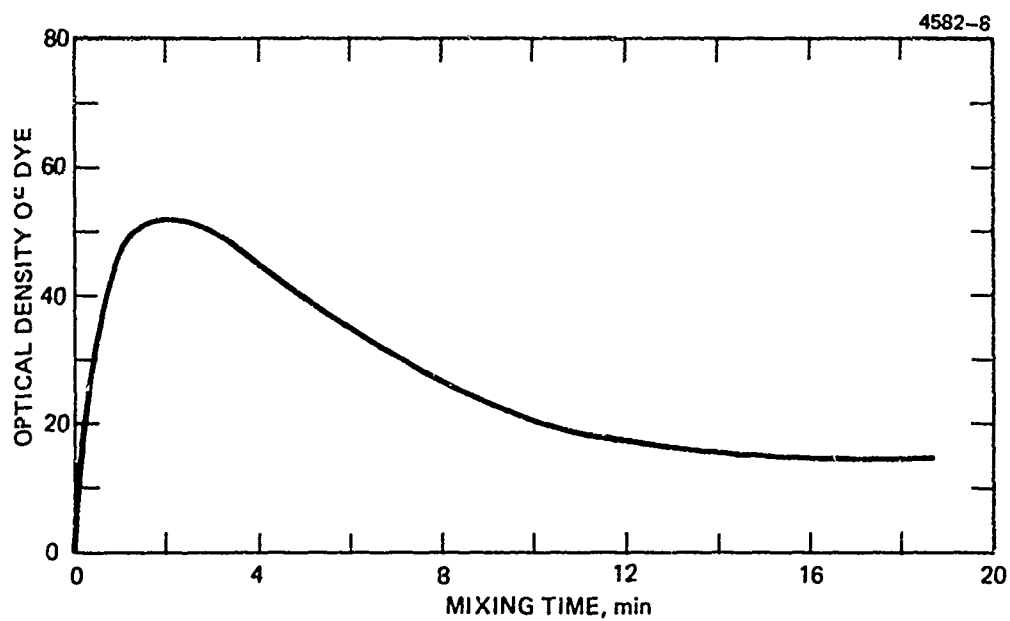tion excess, undissolved dye and accumulated precipitate should
be removed.

32

Fig. 6. Optical density developed at 632.8 nm in 1 cm
path length as a function of the time of mix-
ing of methylene green dye in 1 Molar ammonium
dichromate.

III.   DSDCG Hologram Processing Techniques Development

A.   Methylene Green Dye

4.   SENSITIZING SOLUTION LIFETIME

> The filtered methylene green and dichromate solution will
> retain its ability to sensitize DSDCG for over sixty minutes.

In the previous section it was shown that the mixing of the
dye-dichromate mixture must be properly timed to achieve
optimum optical density. If filtration of the DSDCG sensi-
tizing solution is done after two minutes, the question comes
to mind as to how long the sensitizing solution will still be
good. Figure 7 shows that the optical density of dissolved
dye is a function of both the dye concentration and the age
of the sensitizing solution. The loss of optical density with
time is particularly severe at large dye concentrations, as
expected, since the dye-dichromate reaction is concentration
dependent. At the large dye concentrations, where DSDCG will
be used, only about a 25% density decrease occurs in thirty
minutes and 44% decrease in sixty minutes. We believe that the
sensitizing solution could be used for at least sixty minutes,
but filtration of the precipitated, oxidized dye will be
necessary between sensitizations. It is anticipated that films
sensitized at later times from the same solution will require
somewhat longer exposure times to overcome the decreased density.

It is possible to rejuvenate or recharge the sensitizing solution
after its useful time has been exceeded. Since the concentra-
tion of ammonium dichromate in the sensitizing solution is so
much higher than the dye, it can be assumed that only the dye
requires replenishment. Addition of new methylene green dye,
agitation, and filtration produces a fresh sensitizing solu-
tion. In the production of many DSDCG holograms such sensi-
tizing solution replenishment not only conserves the starting
material chemicals, but also alleviates the problem of dis-
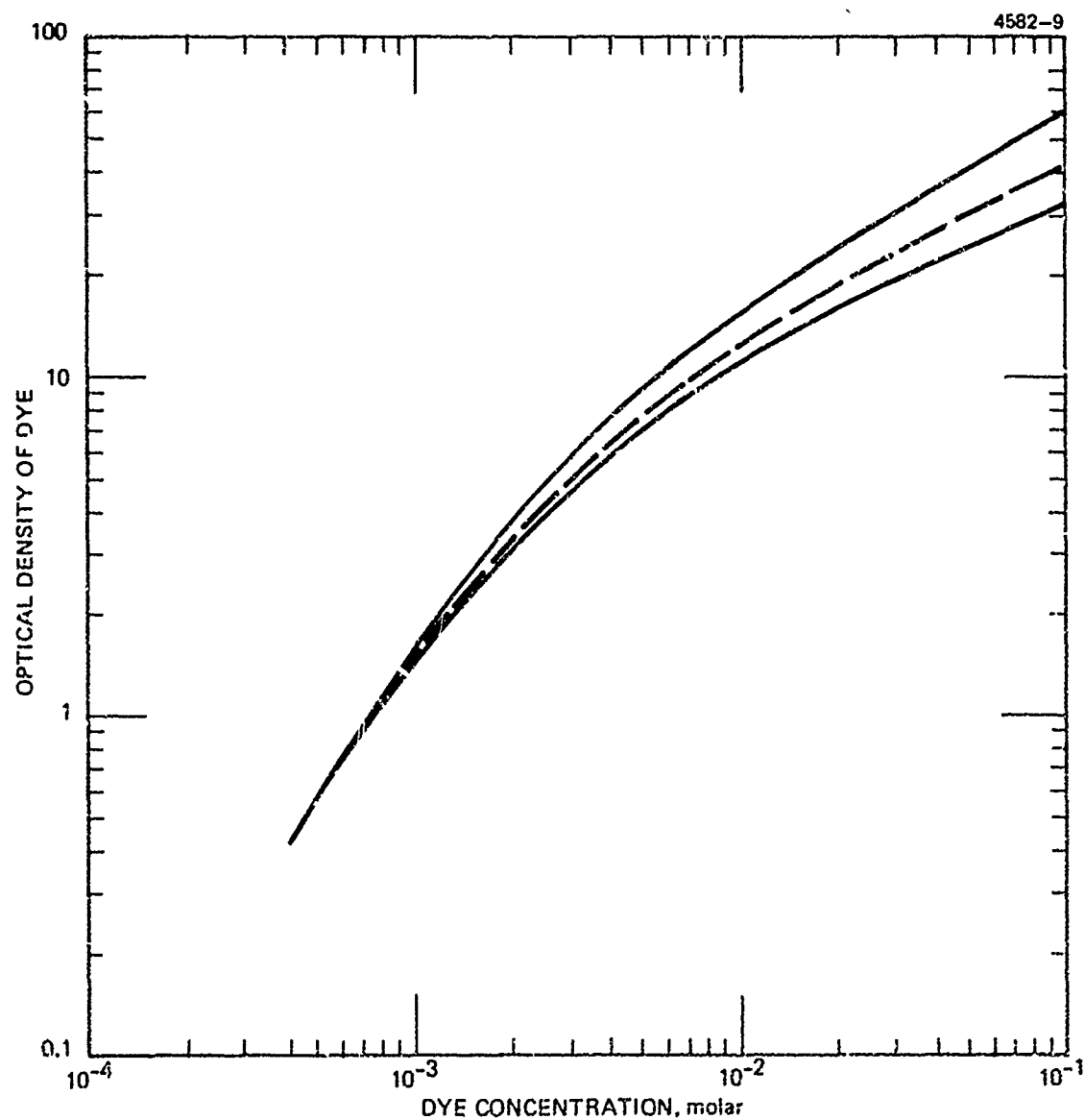posing the spent toxic materials.

34

Fig. 7. Optical density developed at 632.8 nm in 1 cm path
length as a function of methylene green dye concen-
tration in 1 Molar ammonium dichromate solution
immediately after mixing (——); after 30 min (- - -);
afer 30 more minutes (- ---- -).

III.   DSDCG Hologram Processing Techniques Development

B.   Small Aperture Exposure

1.   PLATE PREPARATION TECHNIQUES

Four plate preparation techniques were considered for the
large aperture hologram fabrication.

We extended our scope of photographic plate preparation tech-
niques to include those which anneal or crystallize the gelatin
molecules. The annealing is thought to increase the rigidity
of the gelatin film[7] and orient the molecules in positions
favorable to crosslink formation,[8] thereby increasing film
sensitivity.

Besides the considerations of resulting hologram quality from
each of these processes, we also considered their ease of
implementation into the large hologram processing apparatus.
Tables 3 and 4 show preparation methods that require annealing
through the gradual rise in washing water temperature. An
obvious difficulty with these schemes is in providing sufficient
washing water at the proper temperature over large area holo-
grams. Despite this disadvantage, these two techniques were
further evaluated.

The technique shown in Table 5 omits the annealing cycle, but
the two-stage drying in steps 3, 4 and 7, we believe, serve as
a pseudo-annealing method that toughens the gelatin film.
Table 6 contains the double-hardening technique, producing
very hard films. This method must be coupled with special
development procedures to extract maximum diffraction efficiency.[2]

In the next section we show holographic exposure comparison of
the four dichromated gelatin preparation techniques.

36

Table 3

Dichromated Gelatin Preparation from Kodak 649F Plates with Annealing Cycle[9]

1. Fix in Part A of Kodak Rapid Fixer - 10 minutes.

2. Wash with running water at 90°F for 15 minutes. Start at 70°F and raise temperature at approximately 2.5°F min. to 90°F.

3. Stand in air 1 minute.

4. Rinse in distilled water with 2 drops per liter of Photo-Flo 600 for 30 seconds.

5. Dry completely in room environment.

6. Soak in room temperature water for 2 minutes.

7. Harden in both Part A and Part B of Rapid Fixer for 10 minutes.

8. Wash for 15 minutes at 70°F in running water.

9. Rinse in Photo-Flo solution for 30 seconds.

10. Dry overnight at room temperature.

Table 4

Dichromated Gelatin Preparation from Kodak

649F Plates with Shortened Annealing Cycle[10]

1. Soak in fixer without hardener for 10 minutes.

2. Wash in running water at 90^OF for 15 minutes; start at 68^OF and raise temperature 2.5^OF/min to 90^OF; following wash, lower temperature at same rate to 68^OF.

3. Soak in fixer with hardener for 10 minutes.

4. Wash in running water for 15 minutes.

5. Rinse in distilled water for 1 minute with agitation.

6. Dry overnight at room temperature.

Table 5

Dichromated Gelatin Preparation from Kodak

649F Plates Without Annealing Cycle

1. Fix in Part A of Kodak Rapid Fixer - 10
    minutes.

2. Wash in tap water - 15 minutes.

3. Dry in flowing 55% RH air - 90 minutes.

4. Dry in still 40% RH air - overnight.

5. Presoak in deionized water - 2 minutes.

6. Fix in Part A and B of Kodak Rapid Fixer -
    10 minutes.

7. Repeat steps 2, 3 and 4.

Table 6

Dichromated Gelatin Preparation from Kodak 649F Plates with Two Hardening Cycles[2]

	Step	Time	°C Temperature
1.	Apply Kodak Rapid Fixer (with hardener) mild agitation	15 min.	22
2.	Deionized water wash	20 min.	22
3.	Kodak Photo Flo 200 diluted with deionized water 1:200 volume ratio	30 sec.	22
4.	Squeegee gelatin surface	-	-
5.	Dust-free air dry, 40% RH	Overnight	22
6.	Repeat steps (1) to (5)		
7.	Bake in air atmosphere	2 hrs.	150
8.	Store in 40% RH air		

III.   DSDCG Hologram Processing Techniques Development

B.   Small Aperture Exposure

2.   METHYLENE GREEN SENSITIZATION

> The methylene green sensitizing dye has sufficient light
> absorption in gelatin layers for sensitive holographic
> exposures.

In order to ensure good light penetration into the sensitized
gelatin layer, it is necessary to keep the light-absorbing
species at a sufficiently low level.[11] On the other hand, with
too little absorption in the sensitized layer, the majority
of the exposing light will be wasted. The proper adjustment
of the red light-absorbing properties in dye sensitized dichro-
mated gelatin (DSDCG) is not a simple matter since it is depen-
dent on (1) the dissolved dye concentration in the sensitizing
solution, (2) the amount of swelling of the gelatin layer,
(3) the binding of the dye by the gelatin, and (4) the oxida-
tion of the dye by dichromate after sensitization. The first
variable has been studied and determined, but the last three
are difficult to measure. We chose to take an empirical
approach to determine the best film absorption characteristics.

After sensitization and drying, the optical density was measured
in each of the plates prepared by the various processing methods.
The mean optical densities for the samples were 0.807 for method
of Table 3, 0.626 for Table 4, 0.862 for Table 5, and 0.808
for Table 6. It was expected that plates of Table 6 would have
a lower average density since these plates had the hardest gela-
tin, which would swell the least. Instead, these plates had
densities commensurate with much softer plates. This implies
that the presensitization hardening procedures not only changed
the gelatin swelling properties, but also influenced the affinity
of the gelatin for methylene green.

Figure 8 shows how excessive absorbance can decrease film sen-
sitivity. Samples were prepared by the method of Table 5 and
sensitized with two different dye concentrations. The lower
dye concentration plates are the more sensitive in diffraction
efficiency production. The higher dye plates exhibit the
"umbrella effect," where the top film layers are so dark that
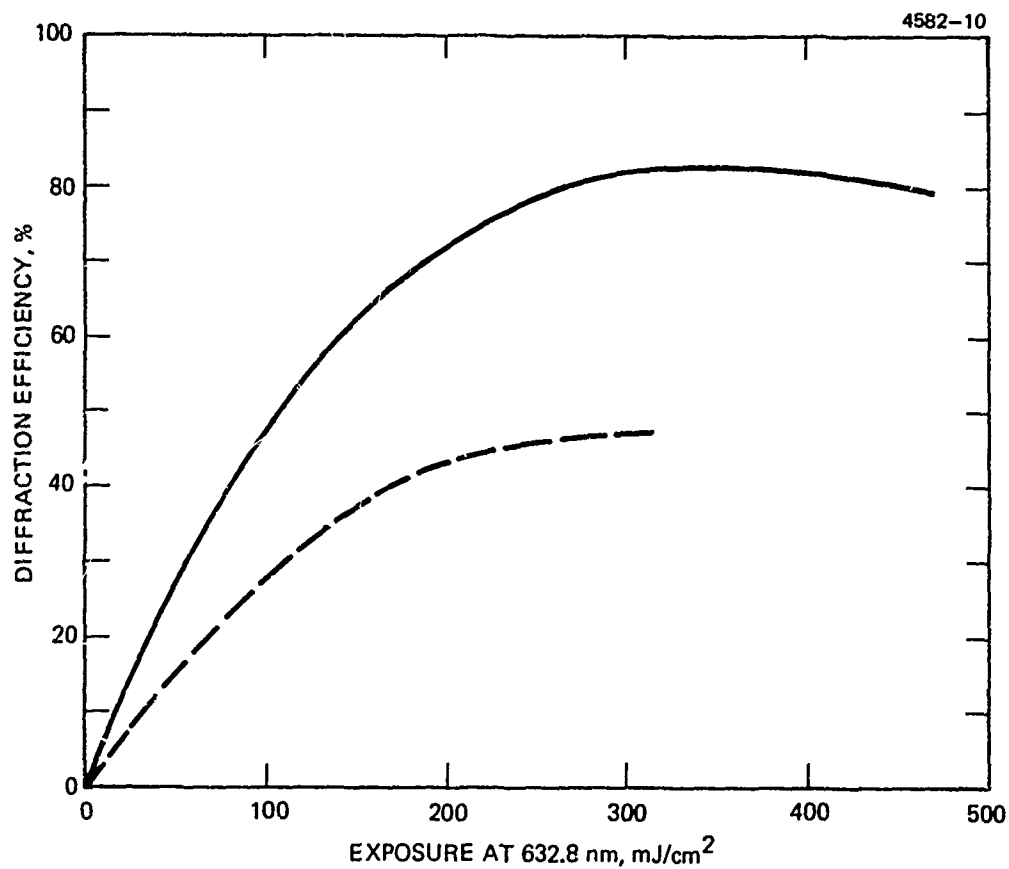they shield lower layers from the image formation light.[12]

Fig. 8. Diffraction efficiency as a function of exposure energy for plates prepared with 10 mg of dye/ml (———) and 20 mg of dye/ml (-----).

All of these preliminary tests were performed with a helium-
neon laser at 632.8 nm, but these results, as expected, were
directly applicable to the 647.1 nm wavelength also. Figure 9
shows that the red absorption spectrum of methylene green is
composed of two primary electronic transitions, which may have
varying efficiencies in converting light energy to crosslinks.
The two wavelengths, as indicated in Fig. 9, are so close
together, relative to the absorption peak separation, that no
significant absorption or sensitivity differences were experi-
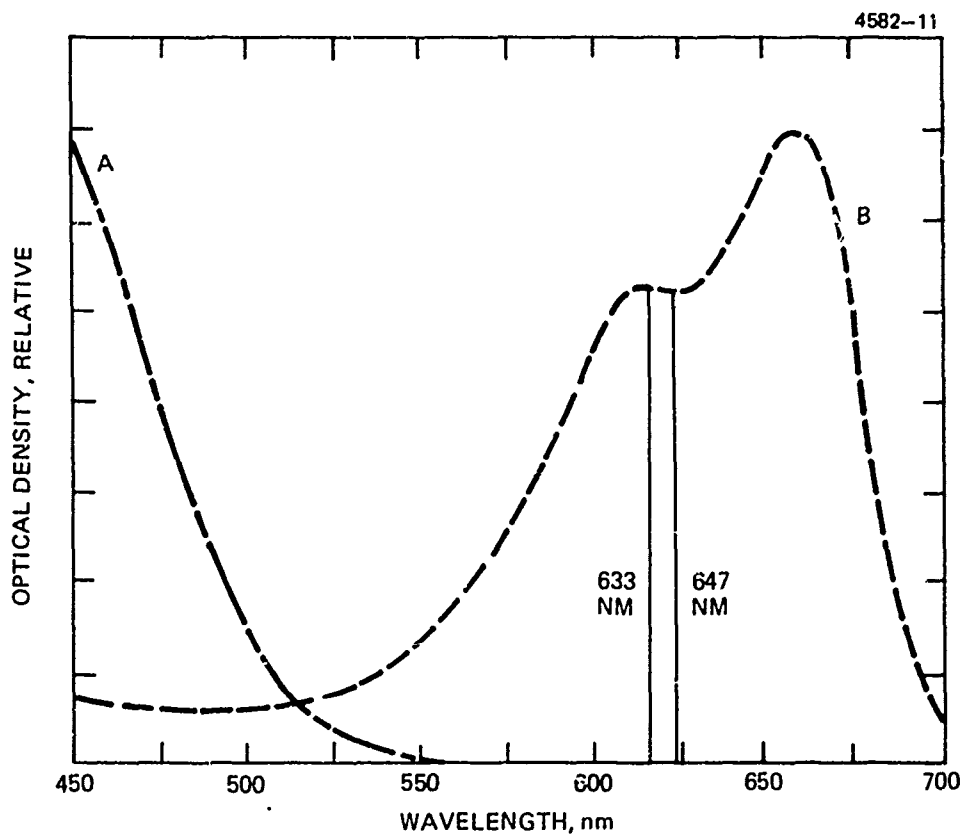mentally observed.

Fig. 9. Relative absorption spectra of dichromate
ion (A) and methylene green dye (B).

III.   DSDCG Hologram Processing Techniques Development

B.   Small Aperture Exposure

3.   RECORDING APPARATUS

A holographic test device with uniform illumination power and high mechanical rigidity was used for materials testing.

To determine the response of any holographic material, it is of critical importance to eliminate physical exposure variables from the exposure apparatus. The presence of optical exposing instabilities leads to the motion of holographic light fringes within the material, causing degraded material performance. Then it is very difficult to assign the relative blame for a poor hologram to the equipment or the holographic material.

In an effort to provide a very stable exposure apparatus, we used a solid aluminum plate with all the optics bolted to it as shown in Fig. 10. The laser beam entered the apparatus from the lower right side, was spatially filtered and expanded, collimated by a lens, and folded on itself by a high reflectivity dielectric mirror. The instrument was designed to provide an interference pattern with a spatial frequency so that a thick hologram would be formed in a 12 micron thic., layer. The average light power distribution varied less than 10% over the exposure area.

This apparatus provided an extremely dimensionally stable holographic materials test fixture as shown by an evaluation with a Michelson interferometer. We inserted a mirror in the sample holder and made it one leg of the interferometer. After thirty minutes, the plate had not moved even a fraction of a fringe, evidencing the stability of the plate holder and supporting structure.

An air shield was provided around the metal base to keep air currents from deforming the wavefront and from influencing the gelatin layer's moisture content. The metal base was secured on four magnetic mounts, which rested on a 4x8 ft. steel table. The table, in turn, was supported by air-inflated vibrational isolation mounts.
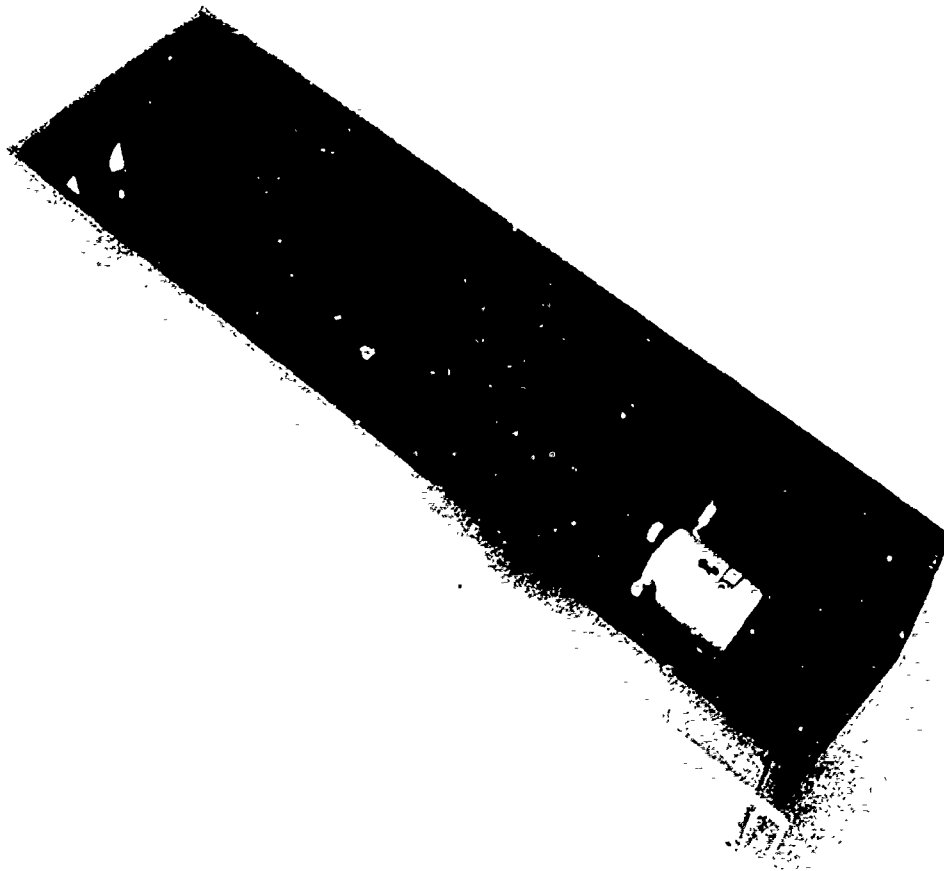
Fig. 10. Stable holographic materials test optical arrangement.

III.   DSDCG Hologram Processing Techniques Development

B.   Small Aperture Exposure

4.   TEST RESULTS

> The plate preparation techniques were evaluated by holographic
> exposure, and two methods showed excellent performance and
> were selected for large plate exposures.

In the previous section we introduced four photographic plate
preparation methods as candidate techniques for the large scale
holograms. We prepared several plates by each of these tech-
niques, and following sensitization with methylene green and
ammonium dichromate, we holographically exposed them in the
stable apparatus shown in Fig. 10.

Following the holographic exposure, in our materials evaluation,
we developed the films and interrogated them at 632.8 nm for
diffraction efficiency and light losses. Figure 11 shows the
results of these tests for three plate preparation techniques.
The method of Table 3 at first appears to be the best, since
the highest diffraction efficiency (defined as the percent of
incident light diffracted into the first order) is achieved
with least exposure. However, in the large photographic plates,
the exposing light power distribution will not be uniform, and
since the diffraction efficiency of the Table 3 method is highly
peaked as a function of exposure, we anticipated the appearance
of non-uniform efficiency. The efficiency non-uniformity could
arise either from underexposure or over-modulation of the phase
shift.

The preparative technique of Table 4 was abandoned since dif-
fraction efficiencies only on the order of 20% could be obtained.
The methods of Tables 5 and 6 were selected as worthy of further
pursuit since the maximum diffraction efficiency peaks are dis-
tributed over a large exposure range. The preparative tech-
nique of Table 5 is preferred since the film is quite light
sensitive, reaching maximum diffraction efficiency between 300
and 400 mJ/cm^2. Also, this technique does not require any
special processing, such as baking or annealing, which would
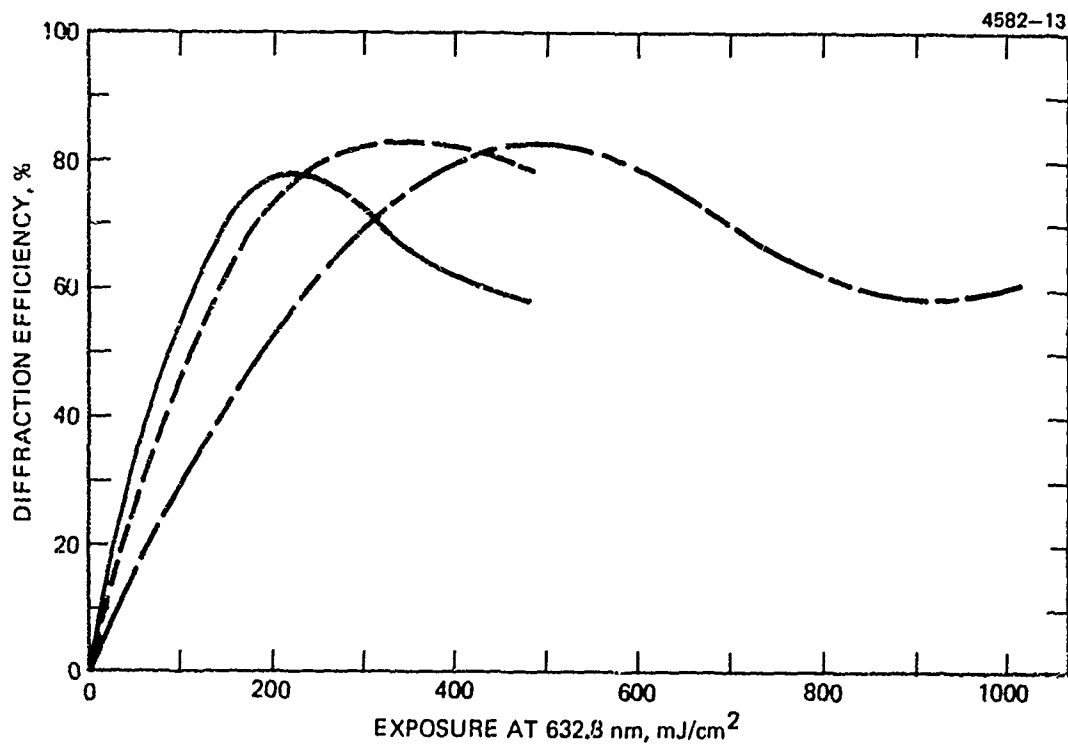present special problems when applied to large scale photo-
graphic plates.

48

Fig. 11. Diffraction efficiency as a function of exposure
for plate preparation method listed in Table 3
(———), Table 5 (------), and Table 6 (- — - —).

49

IV.   DSDCG Hologram Processing Equipment Fabrication

1.   NITROGEN-BURST AGITATION PLATE HOLDER AND PROCESSING
        TANKS

The processing equipment, with minor modification, was con-
structed and successfully used as anticipated in Phase 2
of this program.

The preliminary design of the holographic plate processing
equipment was completed in Phase 2 of this program, and with
minor modifications and alterations, the equipment was con-
structed and utilized. In this section we shall look at the
construction and testing of the processing equipment in the
sequence of plate preparation.

The Type 649F plates as supplied by Kodak have silver salts
imbibed into the photographic gelatin, and these salts must be
removed prior to dichromate sensitization. We used flat photo-
graphic processing trays with 1200 ml of fresh Kodak Rapid
Fixer for each plate. This volume of fixer is ample for
removing the silver salts, and the use of fresh solution assures
reproducible gelatin pre-hardening. In order to uniformly
apply the fixing chemicals onto the plates, we used a two-axis
pneumatic tilt table. This table generates randomly related
sets of right angle waves in a shallow tray containing the
plates to be processed. The small, but adequate, volume of
liquid required to cover the plate is an advantage in mini-
mizing waste chemicals when the tray is used to add a chemical
solution to the plate, or when it is desired to control the
temperatures of the fluid.

Washing of the fixing chemicals was done with deionized water
in ten gallon tanks, shown standing on the floor in Fig. 12.
The stirring was provided by nitrogen-burst agitation built
into the plate holder, shown being held by the technician in
Fig. 12. Originally we had planned to build a nitrogen-burst
agitator in each processing tank, but we found that the holder-
agitator combination could be handled and positioned much more
quickly than separate holder and agitator fixtures. The nitro-
gen burst was provided by a valve actuated by a cam, which
gave a sudden "ON" burst, lasting about three seconds, followed
by about three seconds without flow. Tests showed that for
washing out chemicals absorbed in large plate emulsions, this
agitation method was very efficient and reproducible.

Plate baking was done in an electrically-heated oven, having six inches of refractory insulation around it to prevent temperature non-uniformities from developing. The oven was provided with a temperature sensing circuit that could hold the temperature to within 2°C of the set value.
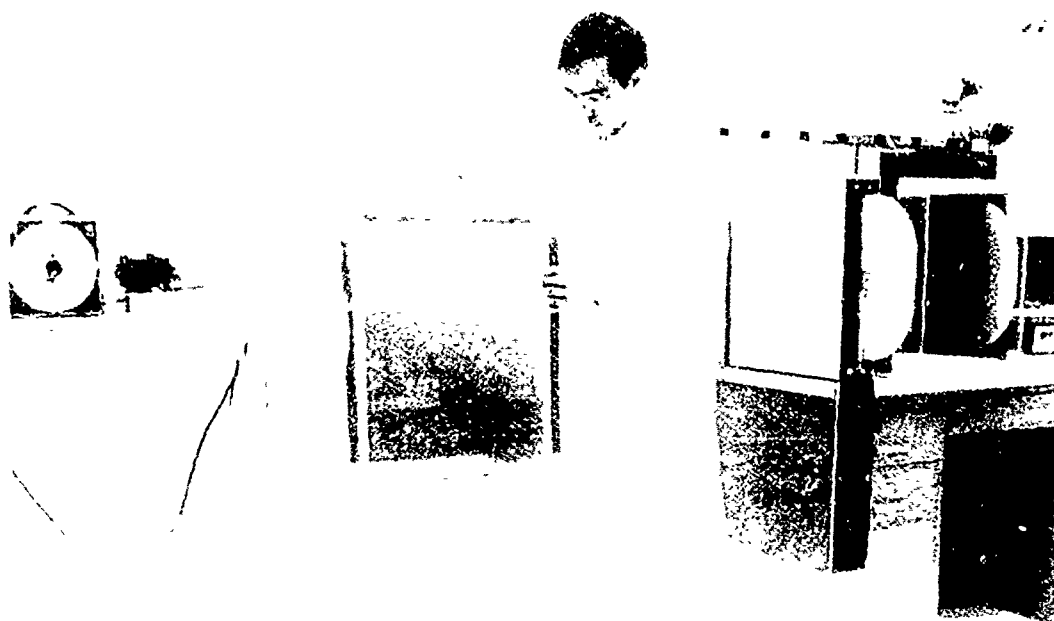
M11039

4582-14

Fig. 12. Chemical processing tanks, agitator/holder, and storage boxes for DSDCG large scale holographic plates.

51

IV.   DSDCG Hologram Processing Equipment Fabrication

2.   HUMIDITY CONTROLLED DRYING CHAMBER

> The processing equipment was designed and constructed to
> provide film uniformity and reproducibility in the post-
> sensitization drying and development.

Although the plate drying following silver salt removal and
washing was accomplished by drying the plates in a laminar flow
clean bench with 55% relative humidity air, the drying stage
following plate sensitization was done in the fixture shown
in Fig. 13. A 24-inch diameter fan directed air through a
fibrous filter before passing over the plates at about a 45°
angle to the plate surface.

The surface of the plates, when wet, is very tacky and
quickly picks up dust particles from the air. The fibrous
filter served as a dust shield for the plate drying area. The
wet air was dehydrated by passing it over open trays of constant
humidity chemical, calcium chloride ($CaCl_2.6H_2O$), placed on a
shelf above the fan and plates. The dried air was then recir-
culated again through the blowing fan.

This entire assembly was enclosed in a light-tight, plywood con-
tainer, provided with temperature and humidity sensors for the
inside air that could be read from the outside. When the wet
plates were dried, the relative humidity would rise to about
65% in the 3 cubic meter volume enclosure before slowly falling
to 40% relative humidity. We found that it was best to operate
the circulating fan intermittently in order to keep the temper-
ature inside the chamber from rising excessively.

During the drying of the sensitized plate, we noticed that the
humidity in the drying chamber was significantly different from
that in the room environment where the exposure was to take place.
To offset the relative humidity "shock" that the sensitized
gelatin plate would experience, we arranged a forced air flow
over the plate during the settling time in the plate holder
prior to exposure. In this way the response of the gelatin
film was made more uniform over the large plate area because
the relative humidity influences film moisture content, and it,
in turn, influences film sensitivity.

Fig. 13. Recircuilating air, light-tight, constant relative humidity drying chamber for large-scale holographic plates.

V.   Full-Scale DSDCG Hologram Fabrication and Test

A.   Full-Scale DSDCG Hologram Processing

1.   PRE-EXPOSURE PROCESSING

> The hologram preparation techniques developed for small plates
> were, with some modification, successfully applied to the
> full scale holograms.

When photographic plates are coated for commercial sale, the
manufacturer is basically interested in only that the plates
perform photographically, giving proper density upon light
exposure and development. The hardness of the gelatin on the
plates is a minor concern to the manufacturer, and his only
concern is that the gelatin does not dissolve from the plate
during photographic development. Since the hardening of
gelatin in photographic plate manufacture involves trade
secrets,[13] we were not able to determine how gelatin hardness
is held in tolerance and had to rely on empirical observa-
tions.

Our original tests on the hardness of Kodak photographic plate
gelatin were carried out on 2 x 2 inch plates by sensitizing
them by increasingly stronger dichromate concentrations
until the films would crystallize. For the plate preparation
methods of Table 5 and 6, these dichromate concentrations
were 0.6 and 0.9 molar, respectively. However, on the large
18 x 18 inch plates, the gelatin in the manufacturer's
coating batch must have been much softer than on the small
plates since sensitization with the 0.6 and 0.9 molar con-
centrations gave plates with severe crystallization, copious
scattering noise, and low diffraction efficiency. We adjusted
the dichromate concentrations to 0.4 and 0.5, respectively,
to eliminate the crystallization problem. Also, the hyper-
sensitizing salt, ammonium nitrate, was left out of the
sensitizing solution to prevent crystallization.

In preparation of the sensitizing solution we found that
when large amounts of methylene green dye (i.e., 10 grams)
were added to the dichromate solution (i.e., 1000 ml), the
dye had a tendency to clump into water-tight pockets. Very
vigorous agitation had to be applied to the mixture to
dissolve the dye. The precipitate formed by the dye and
dichromate during sensitizing solution was removed by fil-
tration through medium speed filter paper. Since the
precipitate has a tendency to clog the filter paper, and
since the speed of filtration is an important factor, as
shown in Figure 6, we accelerated the normal filtration rate
by using large area filters or vacuum filtration methods.

54

The precipitation of oxidized methylene green dye from solution during sensitization presented a special problem. Localized, high concentration sensitizing solution pockets would be formed around the precipitate on the gelatin surface during drip-drying of the plate following sensitization. These precipitate particles, although few in number, significantly scatter the laser light during holographic exposure. We tried several materials set on handles that would act as squeegees for wiping the liquid material from the gelatin surface along with the precipitate particles. These materials included single and double-bladed soft rubber sheets, foam rubber, leather chamois, air blades, and soft plastic. Although each had its own merits, the single soft rubber sheets were the best for removing precipitate without harming the gelatin surface.

Since it is difficult to predict the optical density which sensitization will impart to a film because of the variation in gelatin hardness, we began our sensitization with a nominal 10 mg of methylene green dye per ml of sensitizing solution. Density measurements on the sensitized plates showed that the dye content can be dropped to 7 mg/ml while maintaining adequate red light absorption. The optical density that the plates had after sensitization did not appreciably deteriorate during drying at 40% RH.

With red light illumination, however, the density dropped steadily with increasing light exposure. If it can be assumed that the dye fading rate is the same as in our previous investigation for DSDCG plates, illuminated with 632.8 nm light, a total exposure of 300 mJ/cm^2 should produce about a 2% reduction in red light absorption. This reduction is not thought to significantly affect film sensitivity.

V.   Full-Scale DSDCG Hologram Fabrication and Test

A.   Full-Scale DCDCG Hologram Processing

2.   POST-EXPOSURE PROCESSING

Large scale, high efficiency holograms can be recorded in dye sensitized dichromated gelatin using graded alcohol processing.

When dye sensitized dichromated gelatin plates are holographically exposed, they develop only a small amount of diffraction efficiency. This small efficiency is typically amplified in the development process by the sequential immersion of the plate in a gelatin swelling liquid and a gelatin collapsing liquid. The critical step in this process is in the transfer of the plate from the first solution to the second. Depending on the rate at which the dehydrating alcohol reaches the swollen gelatin surface, large differences in diffraction efficiency can result.

We developed the exposed gelatin plates by first washing them for 20 minutes in deionized water with nitrogen bubble burst agitation. This step effectively removed the unreacted dichromate and most of the sensitizing methylene green dye. When the plate was immersed in the alcohol bath with nitrogen burst agitation, however, the resulting diffraction efficiency was over 70% but varied considerably over the plate area. The efficiency variation was highly correlated to the paths taken by the agitating bubbles rising to the liquid surface.

To overcome this efficiency variation, a modified development procedure was applied, where the holographic plate was bathed in graded alcohol solutions. In going from the water bath to solutions containing 25%, 50%, 75%, 90%, and 100% 2-propanol by volume, the necessity for rapid agitation of the holographic plate was obviated. The gelatin layer, in taking the water-to-alcohol transition in a gradual manner does not generate as much diffraction efficiency as when suddenly shocked with 100% alcohol, and correspondingly we achieved lower diffraction efficiencies with this method. The efficiency was very uniform over the plate surface, corresponding to the holographic exposure energy. Detailed quantitative efficiency measurements will be presented in another section of this report. The graded alcohol baths were applied to the large plates in open trays, causing a large Concentration of alcohol fumes to appear in the vicinity. We found that activated charcoal respirators were necessary for the personnel to prevent pulmonary alcohol intoxication.

After the holograms were developed and dried in dry nitrogen, a cover glass was sealed over the gelatin film to protect it from moisture and abrasion. For the sealant we used a clear epoxy resin, Epotek #305, with a viscosity of about 2,000 cp. The viscosity of the sealant should be low enough to allow spreading over the hologram area, but not so low viscosity that bubble entrapment is excessive. After the two part epoxy adhesive was mixed, it was degassed for bubbles under vacuum. The resin takes about 24 hours to gain a firm hardness, and it does not photodegrade easily with sunlight illumination. The holograms sealed by this method had excellent clarity and low scattering noise. The diffraction efficiency was not significantly changed from the unsealed to the sealed state, indicating that surface relief on the gelatin surface was small in comparison to red light wavelength and the holographic lens was recorded as a volume, phase image without substantial cracks in the gelatin surface.

V.   Full-Scale DSDCG Hologram Fabrication and Test

B.   Full-Scale DSDCG Hologram Exposure

1.   PARAMETERS

> The dynamically stabilized exposure apparatus maintained
> fringe stability during the 2.25 hours required to expose the
> full scale hologram lens on DSDCG.

The fringe control system, developed in Phase 2 program,
servo-locked the axial phase difference between the exposing
beams. Fringe stability was maintained during the 2.25 hours
required to expose the full-scale hologram. This successful
long-time exposure is evidence of the stability integrity of
the complete exposure system.

The krypton ion laser's single frequency 647.1 nm output,
operating under light control, was 400 mW. Higher power
spatial filter objectives were used to improve the illumina-
tion uniformity across the 16" hologram aperture. However,
trade-offs between the degree of uniformity and length of
exposure time resulted in approximately 300 mJ/cm^2 variation
in exposed energy. The exposed energy, at various horizontal
and vertical locations of the hologram aperture, is shown in
Figure 14 for the 2.25 hours exposure period. Further
improvements in exposure uniformity were possible but not
implemented because of lack of time.

The beam ratio of the exposing beams measured 2:1. At the
center of the hologram lens, the energy of the converging
and diverging construction beams was .028 mW/cm^2 and .050
mW/cm^2, respectively. The calculated fringe visibility is
94% of maximum visibility of one for equal intensity beams.

After the 18" square DSDCG plate is positioned in the holo-
gram recording plane, minor adjustment of the fringe control
interferometer is required to center the low spatial fre-
quency control fringes on the detector. This adjustment is
necessary to compensate for slight perturbation of the trans-
mitted construction beams through the glass substrate of the
DSDCG emulsion. However, the adjustment requires typically
less than one minute with the exposure shutter open. The
absorbed energy during this period is negligible compared
to the total exposure energy required.

With the exposure shutter closed, the control output of the
integrator in the control electronics remains constant.
Upon releasing the shutter, the control electronic integrates
phase difference between the construction beams. The control

output drives a piezoelectric translator correcting any phase difference variations during the exposure.
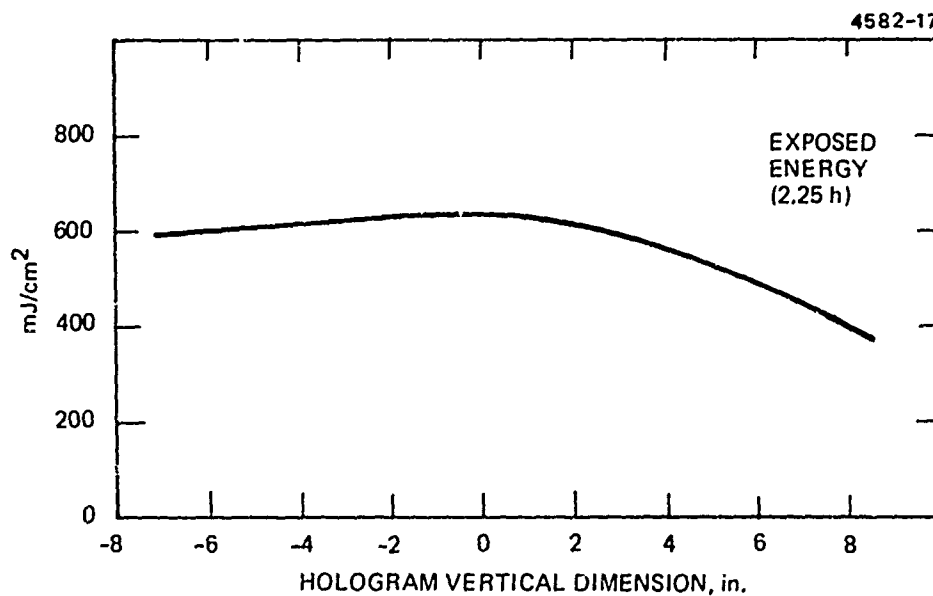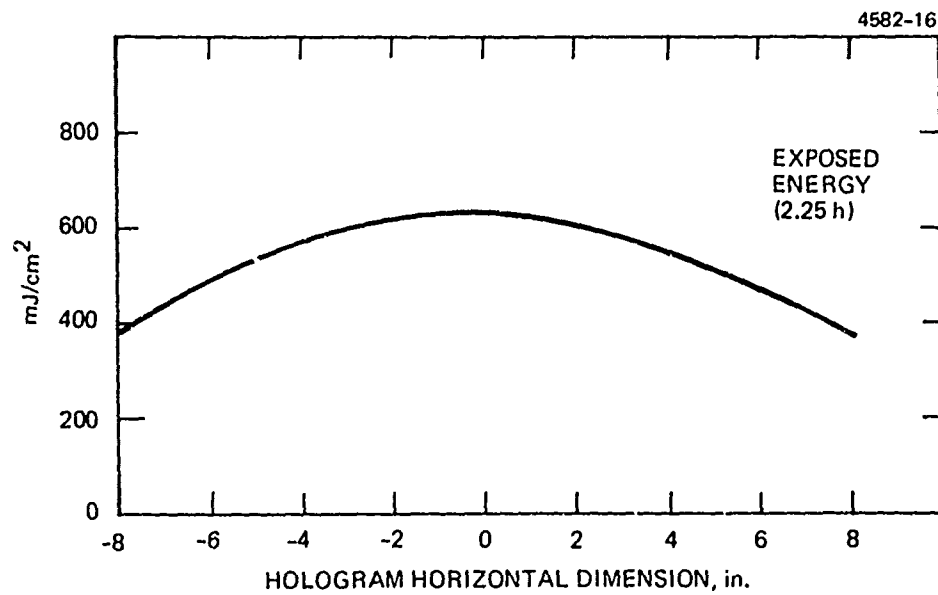
4582-16

4582-17

Fig. 14. Variation in exposed energy across vertical and horizontal dimensions of full-scale hologram lens.

59

V.   Full-Scale DSDCG Hologram Fabrication and Test

C.   Full-Scale Hologram Characteristics

1.   DISPLAY GEOMETRY AND INTERMEDIATE IMAGE PLANE

> The full-scale hologram HUD geometry at 632.8 nm is 48.82°
> off-axis with a 25 in. eye relief. The intermediate image
> plane tilt is 14° at 14.97 inches focal length.

The full-scale hologram recording apparatus was designed and
fabricated for a 50° off-axis symmetric transmission con-
struction geometry. Slight modifications to this construction
geometry is required for optimal 632.8 nm wavelength recon-
struction in a symmetric configuration. This is summarized
in Table 7, and a vertical section of the HHUD geometry of
the full-scale hologram is shown in Figure 15.

Computer ray trace data of the hologram's focal surfaces
are plotted in Figure 16. The relay lens system design
represents a complex task because of the disparity in object
surfaces and is not within the scope of this Phase 3 program.
However, an intermediate image plane can be selected to
provide display imagery from the 4" square diffusing screen
of the acousto-optical laser scanner.

The intermediate image plane is the bisector to the axial
tangent planes of the spheroidal focal surfaces shown in
Figure 16. This image plane is tilted vertically towards
the hologram, 14° from the optical axis normal at the focal
length of the lens, 14.97". The required input size for 25°
circular FOV can be measured from the optical axis to the
extreme field points on the intermediate image plane,
incident points for the $\pm$12.5° field rays.

With the 4" square diffusing screen, tilted 14°, + 3.75 in.
and -3.19 in. is adequate for 25° vertical FOV. A horizontal
dimension of $\pm$3.31 in. is necessary for 25° horizontal FOV.
Residual aberrations will exist in the display imagery of
the intermediate image plane (4" square diffusing screen),
because of the absence of an aberration-correcting relay lens
system.

60

TABLE 7

Full-Scale Transmission Hologram

Construction at 647.1 nm		Reconstruction at 632.8 nm	
Asymmetry angle	0°	(Symmetric)	0°
Off-axis angle	50°		48.82^O
Focal Length	14.58 in.		14.97 in.
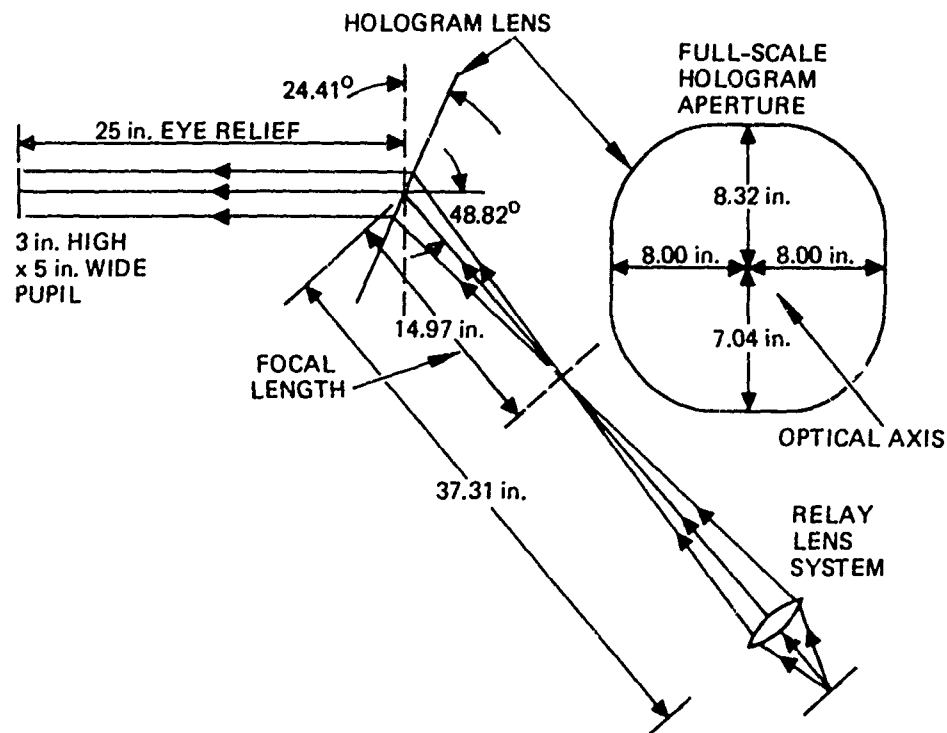
Fig. 15. Full-scale hologram HUD geometry at a dis-
play wavelength of 632.8 nm.

Fig. 16.   Vertical and horizontal section of focal surfaces
           and intermediate image plane.

V.   Full-Scale DSDCG Hologram Fabrication and Test

C.   Full Scale Hologram Characteristics

2.   EFFICIENCY AND SCATTER

The full-scale hologram display geometry at 632.8 nm was confirmed experimentally. Peak diffraction efficiency of 42% was measured with approximately 1-2% scatter.

Symmetry, off-axis angle, and focal length of the full-scale transmission hologram was experimentally measured at 632.8 nm, the operating wavelength of the laser scanner. The display geometry of the full-scale DSDCG hologram lens was confirmed to be 48.82° off-axis, symmetric transmission with a focal length of 14.97 inches. Detailed discussion of the test procedures can be found in Reference 14.

Chief ray efficiency and scatter, measured at 632.8 nm, is plotted in Figure 17. Diffraction efficiency is the percent of incident light diffracted into the first order. Scatter is the percent of incident light loss not accounted for in diffracted and transmitted light, corrected for surface reflections and film absorption. Peak efficiency of 42% was measured at the hologram optical center. With typical reflections of 6-7% and absorption (measured in unexposed regions) of 16%, the scatter of the processed DSDCG hologram is well below 5%.

Note that chief ray efficiency and scatter data was measured and plotted for field angles greater than the ±12.5° FOV. Because chief rays of the HHUD system are construction rays of the hologram lens the graph in Figure 17 also shows the diffraction efficiency variation across the 16" diameter hologram aperture. A direct correlation exists between this variation and the exposure variation (Section V, Topic B1) across the hologram aperture. Consequently, chief rays incident at points of high exposures, near the hologram optical center, had high diffraction efficiencies. Because diffraction efficiency does not appear saturated versus exposure, higher diffraction efficiency could probably be attained with increased exposure.

During a laboratory display setup of the full-scale transmission DSDCG hologram lens, ghost imaging was noticed in the display imagery. Consequently, this secondary imaging was tracked down to actual weak holograms of construction hardware and optics. These holograms were formed by reflections of the construction beams off these construction hardware and optics during the exposure. The overall

64

intermodulated effect of these weak holograms is to produce
faint shadow-like images causing slight contrast reduction
and resolution loss. These secondary holograms can be
eliminated with antireflection coatings of problem optical
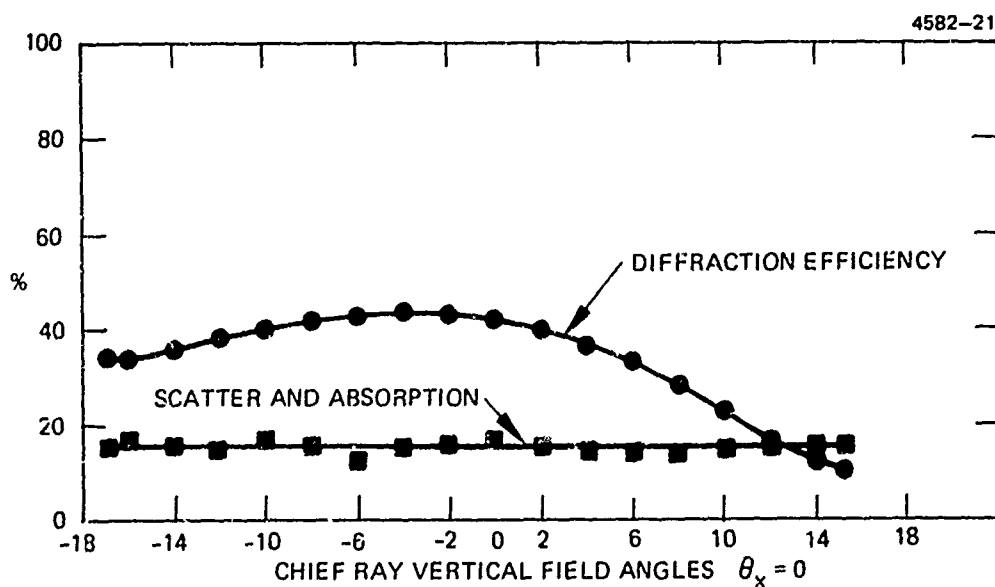surfaces and re-anodizing problem construction hardwares.
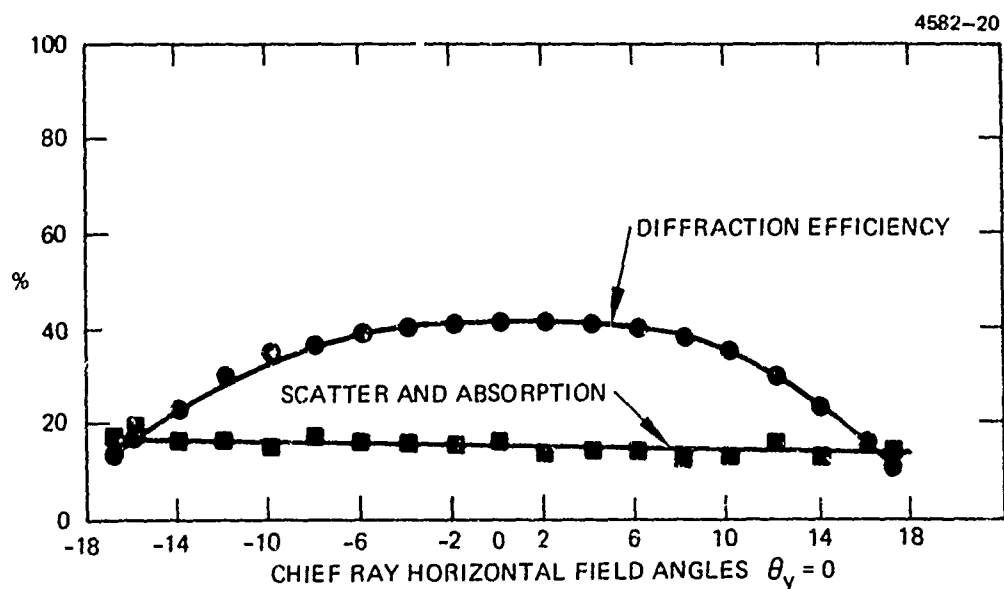
Fig. 17. Vertical and horizontal chief ray efficiency
and scatter.

VI.   Reflection Hologram Collimator/Combiner Design Study

A.   Introduction

1.   BACKGROUND, OBJECTIVE AND APPROACH

The major objective of the NADC-HHUD Optical Design Study is to
establish the limits on the use of flat reflection hologram
lenses in head-up display.

The principal elements in the Holographic Heads-Up Display
(HHUD) are schematically illustrated in Figure 18.   An inter-
mediate image of the object surface is formed by a relay lens.
This intermediate image is located at the focal surface of a
flat plate holographic optical element which is used as an
eyepiece to present a collimated image of the object to the
eyes located in the exit pupil.   The relay lens is located
close to the entrance pupil to the holographic lens in order
to minimize its size.

The reflection efficiency of the holographic element is highly
wavelength and angle dependent.   The holographic element there-
fore performs the dual functions of (a) eyepiece for the display
and (b) combiner glass so that the display is viewed against
the outside world seen through the holographic element.   The
angular sensitivity of the holographic element's reflection
efficiency requires that the holographic element be constructed
with point sources located close to the desired entrance and
exit pupils.   This ensures that high reflection efficiency of
the chief rays occurs and a wide field of view (FOV) optical
system is obtained.

The major objective of the NADC-HHUD Optical Design Study has
been to establish the limits on the use of a flat reflective
holographic optical element in the head-up display (HUD) con-
figuration described above.   To this end, the study was divided
into two phases: The first was a general parametric study of
flat holograms operating in a reflective mode, see Section VI-B.
The principal parameters of interest were 1) the off-axis
angle, ϕ, and focal length, f, of the holographic element,
2) tilts and curvatures of the focal surfaces, and 3) the amount
of coma present.   From the information gained in this phase of
the study, a holographic configuration of optimum parameters
was chosen as the starting point for the second phase of the
study — the design of a complete head-up display.

66

R₁ = 25 in.

HOLOGRAM

EXIT PUPIL

ϕ

INTERMEDIATE
IMAGE

f

RELAY LENS
(CLOSE TO HOLOGRAM
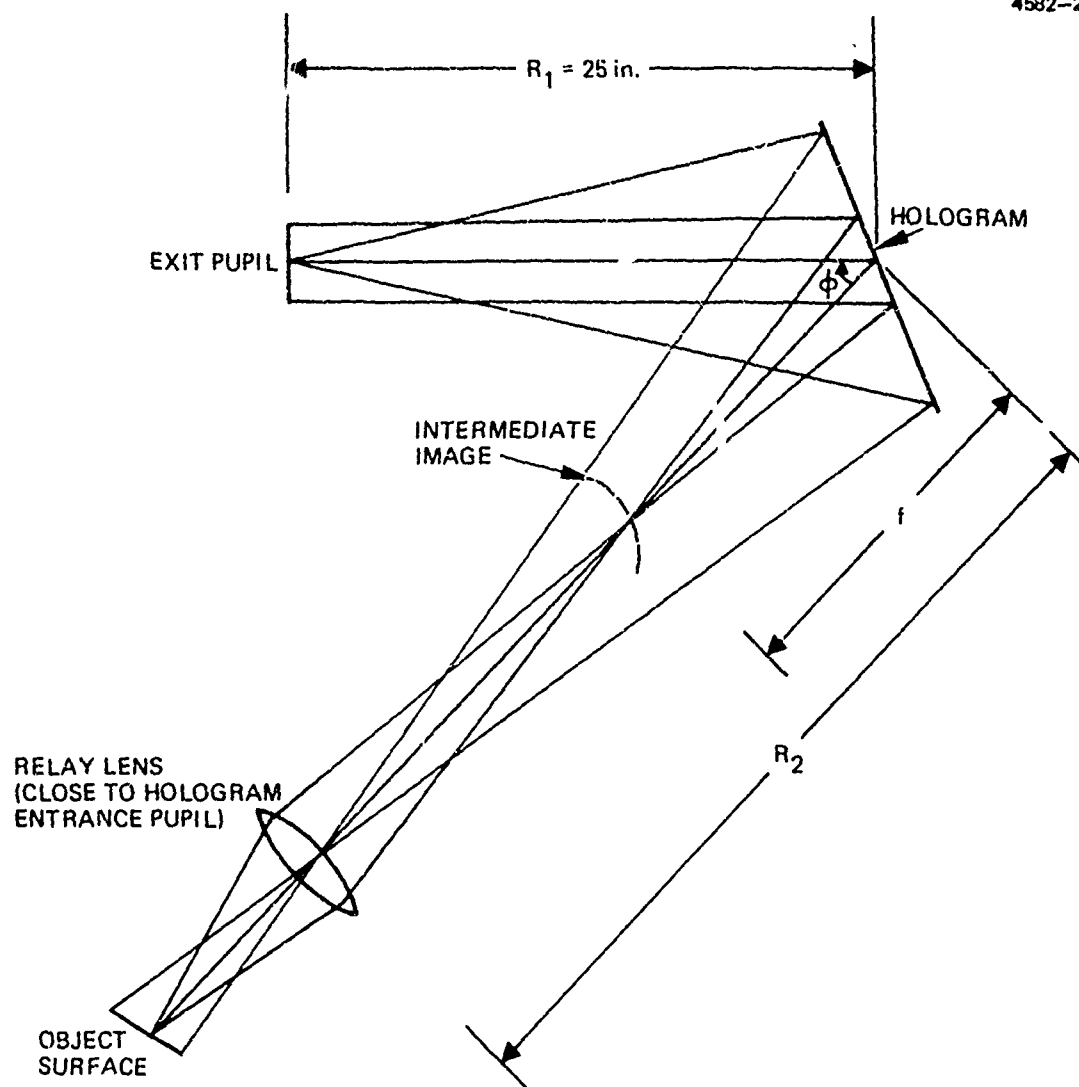ENTRANCE PUPIL)

R₂

OBJECT
SURFACE

Fig. 18. HHUD optical concept and paraxial considerations
in hologram parametric tradeoff.

VI.   Reflection Hologram Collimator/Combiner Design Study

A.   Introduction

2.   DESIGN OBJECTIVES AND RESULTS

> Pupil errors in the final configuration of the HHUD design
> were held to less than 5 mrad over the 25° FOV from a 3"
> high by 5" wide "racetrack" exit pupil at an eye relief of
> 25 inches.

Design objectives for the display are given in column I,
Table 8. The field of view is large ($\pm$ 12.5 deg.), as is the
exit pupil (3 in. x 5 in.). Performance objectives were in
the form of requirements for binocular disparity and collima-
tion error (or accuracy). The results of the design effort
are shown in column II, Table 8. The present design nearly
meets the requirements over the entire field of view and over
a "racetrack" shaped exit pupil of 5 in. major axis and 3 in.
minor axis. Larger errors, exceeding 5 mrad, exist outside
the "racetrack," i.e., in the extreme corners of the 3 in. x
5 in. rectangular pupil. This degradation at the outer
corners is thought to be a limitation imposed by the present
relay lens design rather than a property of the holographic
element. The effective f-number of the relay lens is
f/0.95 for the diagonal dimension of the pupil; this f-number
is very low, and it stretches the limits of the triplet
derivative used for the relay lens design.

The final configuration of the HHUD design has the following
additional principal features: (1) a curved folding mirror to
improve packaging and to reduce the relay lens size, and (2)
cylindrical and tilted surfaces in the relay lens to compen-
sate for aberrations in the holographic element. This design
evolved with no guidelines for a cockpit envelope and should
be treated as such. The geometry can be varied within limits
and can be configured to fit in aircraft with large cockpits
such as helicopters. Flat plate HHUD designs for fighter
cockpits would probably require giving up some vertical FOV
or exit pupil size.

Table 8. HHUD Optical Design Objectives and Results

Parameter	I. Objective		II. Value	
	Horizontal	Vertical	Horizontal	Vertical
Field of View, deg.	25	25	25	25
Exit Pupil, in.	5	3	5*	3*
Eye Relief, in.	25	25	25	25
System EFL, in.	9	9	9	9
System f-Number	1.8	3.0	1.8	3.0
Object Surface Diameter, in.	4	4	4	4
Object Surface Tilt, deg.	-	-	0	17.4
Hologram EFL, in.	-	-	14.9	14.9
Hologram Off-Axis Angle, deg.	-	-	0	43
Hologram Size, in.	-	-	~ 16	~ 15
Relay Lens Magnification	-	-	1.66	1.66
Relay Lens Size, in.	-	-	~ 5	~ 4
Resolution, mr.	1	1	< 1	< 1
Optical Efficieny	80%	80%	88%+	88%+
Binocular Disparity, mr.				
a) over central 15°	2.5	1.0	~ 2.0	~ 2.0
b) 15° to 25°	2.5	1.0	~ 2.5	~ 2.5
Collimation Error (accuracy), mr.				
a) over central 15°	1.0	1.0	~ 1.5	~ 1.5
b) 15° to 25°	1.0	1.0	~ 2.0	~ 1.5

*Nominal racetrack shape
+ Peak value; 60% average across pupil

VI.   Reflection Hologram Collimator/Combiner Design Study

B.   Parametric Study

1.   SCOPE OF THE PARAMETRIC STUDY

> The scope of the parametric study was defined by general
> paraxial considerations of the f# and size of the hologram
> and relay as related to the pupil locations and hologram
> focal length.

The scope of the parametric study was set by general paraxial
considerations. These considerations, as illustrated in Figure
18 are a) the location of the pupils and the hologram focal
length, b) the hologram and relay lens f-numbers, and c) the
diameter of the relay optics.

To maintain maximum efficiency over the entire field of view,
it is necessary to construct the hologram using point sources
located near the entrance and exit pupils to be used in the
display configuration. The distance form the exit pupil to
the hologram, R_1, is required to be 25 inches, see Table 8.
The entrance-pupil-to-hologram length, R_2, and the focal length,
f, are then related by

$$\frac{1}{f} = \frac{1}{R_1} + \frac{1}{R_2}$$

and the f-number of the hologram, F_H, is

$$F_H = f/D$$

where D is the exit pupil dimension. Further, the nominal size
of the relay lens, D_R, is determined by the size of the hologram
exit pupil; the effective f-number of the relay lens, F_R, is
determined by F_H and F_S where F_S is the overall optical system
f-number:

$$D_R = \frac{R_2}{R_1} D$$

$$\frac{1}{F_R} = \frac{1}{F_S} + \frac{1}{F_H}$$

Figure 19a shows generally how the f-number of the hologram
and the relay are related to R_2 and the hologram focal length,
f. The relay can be seen to be very fast for small R_2 (small f).

70

Figure 19b shows how large the diameter of the relay optics can get for large R_2 (large f).

With these facts in mind, the scope of the parametric study was defined in terms of two properties: The hologram focal length and the off-axis angle, ϕ. Holograms with focal lengths of 10, 12, 14, and 16 inches and off-axis angles of 20, 40, 60 and 80 degrees were investigated. Counting all possible combinations, the study involved 16 different configurations.
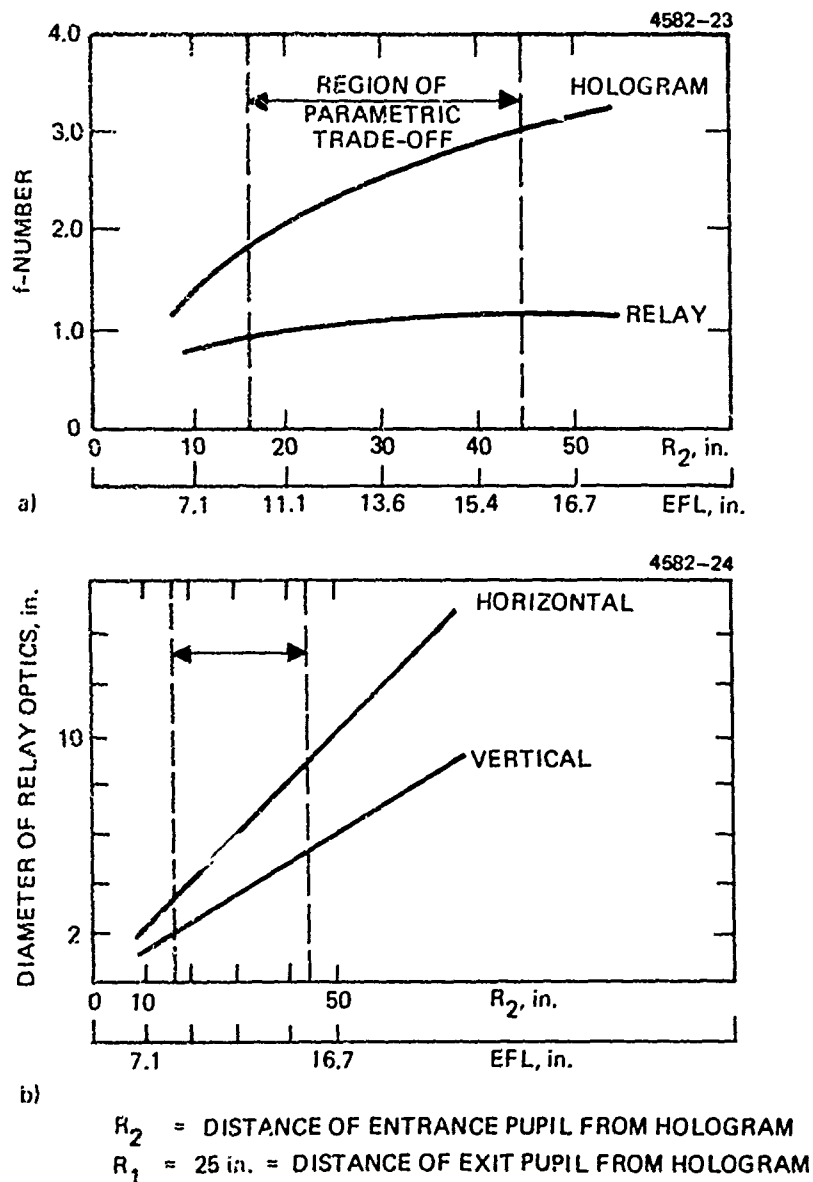

R$_2$ = DISTANCE OF ENTRANCE PUPIL FROM HOLOGRAM

R$_1$ = 25 in. = DISTANCE OF EXIT PUPIL FROM HOLOGRAM

Fig. 19. Paraxial interrelationships between (a) hologram and relay lens f-numbers and (b) hologram focal length and relay lens size.
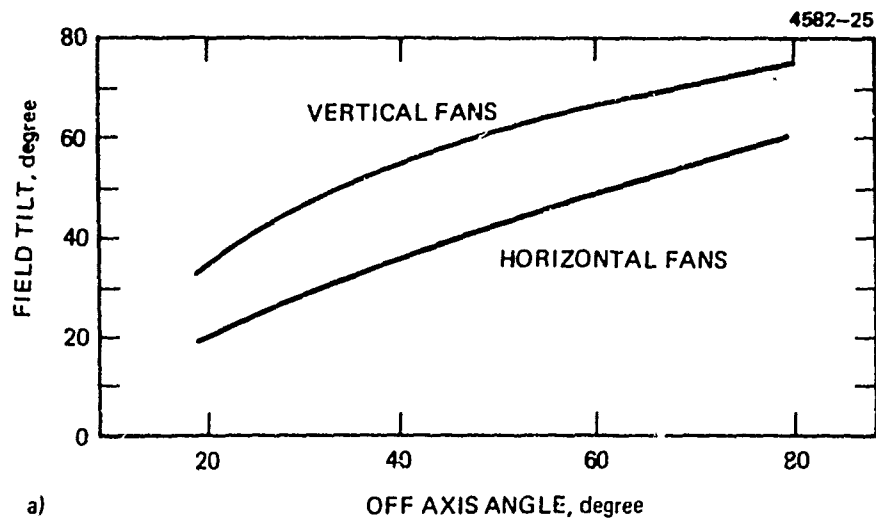
71

VI.   Reflection Hologram Collimator/Combiner Design Study

B.   Parametric Study

2.   FOCAL SURFACE TILTS

The focal surface tilts of off-axis holograms increase with
increasing off-axis angle and are nearly independent of focal
length.

Focal surface tilts of off-axis holograms in general have two
separate focal surfaces, one for fans of rays traced in the
plane of symmetry (horizontal) and one for fans of rays traced
in the plane of asymmetry (vertical). These two focal surfaces
are tilted with respect to the optical axis. The direction
of the tilts tends to bring the focal surfaces parallel to the
hologram. More importantly, the focal surface defined by
vertical fans is tilted at a greater angle than the surface
defined by horizontal fans. This disparity in tilts is quite
a problem because there can only be one tilt to the object
surface; the problem is ultimately solved with cylindrical
elements in the relay. Figure 20 shows that both focal
surface tilts increase with increasing off-axis angle and are
nearly independent of focal length.

4582-25

4582-26
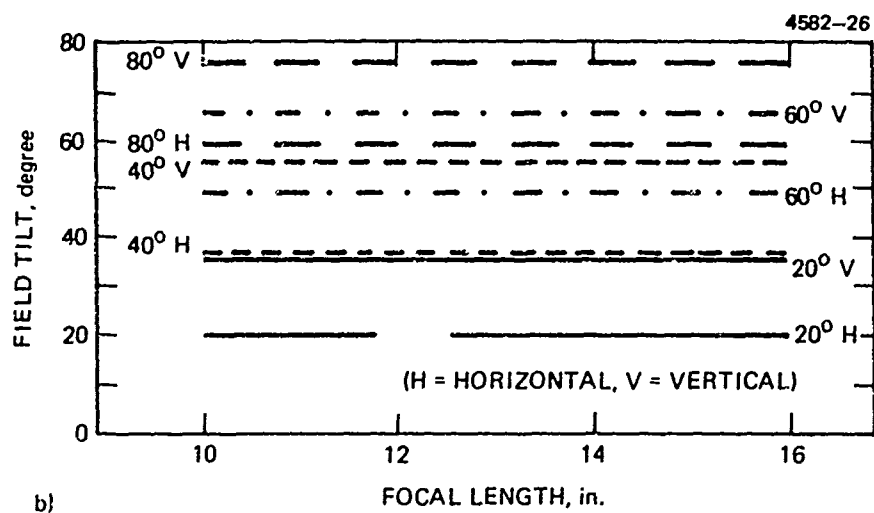
Fig. 20. Variation of field tilt. (a) off-axis
angle. (b) Focal length.

73

VI.   Reflection Hologram Collimator/Combiner Design Study

B.   Parametric Study

3.   FIELD CURVATURES

Reconciling field curvatures of the toroidal focal surfaces
is a major factor in choosing the holographic lens configura-
tion.

Field curvature — in addition to being tilted, the focal sur-
faces are generally toroidal, i.e., having different horizontal
and vertical curvatures. Reconciling these four curvatures
was a major factor in choosing a baseline holographic configura-
tion.

Figures 21 and 22 point out the wide variation in field
curvatures. However, it should be noted that the differences
between the four curvatures is minimized when the focal length
is in the region of 14 to 16 inches and the off-axis angle is
about 40 to 60 degrees. In particular, the curves shown in
Figures 21 and 22 intersect at certain points at which two of
the four field curvatures are equal. It is important to obtain
nearby equal field curvatures because large inequalities are
very difficult to correct in the relay lens.

Figure 23 is an alternate way of graphing the information about
field curvatures and makes use of the intersections of curves
on Figures 21 and 22. Reference to the legend on Figure 23 shows
that lines A, B, C and D represent conditions (values of focal
length and ϕ) where certain field curvatures are equal. Of
interest is the near-intersection of lines A, C and D. In
this region, three of the four field curvatures are equal.
This situation where three field curvatures are equal is also
obtained at the intersection of lines B and C. From an optical
design standpoint, this equality of field curvatures is very
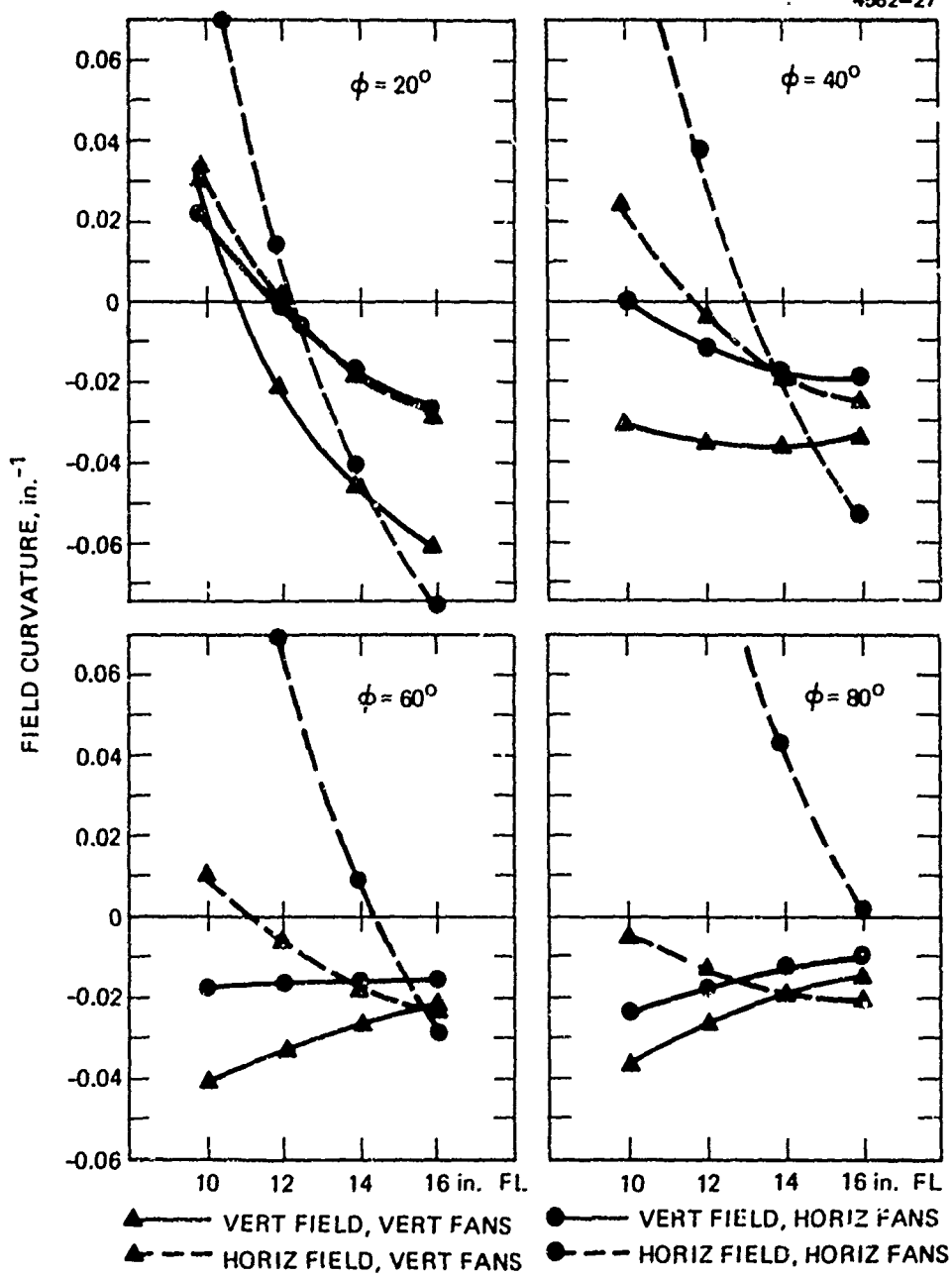desirable.

74

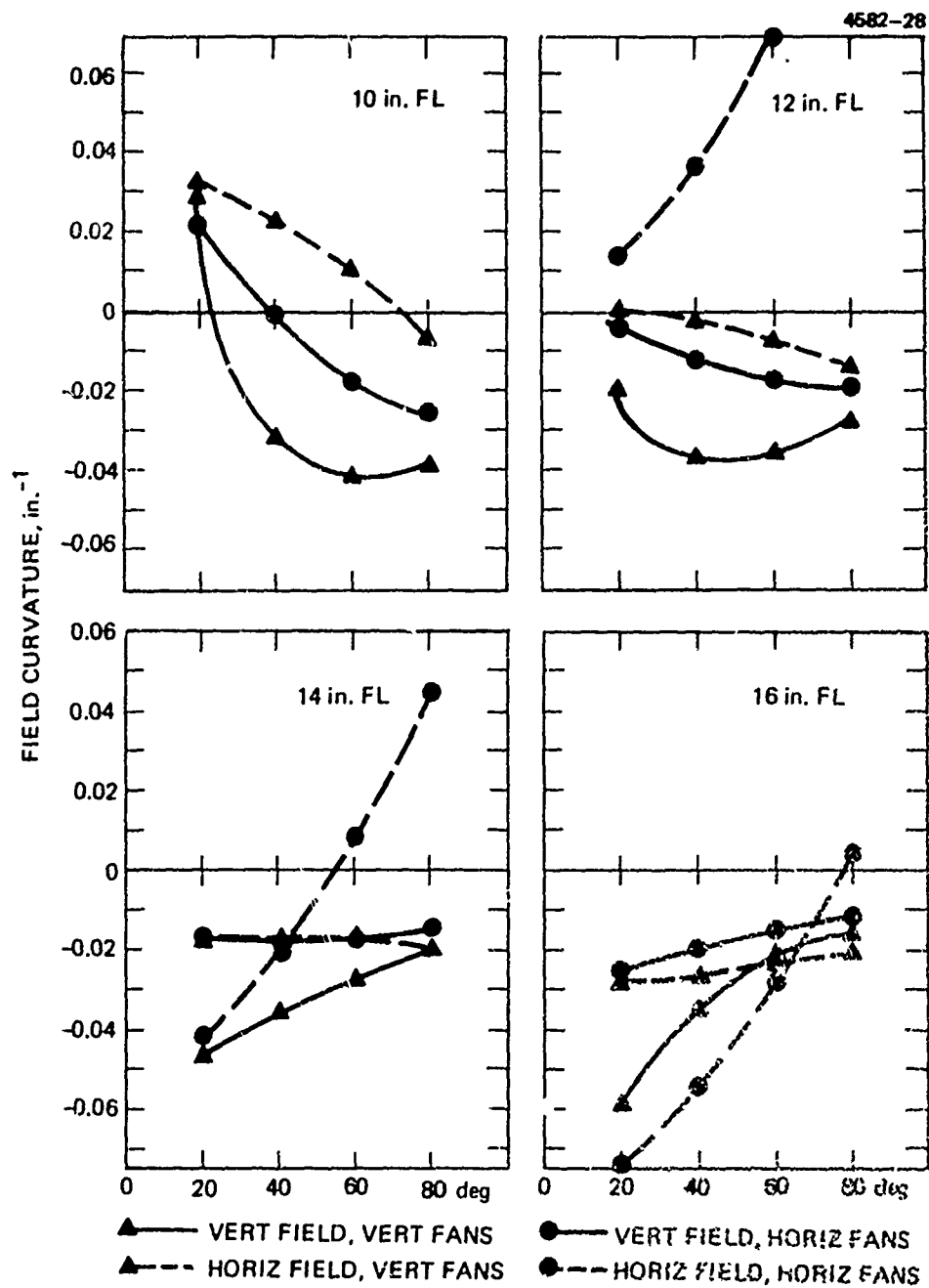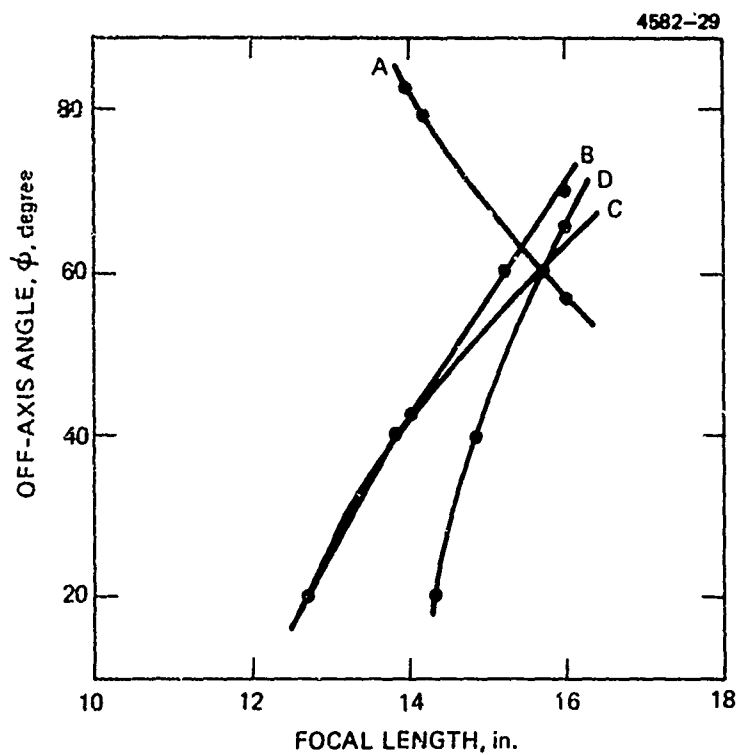Fig. 21. Variation of field curvatures with focal length for different off-axis angles, ϕ.

4582-28

Fig. 22.   Variation of field curvatures with off-
axis angle for different focal lengths.

76

A — HORIZONTAL AND VERTICAL CURVATURES DEFINED
BY VERTICAL FANS ARE EQUAL

B — HORIZONTAL AND VERTICAL CURVATURES DEFINED
BY HORIZONTAL FANS ARE EQUAL

C — HORIZONTAL CURVATURE DEFINED BY VERTICAL
FANS = HORIZONTAL CURVATURE DEFINED BY
HORIZONTAL FANS

D — VERTICAL CURVATURE DEFINED BY VERTICAL
FANS = HORIZONTAL CURVATURE DEFINED BY
HORIZONTAL FANS

Fig. 23.   Selection of near equal field
curvatures.

VI.   Reflection Hologram Collimator/Combiner Design Study

B.   Parametric Study

4.   ABERRATIONS

Coma, the dominant aberration in symmetric reflection holo-
grams, is minimized for small off-axis angles and large focal
lengths.

Aberrations — Coma is the dominant aberration, but some spher-
ical aberration is also present. The holograms considered
in the trade-off were constrained to operate in a symmetric
fashion, where the normal of the hologram bisects the off-
axis angle. This arrangement eliminates axial astigmatism
and minimizes dispersion. Small off-axis angles and large
focal lengths are indicated by Figures 24 for the minimization
of coma. Further, at large focal lengths the coma is nearly
constant across the field of view.

In addition to the above, there exists an aberration made
apparent by fans traced from horizontal object points. There
is a total lack of symmetry across the pupil of these fans,
which causes horizontal image errors for fans of rays traced
in the vertical section, and vertical image errors for fans
of rays traced in the horizontal section. These image errors
are usually small in concentric optical systems, but have to
be considered during the optimization of a highly off-axis
optical system. They were not considered as part of the
holographic element trade-off, but were compensated for during
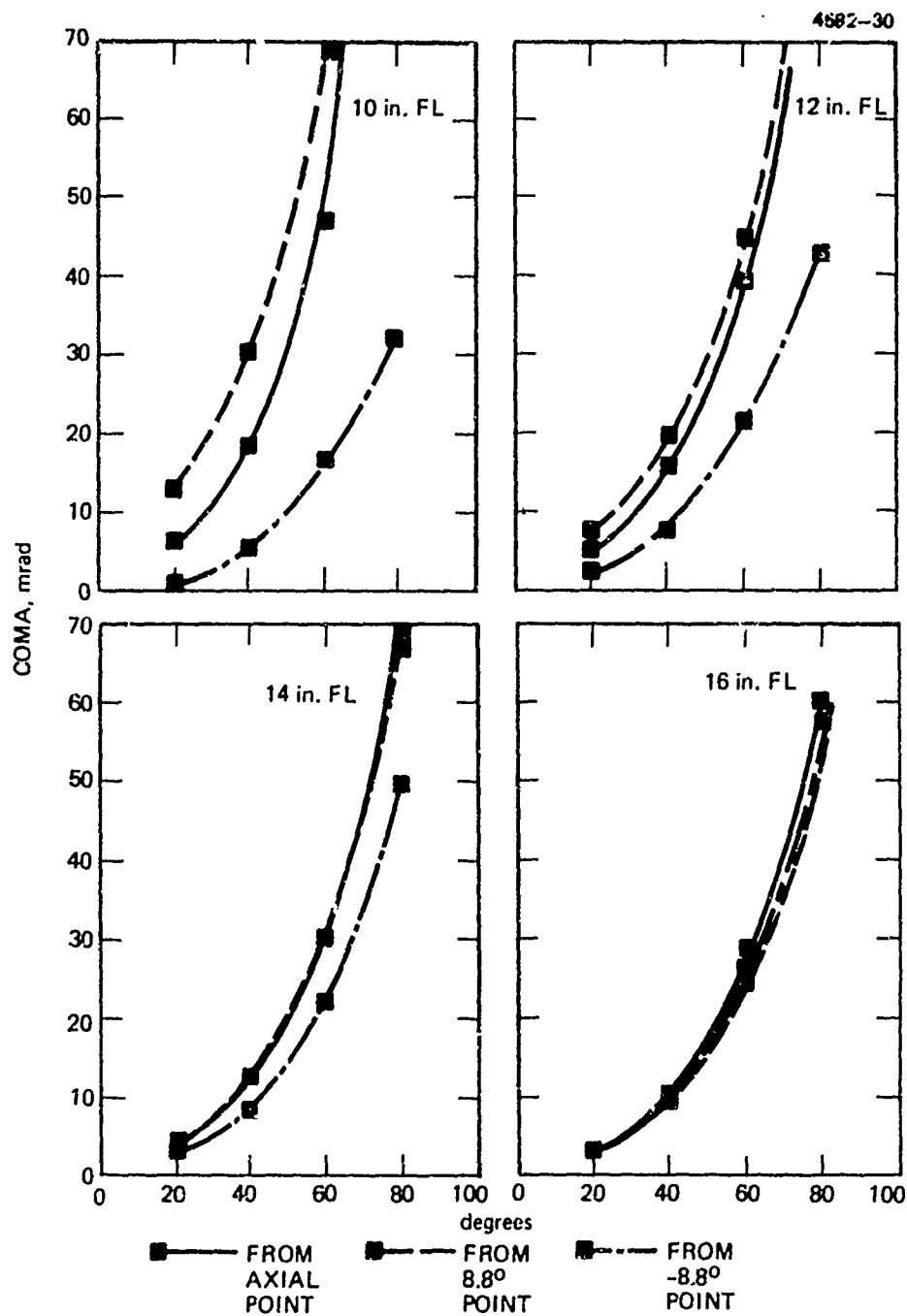the HHUD optical system design.

Fig. 24.   Variation of coma with off-axis angle for
           different focal lengths.

79

VI.   Reflection Hologram Collimator/Combiner Design Study

C.   Baseline Hologram

1.   PARAMETERS

The baseline hologram is a 43° off-axis symmetric reflection hologram lens with a focal length of 14.9 inches.

The parameters chosen for the baseline hologram are a focal length of 14.9 in. and an off-axis angle of 43°. Two of the four field curvatures are equal. Column I of Table 9 summarizes the properties of this baseline hologram. Figure 25a shows the pupils of the hologram along with intermediate focal surfaces formed by vertical fans.

While we were not constrained to any particular cockpit geometry in this design, it was reasonable to assume that (a) a fold would be needed in the optical path between the entrance pupil and the hologram, and (b) the large focal length implied an overly large relay lens. Using a mirror with some optical power to make this fold, we were able to reduce the pupil-to-hologram distance from 36.9 inches to 29.9 inches. Another result of the addition of the folding mirror, and one having an even greater impact on the design, was the reduction in the size of the relay elements from approximately 7.5 inches to about 5 inches. Reference to column II of Table 9 shows that the curved folding mirror produced other small changes and indeed helped the balancing of field curvatures. The hologram and folding mirror produced other small changes and indeed helped the balancing of field curvatures. The hologram and folding mirror are pictured in Figure 25b.

80

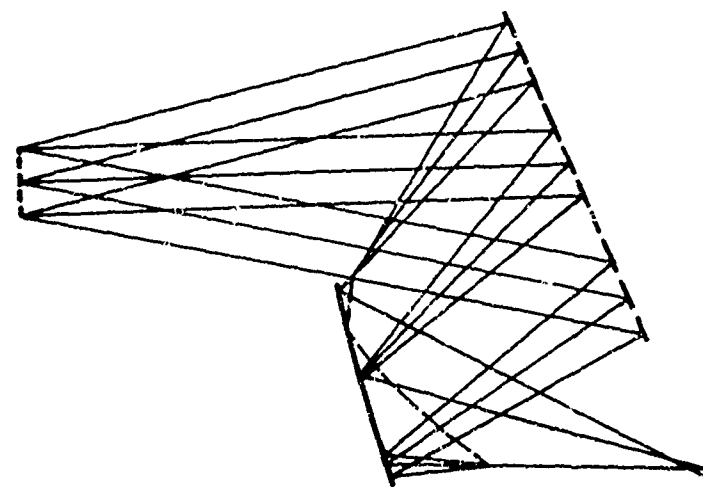TABLE 9. Properties of Baseline Hologram

Property	I Before Folding Mirror	II After Folding Mirror
Off-Axis Angle, deg.	43	43
Focal Length, in.	14.90	14.86
R_2, Entrance Pupil to Hologram, in.	36.9	29.9
Implied Relay Size, in.	∿ 7.5	∿ 5.0
For Vertical Fans		
Field Tilt, deg.	56.7	56.6
Vertical Radius, in.	29.6	20.6
Horizontal Radius, in.	46.2	23.7
For Horizontal Fans		
Field Tilt, deg.	37.5	38.2
Vertical Radius, in.	53.6	25.7
Horizontal Radius, in.	29.8	19.7

EXIT
PUPIL

HORIZONTAL FAN
FOCAL SURFACE

VERTICAL
FAN FOCAL
SURFACE

ENTRANCE PUPIL
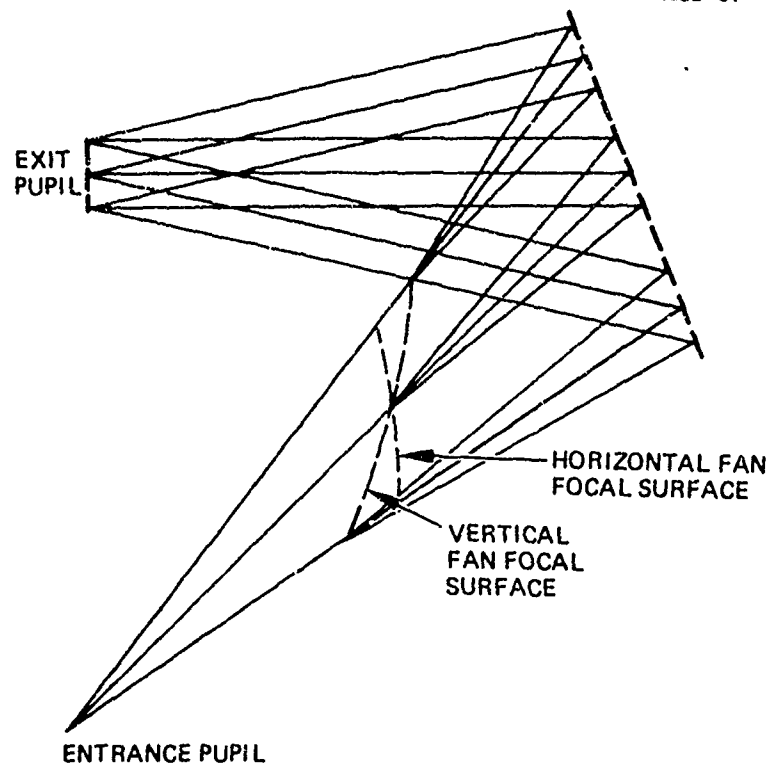
A)   WITHOUT FOLDING MIRROR

4582-32

B)   WITH FOLDING MIRROR

Fig. 25.   Vertical section of hologram.

VI.   Reflection Hologram Collimator/Combiner Design Study

C.   Baseline Hologram

2.   GEOMETRICAL ABERRATIONS

> The geometrical aberrations, primarily coma, of the baseline
> hologram is approximately 13 mrad on axis.

The geometrical aberrations of the baseline holographic
configuration are given in Figures 26a and 26b. As pre-
viously mentioned, coma dominates, amounting to about 13 mrad
on axis. The aforementioned lack of symmetry for horizontal
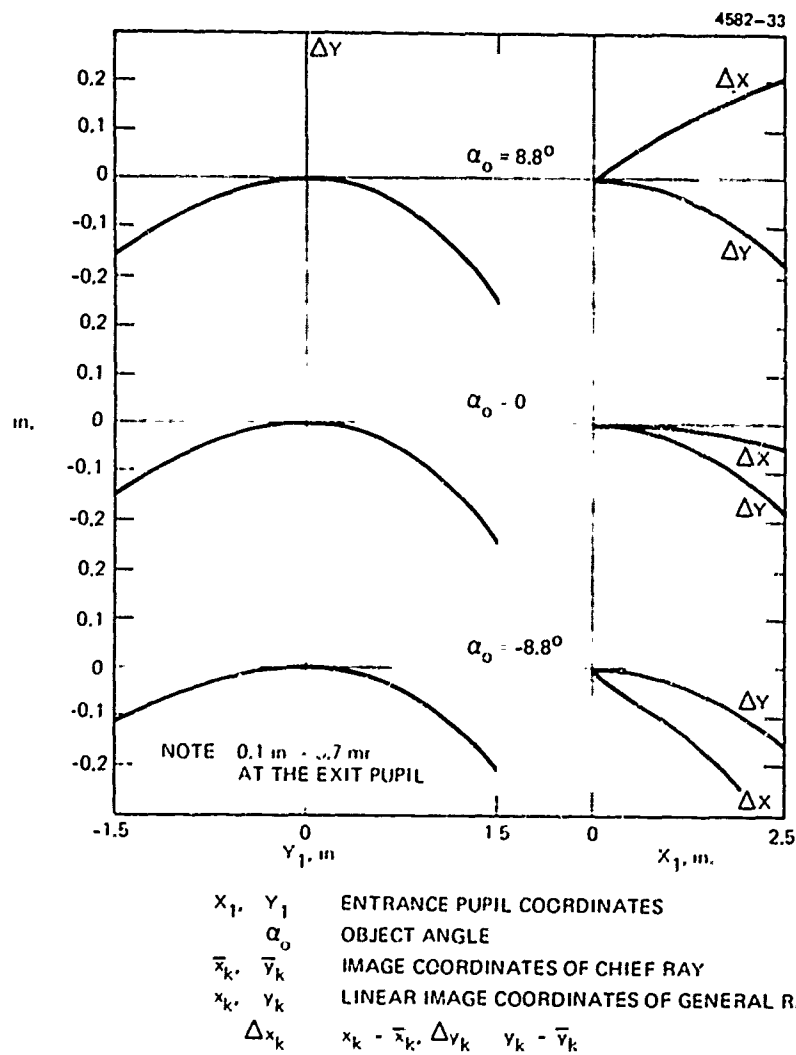field points is clearly shown in Figure 26.

84

Preceding page blank

4582-33

X_1, Y_1 ENTRANCE PUPIL COORDINATES
α_o OBJECT ANGLE
$\bar{x}_k, \bar{y}_k$ IMAGE COORDINATES OF CHIEF RAY
x_k, y_k LINEAR IMAGE COORDINATES OF GENERAL RAY
Δx_k $x_k - \bar{x}_k, \Delta y_k$ $y_k - \bar{y}_k$

Fig. 26(a). Geometrical aberrations of baseline hologram for vertical field angles, α_o.
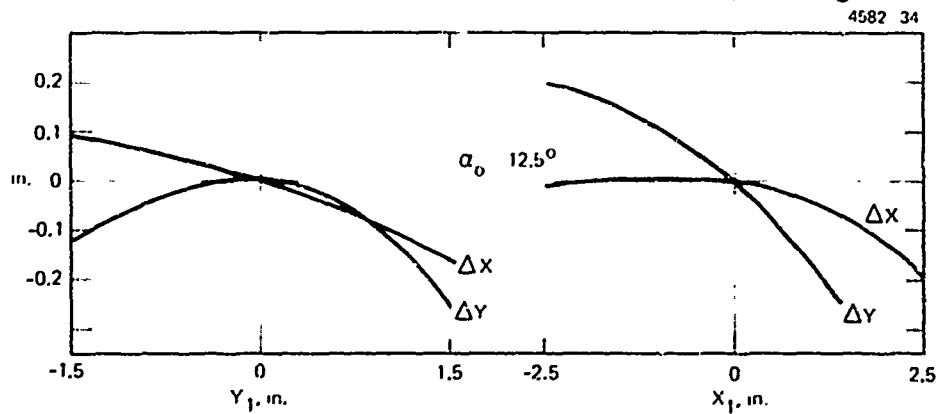
Fig. 26(b). Geometrical aberrations of baseline hologram for horizontal field angle of 12.5 degrees.

85

VI.   Reflection Hologram Collimator/Combiner Design Study

C.   Baseline Hologram

3.   CONSTRUCTION BEAMS

The baseline hologram is constructed with point sources centered at the entrance and exit pupil of the HUD system.

The hologram is constructed using two point sources centered at the desired pupil locations. The beams associated with these points can be termed the reference beam and the object beam. The holographic element construction optics are shown in Figure 27. The reference beam simply diverges from point R located at the exit pupil. The object beam converges to point 0 at the entrance pupil. The f/1, 36 inch EFL spherical mirror in the object beam and the cylindrical elements in the object beam were designed, specified, and procured as part of Phase 2 of the Flyable Hologram Lens Development Program.[3] These cylindrical elements are used to correct aberrations inherent in the off-axis use of the spherical mirror so that the aberrations in the object beam are insignificant.
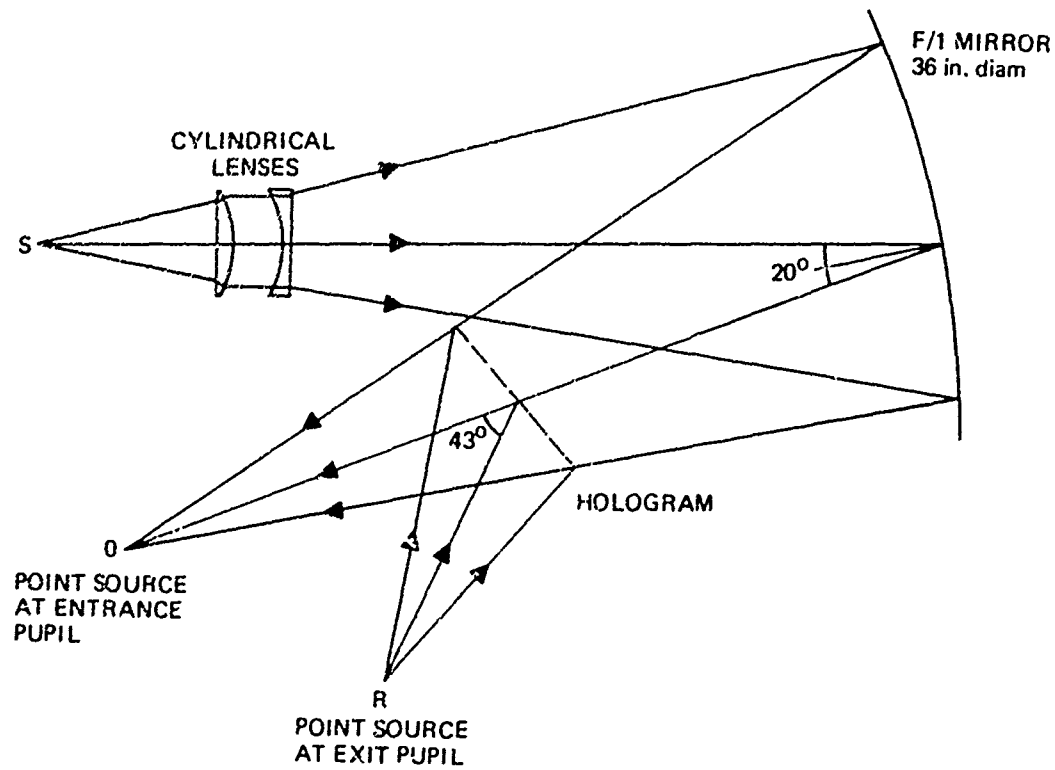
4582-35

Fig. 27. Holographic element construction optics.

87

VI.   Reflection Hologram Collimator/Combiner Design Study

D.   HHUD Relay Lens Design

1.   PRELIMINARY DESIGN

A Cooke triplet was chosen as a starting relay lens form used
to image the object plane onto the focal surface of the
hologram.

A relay lens is necessary to image the object plane onto the
focal surface of the hologram. While the object plane may be
either the diffusing screen of a laser spot scanner or the
CRT display, exact method of display has little bearing on the
design beyond the assumption of monochromaticity. Paraxial
calculations showed that the relay lens must have those pro-
perties listed in Table 10. The relay lens is somewhat fast
as was foreseen. A derivative of a Cooke triplet was chosen
as a starting point (Figure 28), and the relay lens was
optimized to roughly a 3 mrad system using a combination of
3rd order, 5th order, and real-ray aberrations. Figure 29
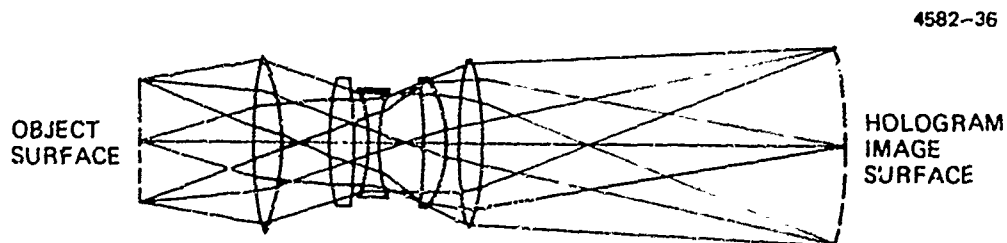shows the geometrical aberrations of this interim relay.

4582-36

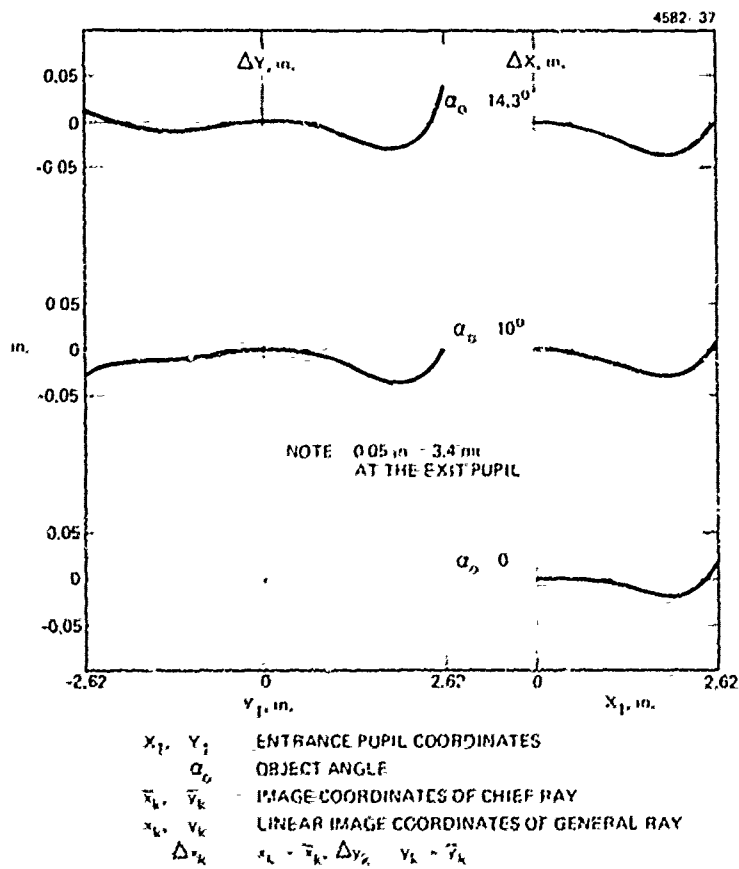Fig. 28. Preliminary design of the relay lens.

88

Fig. 29. Geometrical aberration at the inter-
mediate image of the relay lens.

Table 10

Paraxial Properties of the Relay Lens

Characteristic	Value
Distance from Hologram,	29.9
Magnification	1.66X
Focal Length, in.	5.64
f-Number	
Horizontal	1.13
Vertical	1.88
Diameter of Optics, in.	5
Object Surface Size, in.	$\sim$ 4

VI.   Reflection Hologram Collimator/Combiner Design Study

D.   HHUD Relay Lens Design

2.   OPTICAL SYSTEM DESIGN OPTIMIZATION

> Optical system design optimization is performed on head-up
> display configuration, the combination of the baseline
> hologram geometry with a preliminary relay lens design.

At this point, with the hologram and relay lens designs
established separately, what remained was to combine them in
the head-up display configuration and perform the detailed
optical system design optimization. Merely placing the relay
lens at the entrance pupil of the hologram neglects the
fact that the hologram has two separate image surfaces tilted
at different angles. A method is needed by which the two could
be made to coincide. It is preferable to find a means of
controlling the focal surface defined by vertical fans, since
it is tilted at a greater angle.

The solution to this problem involves the use of cylindrical
lenses. A negative cylindrical lens was placed between the
folding mirror and the relay, just after the hologram image
surface, see Figure 30. It is tilted 22 degrees in the
direction opposite to the tilt of the hologram image surface.
Its orientation is such that the cylindrical axis is horizontal
and the element is much closer to the hologram image surface
at the bottom than at the top. The net effect is that the
lens exhibits power for vertical fans and acts to set the
focal surface (for vertical fans) in a more upright position.
The focal surface for horizontal fans is also affected some-
what, so that the superposition of the two surfaces results
in one which is tilted at approximately 45 degrees.

A second cylindrical lens, used to correct the astigmatism
introduced by the first, is placed between the fourth and fifth
elements of the relay lens; its cylindrical axis is also hori-
zontal. The resulting HHUD could be deemed a 12 mrad system
with coma as the dominant aberration.

The elimination of the large coma contribution and the final
optimization of the system are the next concerns. Again,
experience led us to believe that either decentering or tilting
relay elements and surfaces would help to bring down the amount
of coma. We determined that tilting surfaces offered a more
efficient means of correction than decentering them. We were
also able to "manually" approximate a solution well enough so
that the automatic optimization procedure of the computer
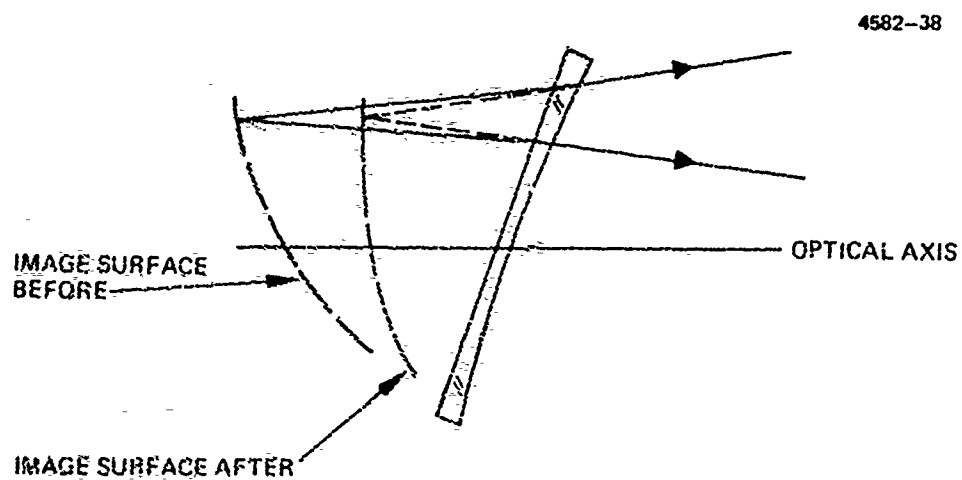program had no trouble converging.

82

4582-38

OPTICAL AXIS

IMAGE SURFACE
BEFORE

IMAGE SURFACE AFTER

Fig. 30. Matching field tilts using a tilted cylindri-
cal field lens.

VI.   Reflection Hologram Collimator/Combiner Design Study

D.   HHUD Relay Lens Design

3.   HHUD OPTICAL SYSTEM

Geometrical aberrations of the final HHUD optical system are
within 5 mrad along the 3 inches vertical and 5 inches
horizontal axis of the pupil.

The resulting HHUD optical design is depicted in Figures 31
and 32. The object surface tilt has decreased from 32.4 to
17.4 degrees. The geometrical aberrations are shown in
Figures 33a and 33b. With the possible exception of the
-12.5 degree vertical field point, it would appear that we
have a 1.5 to 2.0 mrad system. This conclusion is partially
misleading, in that Figures 33a and 33b represent only those
fans traced along the x and y axes of the pupil; no informa-
tion is given about the rest of the 3 inch by 5 inch rec-
tangle. A more detailed analysis covering the whole pupil
and using the specified errors of binocular disparity and
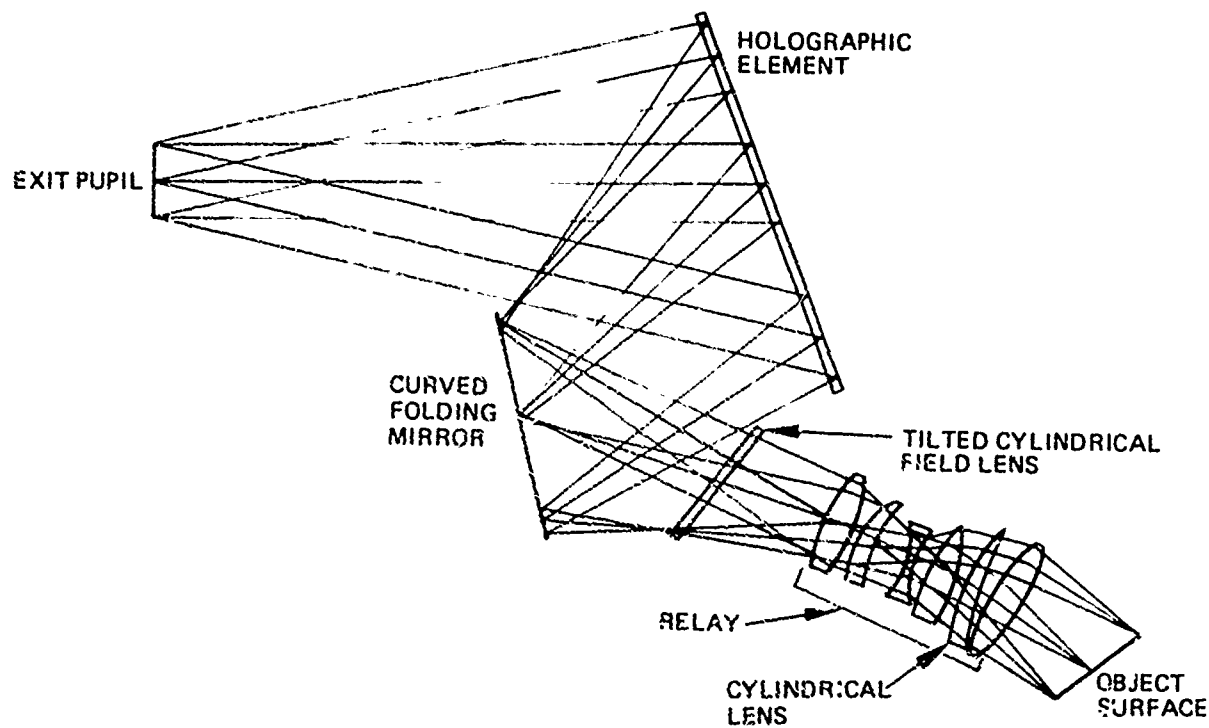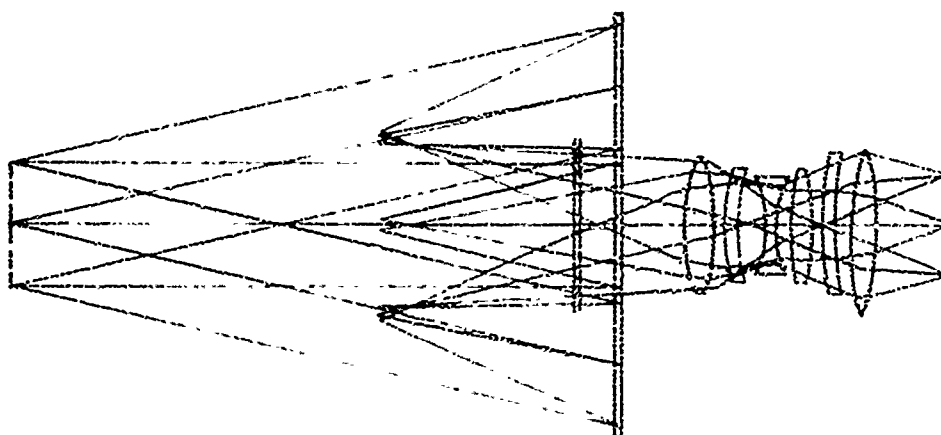collimation error was therefore performed.

4582-40

EXIT PUPIL

HOLOGRAPHIC
ELEMENT

CURVED
FOLDING
MIRROR

TILTED CYLINDRICAL
FIELD LENS

RELAY

CYLINDRICAL
LENS

OBJECT
SURFACE

Fig. 31.   Vertical section of HHUD.

4582-39

Fig. 32.   Horizontal section of HHUD.

95
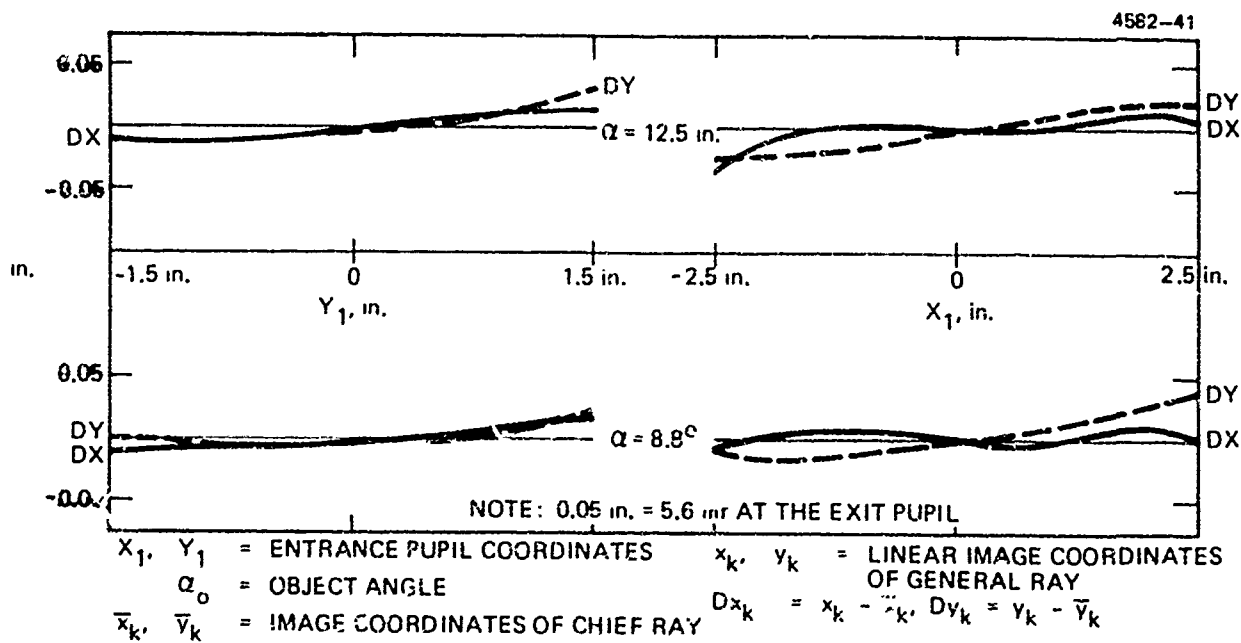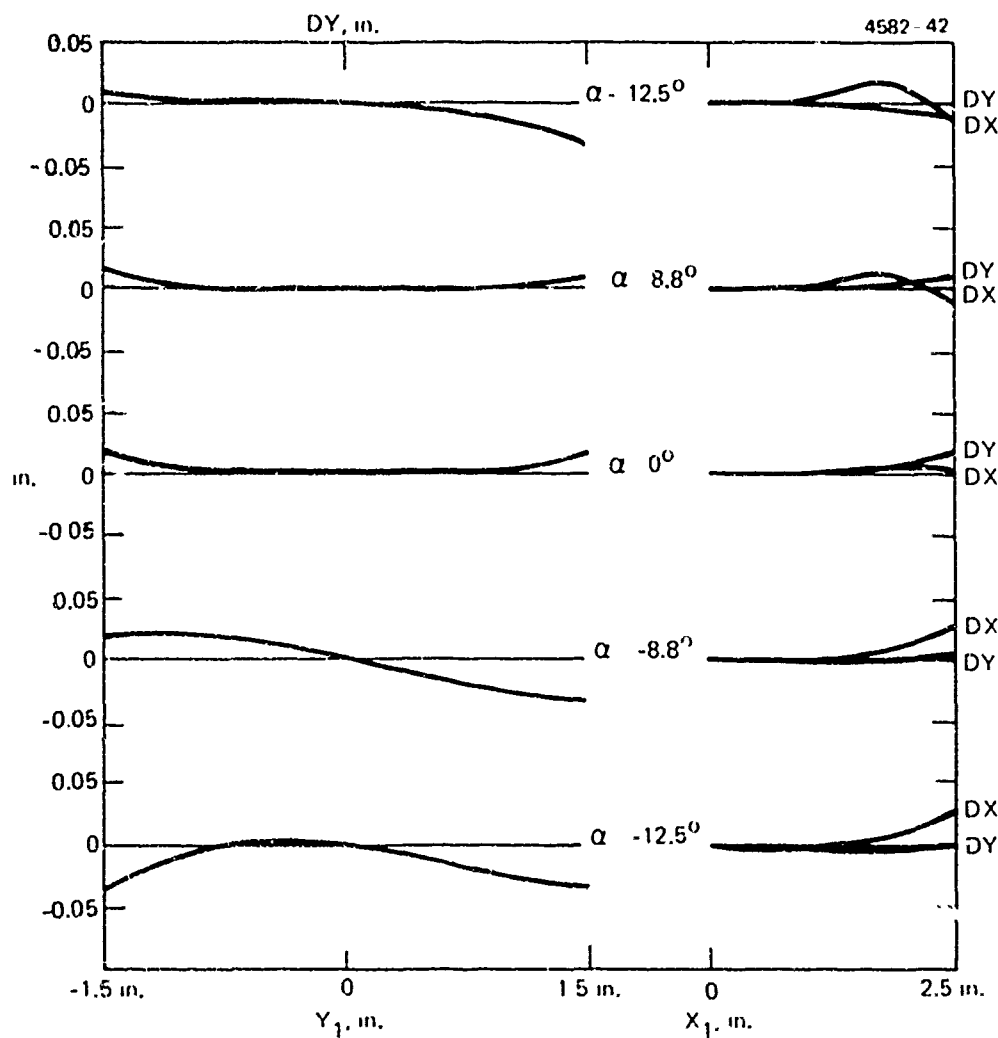
Fig. 33(a). Geometrical aberrations of hHUD (horizontal field
angles).

Fig. 33(b). Geometrical aberrations of HUD (vertical field angles).

VI.   Reflection Hologram Collimator/Combiner Design Study

E.   HHUD Performance Evaluation

1.   DEFINITION — BINOCULAR DISPARITY AND COLLIMATION ERRORS

Binocular disparity is a comparison of the image seen by the
left eye to that seen by the right eye. Collimation error is
a measure of the variation of image location.

Binocular disparity (BD) is a comparison of the image seen by
the left eye to that seen by the right eye. If $D\alpha$ and $D\beta$
denote the horizontal and vertical angular deviations of a
ray from the reference ray, and if "left" and "right" refer
to the eyes, then horizontal and vertical binocular disparity
are defined by (see Figure 34a):

$$BDX = D\alpha_{left} - D\alpha_{right}$$

$$BDY = D\beta_{left} - D\beta_{right}$$

Collimation error (CE), also called accuracy, measures the
variation of image location, for a given point in the image,
as the viewer's eye moves within the exit pupil. It is the
variation in the average position of the point which is seen
by both eyes and is defined by

$$CEX = (D\alpha_{left} + D\alpha_{right})/2$$

$$CEY = (D\beta_{left} + D\beta_{right})/2$$

The scheme used to evaluate these quantities over the whole
pupil and for the entire field of view is described below,
and is illustrated in Figure 34b. The first step is to choose
a field angle. The degree of symmetry depends on whether the
field angle is vertical or horizontal. For vertical field
angles the system exhibits bilateral symmetry: only half of
the pupil need be considered because the other half is
identical. For horizontal field angles there is no symmetry
and the performance across the whole pupil must be examined.

The second step is to trace rays across the pupil (or half

pupil) from the chosen field angle and evaluate the angular
image errors, Dα and Dβ. The rays are traced across the
pupil in a raster fashion: left (L) to right (R), top to
bottom along seven horizontal lines separated by 0.5 inch.
Binocular disparity and collimation error are calculated from
the above equations using two rays separated by an assumed
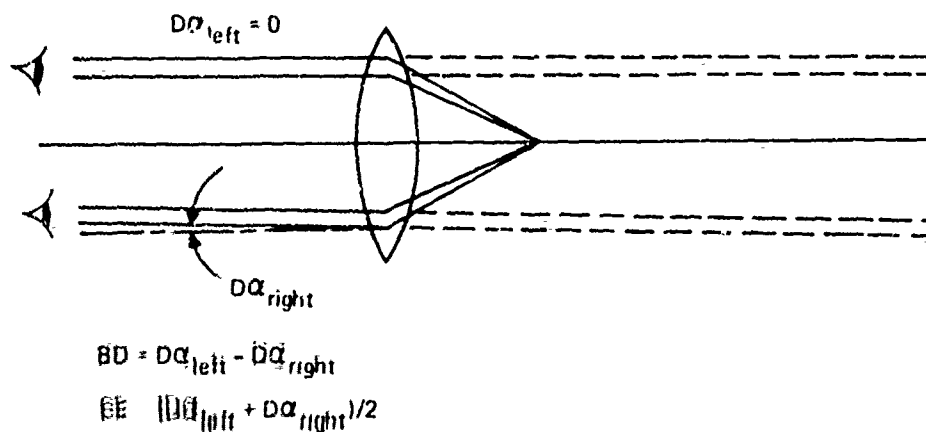interpupillary distance of 2.5 inches.

4582-43

$$BD = D\alpha_{left} - D\alpha_{right}$$

$$CE = |(D\alpha_{left} + D\alpha_{right})/2|$$

Fig. 34a. Definition of binocular disparity and col-
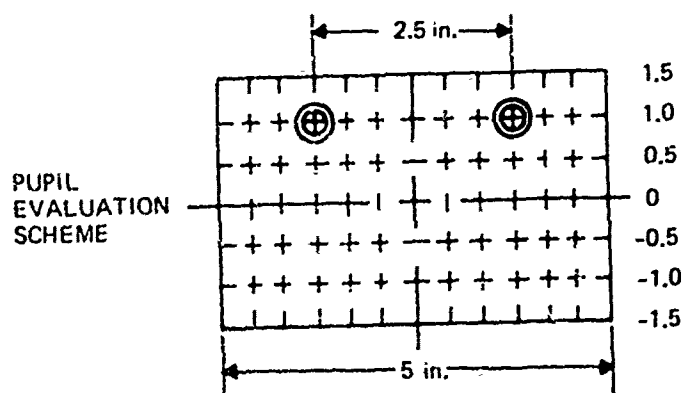limation error.

4582-44

Fig. 34b. Rays traced through the
exit pupil for the evalu-
ation of BD and CE.

99

VI.   Reflection Hologram Collimator/Combiner Design Study

E.   HHUD Performance Evaluation

2.   DATA – BINOCULAR DISPARITY AND COLLIMATION ERRORS

Over most of the 25° circular field and much of the 3" x 5"
exit pupil of the designed HHUD system, pupil errors are within
1 or 2 mrad.

One can consult Figure 35 and find values for binocular dis-
parity and collimation error, both horizontal and vertical.
Each figure gives data for one field angle and sufficient eye
positions to cover the whole pupil. Out of this large
amount of information, some conclusions become clear:

   a.   Over most of the field and much of the pupil, these
        curves agree with the geometrical aberrations shown
        in Figure 33a and b, i.e., that the system exhibits
        1 to 2 mrad of error.

   b.   Close inspection of Figure 35 shows that the signi-
        ficant departures from the 1 to 2 mrad level occur
        generally for the corners of the pupil. This is
        true for all field points.

To achieve the specified performance over the entire 3 x 5 inch
rectangular pupil seems unlikely with the present design.
It is therefore recommended that a racetrack shaped pupil be
used; this pupil would have extreme dimensions of 3 inches
vertical by 5 inches horizontal, but would not include the
corners of the 3 x 5 inch rectangular pupil. As was mentioned
previously, the drop in performance in the corners of the
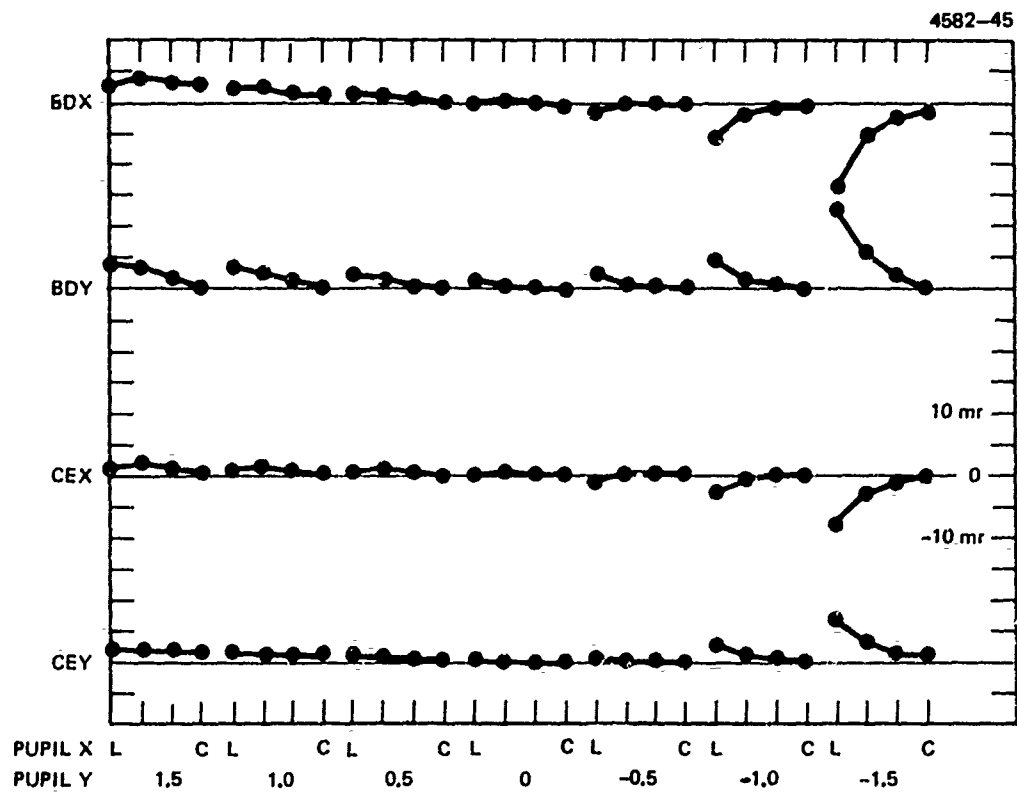pupil is believed to be a limitation of the relay lens design
form.

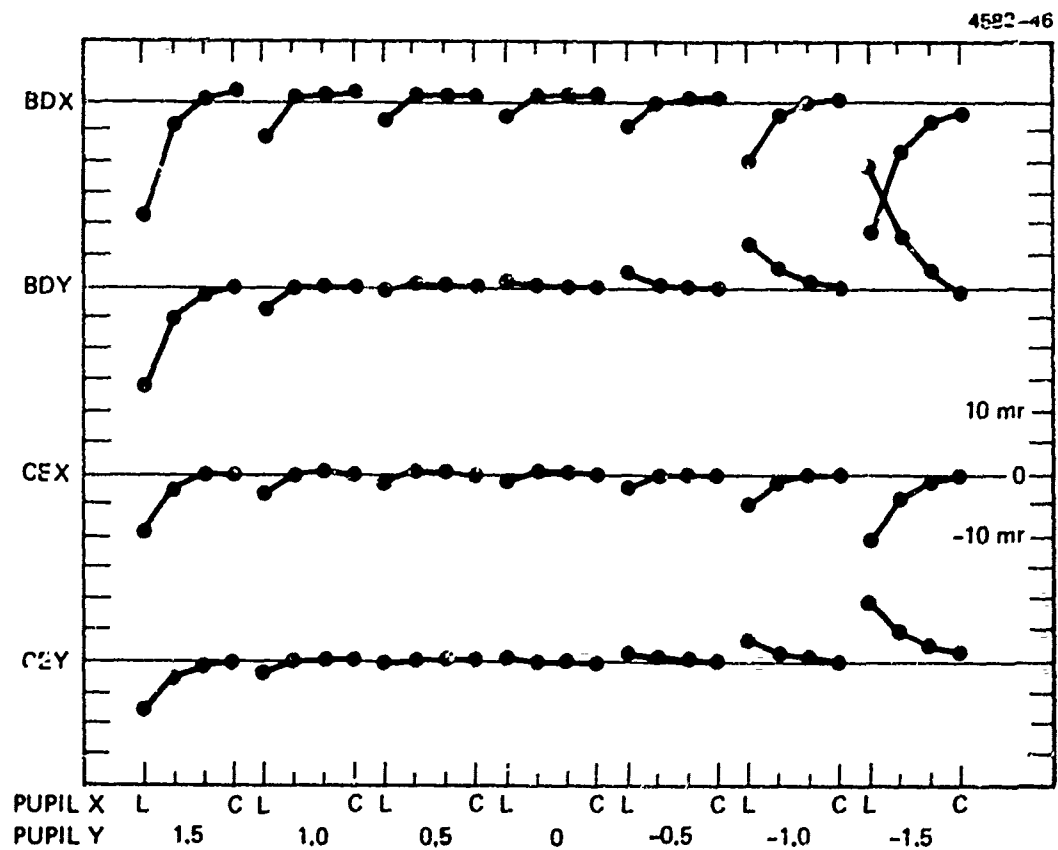Fig. 35. Binocular disparity (BD) and collimation error (CE) on axis.

101

Fig. 35. Binocular disparity (BD) and collimation error (CE) at vertical field angle of 8.8 degrees.

Fig. 35. Binocular disparity (BD) and collimation error (CE) at vertical field angle of 12.5 degrees.

Fig. 35. Binocular disparity (BD) and collimation error (CE) at vertical field angle of -8.8 degrees.
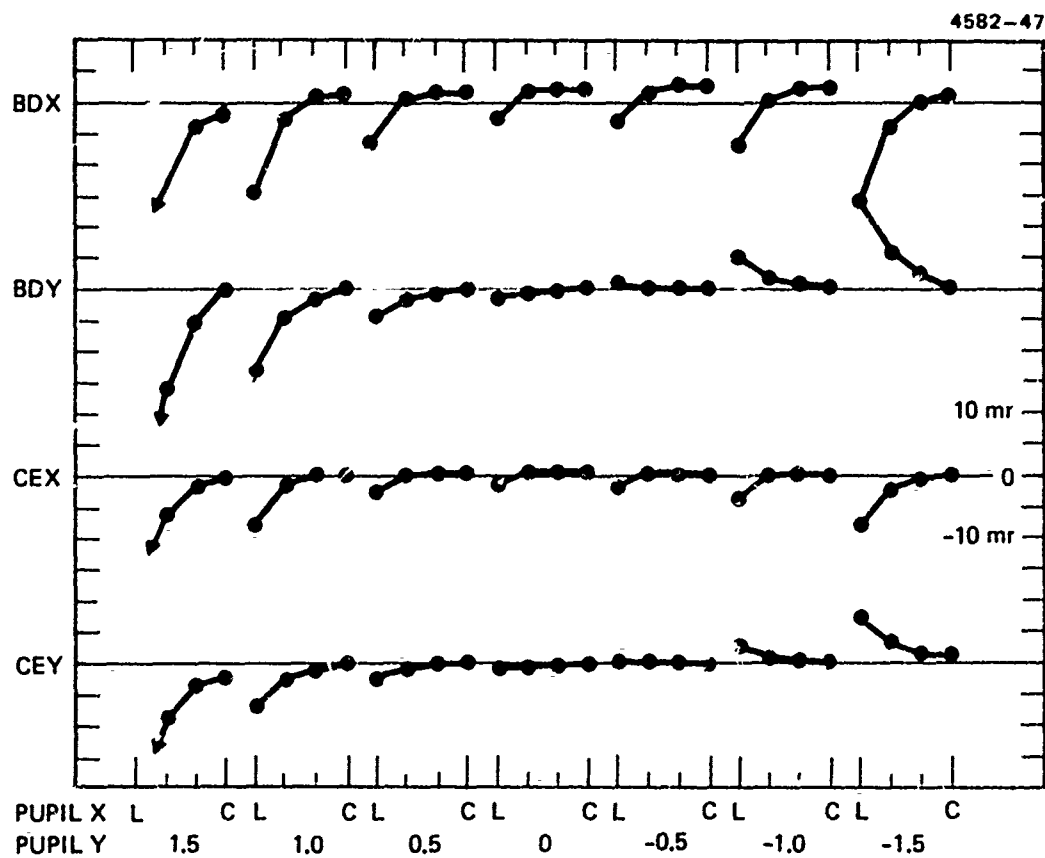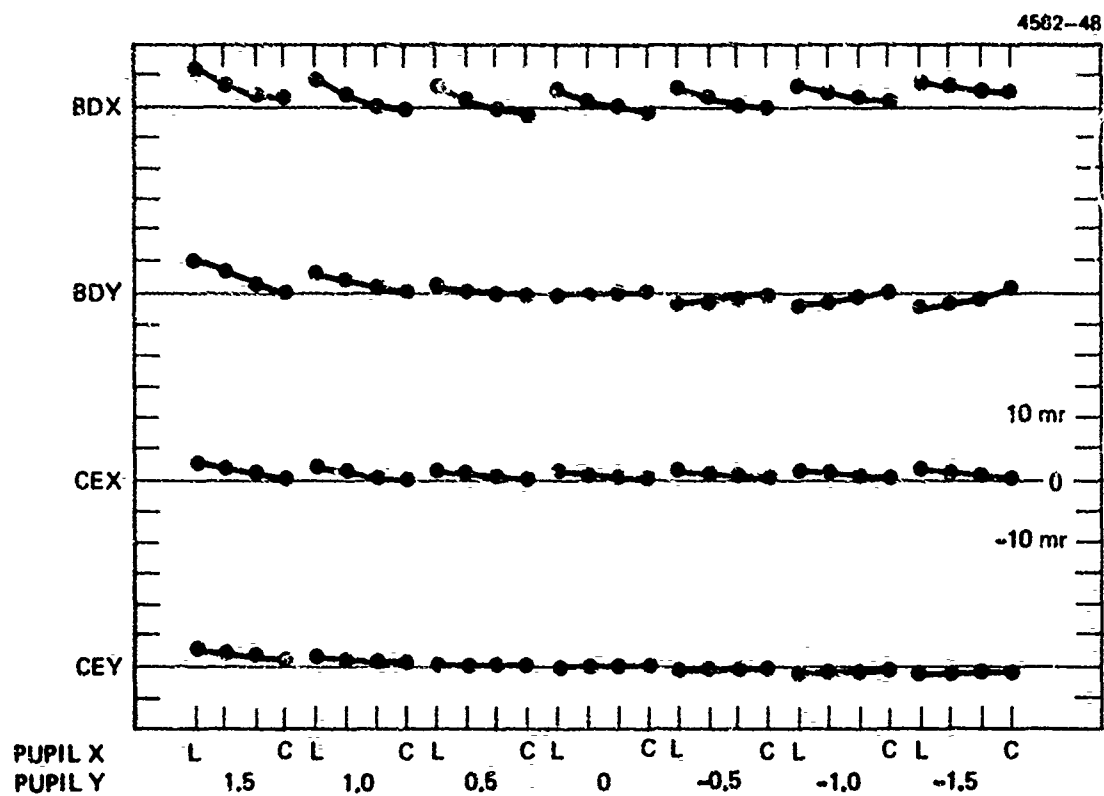
4582-48

Fig. 35. Binocular disparity (BD) and collimation errors (CE) at vertical field angle of -12.5 degrees.
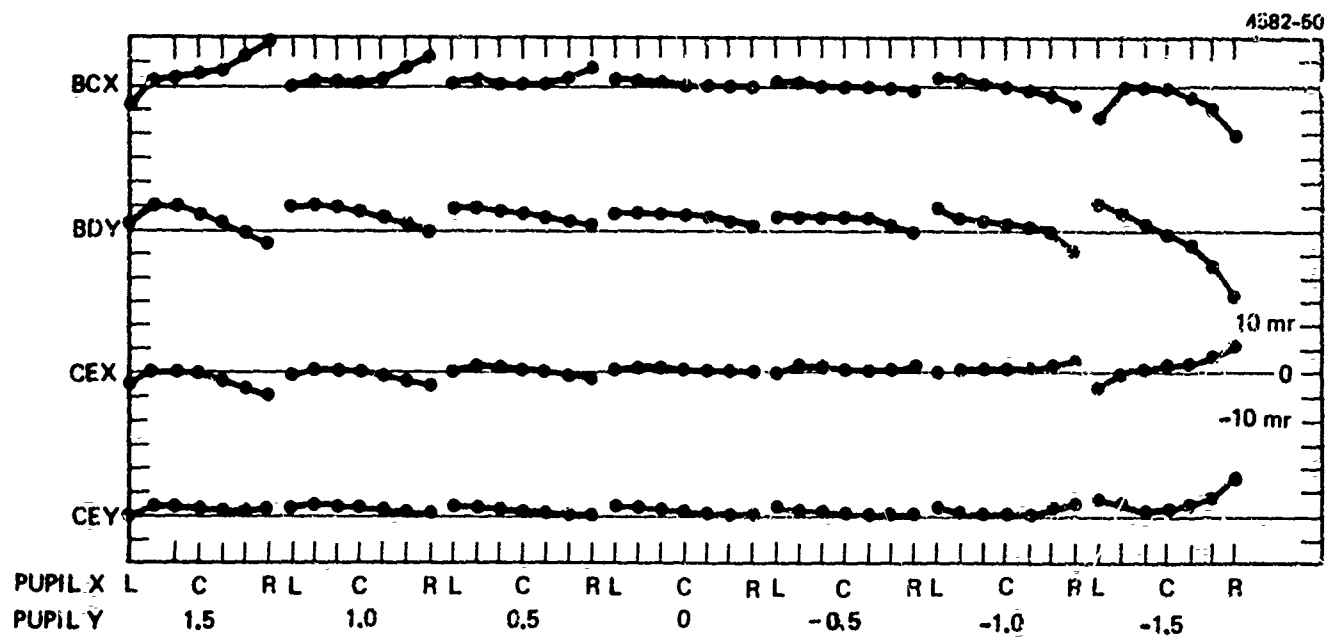
Fig. 35. Binocular disparity (BD) and collimation error (CE) at horizontal field angle of 8.8 degrees.
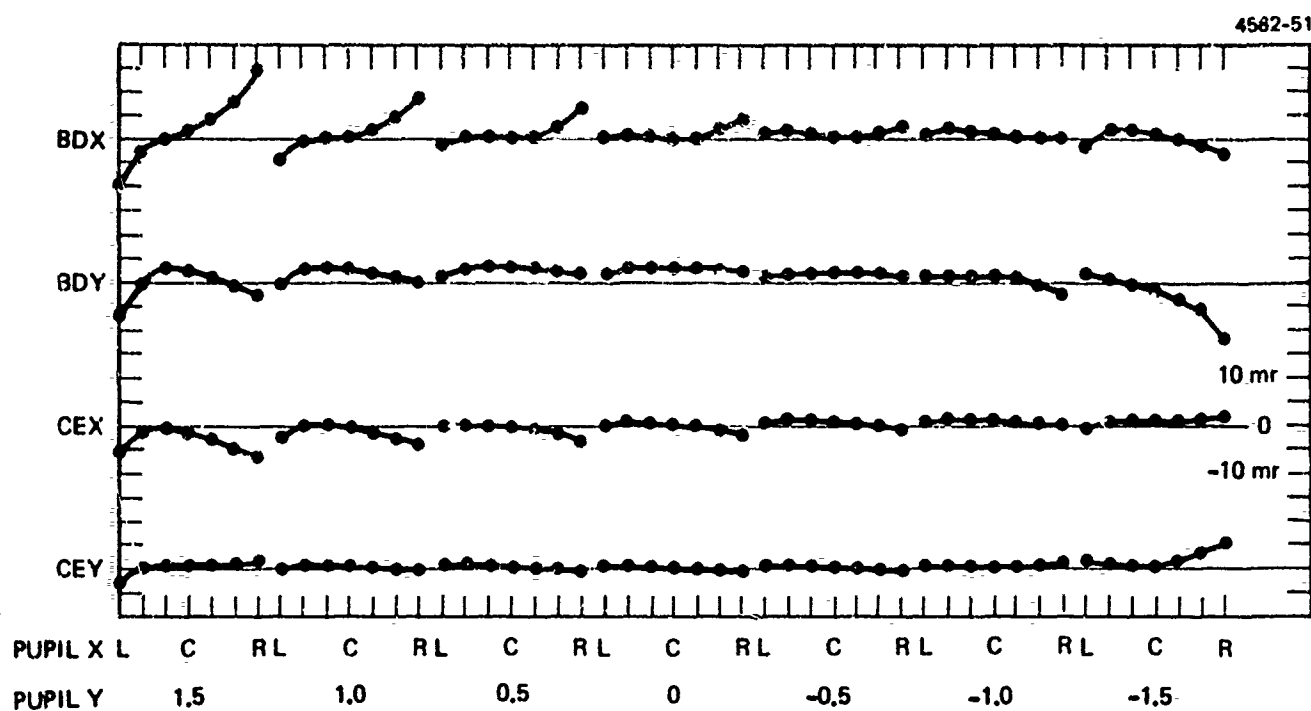
Fig. 35.   Binocular disparity (BD) and collimation error (CE) at horizont-
al field angle of 12.5 degrees.

VII. T90-N8-21.9 Transmission Hologram Lens

1. SYSTEM PARAMETER

> T90-N8-21.9 is a 90° off-axis, 8° asymmetric, transmission hologram lens element with a 34.5" eye relief and a 21.9" focal length.

The T90-N8-21.9 is a 90° off-axis, 8° asymmetric, transmission hologram lens element with an eye relief of 34.5" and a focal length of 21.9". The operating wavelength is 632.8 nm. The HUD configuration for which this hologram lens was con-structed is shown in Figure 36. The input to the display is the 4" square diffusing screen of the acousto-optical laser scanning system. Imaging is done at an astigmatism minimized intermediate image plane. This imagery will exhibit residual aberrations, because there is no aberration-correcting relay lens optical system.

The hologram aperture is 8" in diameter recorded on Kodak 120-01 silver halide emulsion and bromine bleached.[16] Instantaneous vertical field of view for one eye at the pupil center is + 4.40° and - 3.65°. Instantaneous horizontal field of view is ± 6.61°. Single binocular vision can be maintained for eyes at the 34.5" eye relief distance. For a nominal 63 mm separated pair of eyes centered at the exit

pupil, binocular FOV for each eye is + 4.16° and - 3.49° vertical, ± 4.56° horizontal. The relationship of the hologram size to the system parameters is shown in Figure 37.

108

4 in. SQUARE DIFFUSING SCREEN
OF ACOUSTO-OPTICAL
LASER SCANNER

27°

21.9 in. FOCAL LENGTH

34.5 in.
EYE RELIEF

EYE
POSITION

37°

8 in. diam
HOLOGRAM LENS

WINDSCREEN

37°
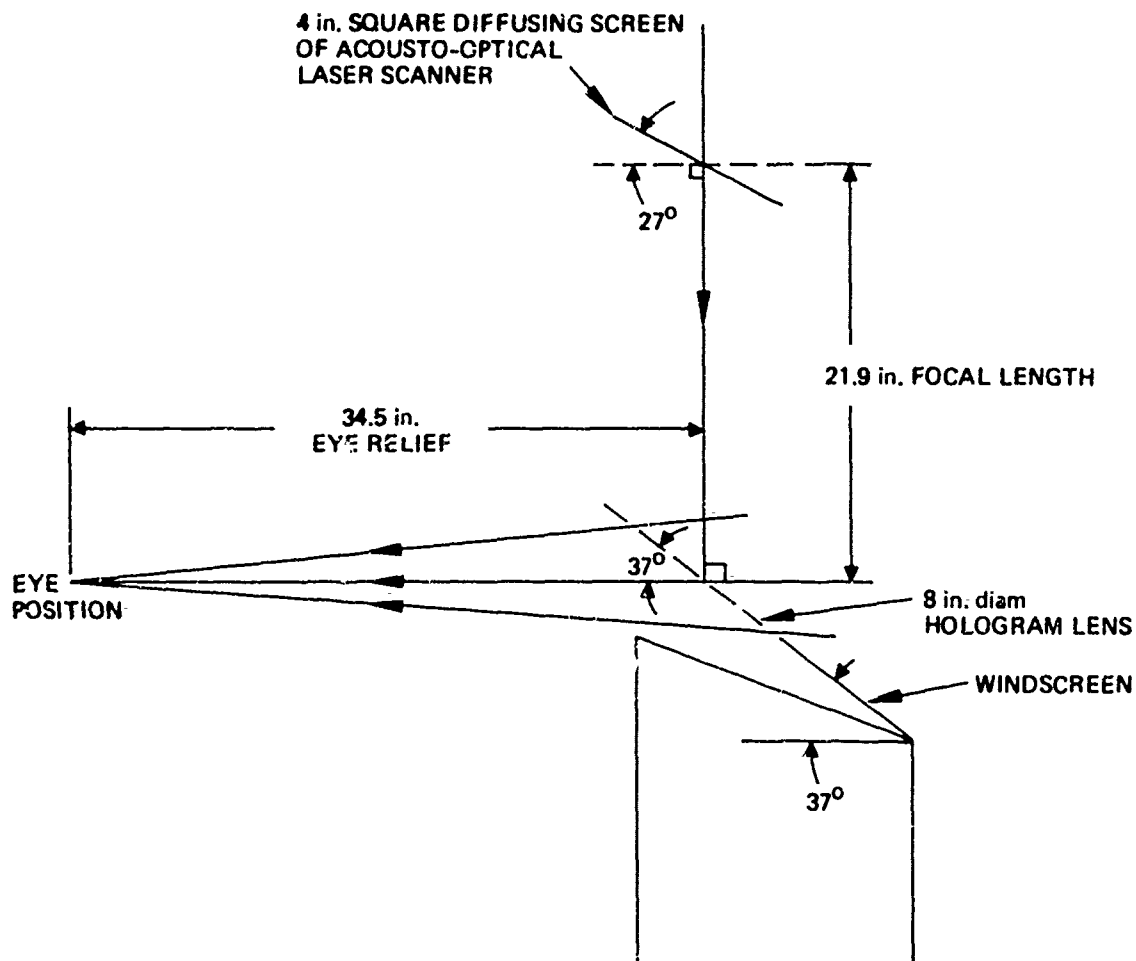
Fig. 36.   The T90-N8-21.9 HUD configuration.

4582-53

HORIZONTAL VIEW

HOLOGRAM

6.61°

34.5 in.

4 in.

a. MONOCULAR
VIEWING

6.61°

4 in.

EYE POSITION

4 in.

4.40°

34.5 in.

4 in.

3.66°

37°

VERTICAL VIEW

HOLOGRAM

4582-54

HORIZONTAL VIEW

HOLOGRAM

1.25 in.

4.56°

EYES
POSITION

34.5 in.

4 in.

1.25 in.

4.56°

4 in.

b. BINOCULAR
VIEWING

3.8 in.

4.16°

3.8 in.

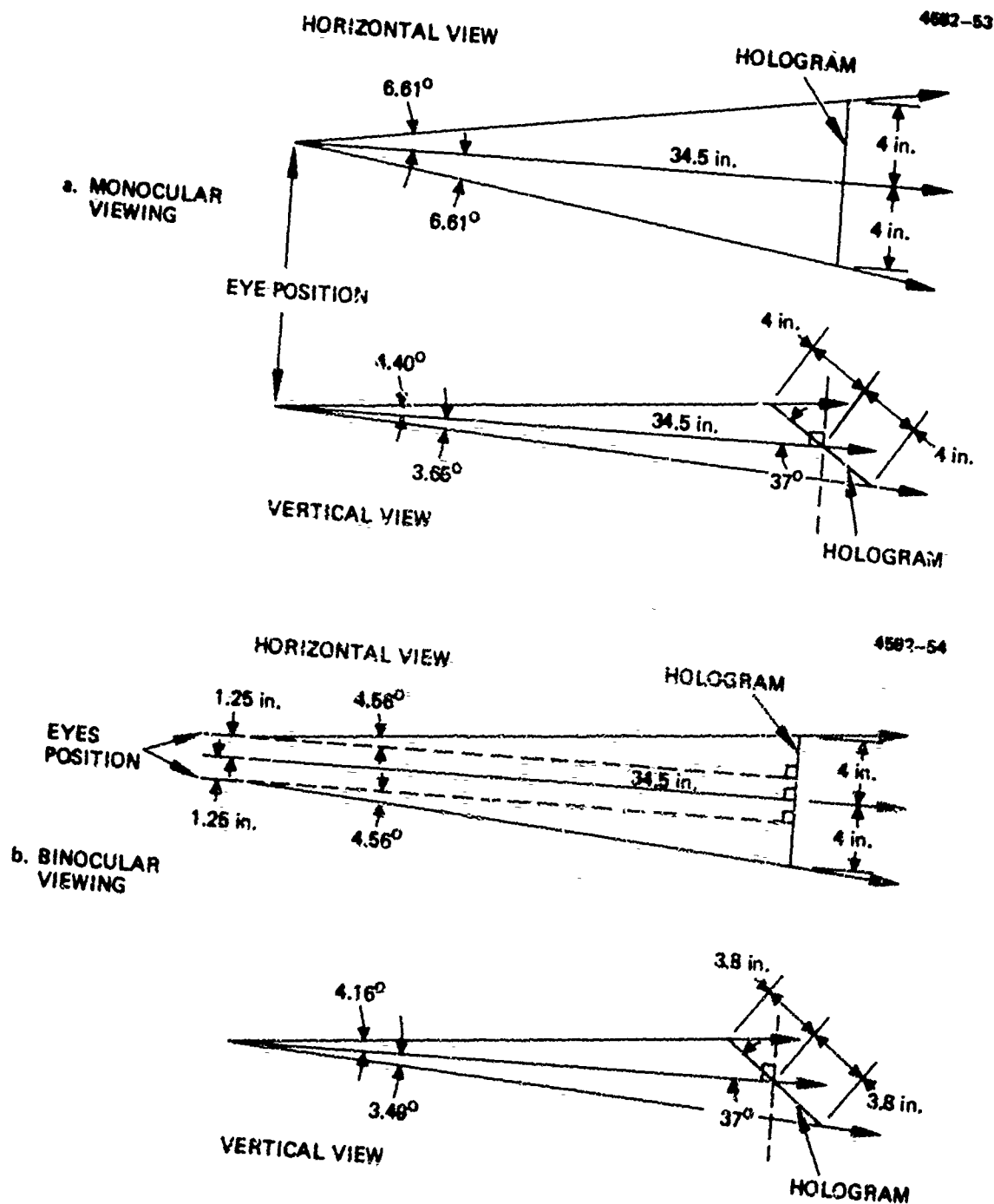3.49°

37°

VERTICAL VIEW

HOLOGRAM

Fig. 37. The relationship of the 8 in. diameter hologram size to the
system parameters.

110

VII.   T90-N8-21.9 Transmission Hologram Lens

2.   CONSTRUCTION BEAM OPTICAL SYSTEM

> The construction beam optical system for the T90-N8-21.9 lens
> is based on the "continuous lens" concept invented at Hughes
> Research Laboratories.

The basic "continuous lens" design concept, invented at Hughes
Research Laboratories by Gaylord Moss, was used in designing
the construction beam optical system for a 90° off-axis, 8°
asymmetric transmission hologram lens. However, point source
construction beams for asymmetric hologram configurations
introduce axial astigmatism as well as a large amount of
astigmatism across the field. Computer simulations of the
hologram construction and corresponding reconstruction charac-
teristics were made. Axial astigmatism was eliminated with
26.30" of astigmatism in one of the construction beams.

A schematic of the construction system, fabricated to expose
the T90-N8-21.9 transmission lens, is shown in Figure 38.
Construction optics consist of plane mirrors, spatial filters,
beamsplitters, and a 14.38" diameter, 60" radius of curvature
spherical mirror. A diverging point source is located 34.5"
from the hologram center. The proper amount of astigmatism
in the converging construction beam was obtained by using the
off-axis aberration of the spherical mirror. The included
angle between the construction beams is 90° at the center of
the hologram recording plane. The angle between the bisector
of this 90° included angle and the hologram recording plane
normal is 8°.

The construction system was assembled on a honeycomb optical
table supported with pneumatic mounts which dampen floor
vibrations. Shielding was provided to minimize atmospheric
disturbances. The construction wavelength was the 632.8 nm
spectral line from a 50 mw helium-neon laser. Path lengths
of the construction beams were matched to the hologram record-
ing plane center.

Preceding page blank   112

14.38 in, diam
60 in. RADIUS OF CURVATURE
SPHERICAL MIRROR

24.1°

20 in. 8°

HOLOGRAM RECORDING PLANE

37°

90°

45°

34.5 in.

55.25 in.

33.69 in.

AXIAL DISTANCE FROM HOLOGRAM

59.99

26.30 in. ASTIGMATISM

PLANE MIRROR
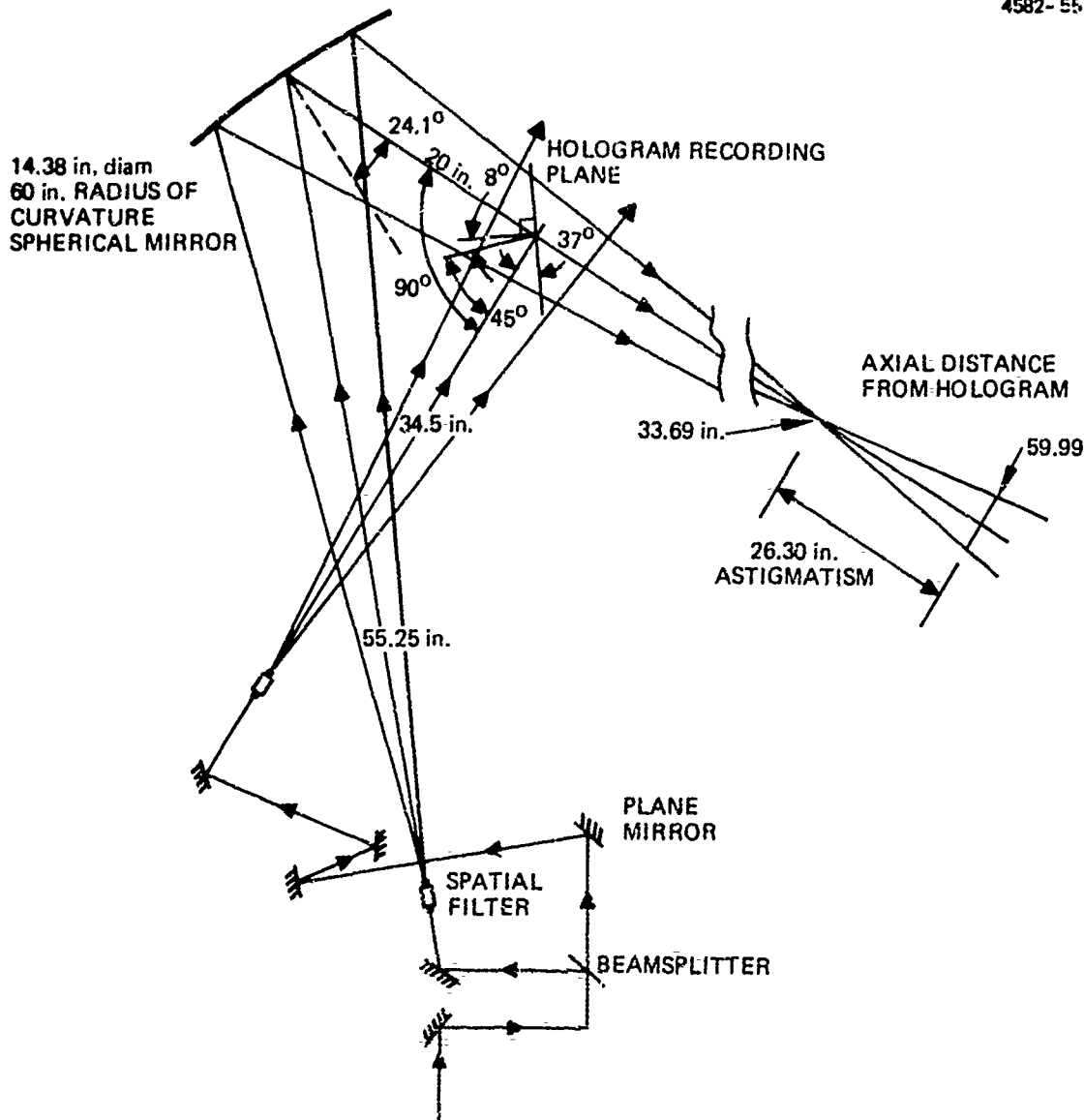
SPATIAL FILTER

BEAMSPLITTER

Fig. 38.   The construction system for 90° off-axis, 8° asymmetric, transmission hologram lens.

VII. T90-N8-21.9 Transmission Hologram Lens

3. HOLOGRAM LENS FABRICATION

> The T90-N8-21.9 hologram lens is exposed on 8" x 10" s.lver
> halide emulsion and bromine vapor bleached.

The T90-N8-21.9 transmission hologram lens was recorded on
6-μm thick, silver halide emulsion (Kodak type 120-01 plates,
8 in. x 10 in.). The resulting amplitude hologram was
converted to a phase hologram with bromine vapor bleaching.

A uniform coverage of the 50.27 in.^{2} area of the hologram
aperture resulted in recording beams energy of 2.3 μW/cm^2 and
2.0 μW/cm^2 (measured at the hologram recording plane). An
exposure of 65 seconds was required to obtain an exposed
energy of 280 μJ/cm^2. The exposed hologram was processed
in 21°C solutions with agitation: 5 minutes in Kodak D-19
developer; 1 minute wash in water; 5 minutes in Kodak fixer
with hardener. The processed density of the amplitude
hologram was 2.0 ND. The air dried amplitude hologram was
then bromine vapor bleached.

Efficiency and scatter was measured at 632.8 nm, the operating
wavelength of the bleached silver halide hologram lens.
Diffraction efficiency was 11% with 8% scatter. The 8" diam-
eter T90-N8-21.9 hologram lens is sealed (Epotek 310 optical
adhesive) on a 1/4" thick glass substrate with dimensions,
as specified by NADC shown in Figure 39. This substrate
can be mounted in the AIMIS demonstrator to display laser
symbology with the hologram lens element.

The efficiency and scatter values are similar to that of the
half-scale, 40° off-axis, symmetric transmission lens delivered
to NADC in Phase 1 program. There are several probable causes
for this low efficiency. The spatial frequency recorded at
the center of the T90-N8-21.9 lens is 2218 cycles/mm. The
hologram recording plane must be restricted from motion a
fraction of 4.50 x 10^{-7} meter. A major cause of instability
was the heat generated by the laser which was positioned on
a platform attached to the underside of the honeycomb table.
This thermal energy tends to warp the stainless steel surface
of the optical table. This type of instability is typically
random and cannot be corrected with a fringe stabilizing
system of the type developed in Phase 2 program.

Despite the low efficiency, the T90-N8-21.9 transmission
hologram lens will adequately display laser symbology in the
AIMIS demonstrator. The characteristics of the holographic
element are discussed in the next topic. Residual aberration
will remain in the imagery due to the absence of an aberration
correcting lens system. However, the holographic lens element
demonstrates that a complex lens function can be achieved with
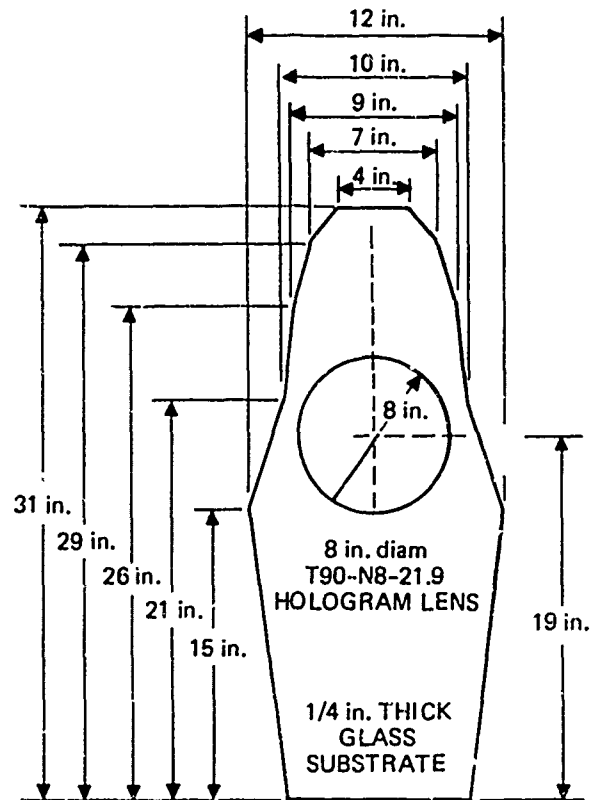hologram optics.

4582—56

Fig. 39. The T90-N8-21.9 hologram lens
is protected between 0.040 in.
thick (8 in. x 10 in.) and
0.25 in. thick glass sub-
strates.

VII.   T90-N8-21.9 Transmission Hologram Lens

4.   INTERMEDIATE IMAGE PLANE AND CHIEF RAY EFFICIENCY

> The T90-N8-21.9 hologram lens' image plane has a tilt of 27° from the optical axis normal at a 21.9" focal length.

The T90-N8-21.9 hologram lens' image plane has a 27° tilt from the optical axis normal. The focal length of the element is 21.9 in. The image plane is the bisector plane between the axial tangental planes of the horizontal and vertical spheroidal focal surfaces. Figure 40 shows vertical and horizontal sections of the focal surfaces. The data points, theoretical and experimental, are foci locations of ray traces of col-limated   chief ray bundle entering the hologram lens at various field angles. A detailed description of the experi-mental procedure for locating the intermediate image plane can be found in the Test Procedures.[14]

The 27° tilted image plane is a plane of best focus for imaging without a relay lens system. Note that there are residual aberrations due to the astigmatism across the field. Relay systems are generally designed to image vertical and horizontal ray fans onto their respective focal surfaces, correcting astigmatism.

However, good projected imagery has been seen in a laboratory set-up with diffused 632.8 nm illumination of photographic slides at the image plane. To display laser symbology with the acousto-optical laser scanner, the 4" square diffusing screen should be located at the intermediate image plane.

The image size for monocular viewing ($+ 4.25^\circ/- 3.50^\circ$ vertical FOV and $\pm 6^\circ$ horizontal FOV) is $+ 1.25"/- 1.13"$ vertical and $\pm 2.31"$ horizontal. For binocular viewing, the vertical FOV is slightly vignetted, $+ 4.16^\circ/- 3.49^\circ$, due to the hologram aperture size. A horizontal image plane dimension of $\pm 1.75"$ is sufficient to allow each eye (63 mm apart) $\pm 4.5^\circ$ FOV. These image plane dimensions are measured directly from data in Figure 40.

Chief ray efficiency was measured as a function of vertical and horizontal field angles, Figure 41. Theoretically, chief ray efficiency should be high due to no angular or wavelength shifts between construction and reconstruction geometry. However, the construction beams were path length matched to the center of the hologram. The degree of coherence and fringe visibility are maximum at this point. Consequently, diffraction efficiency is also maximum. Path length difference between construction rays gradually increase for points away

116

from the center of the lens. Reduction in coherence and visibility between the construction beams causes chief ray efficiency roll-offs as the field angle increases. By increasing the coherence length of the recording laser source, an improvement in chief ray uniformity can be expected.
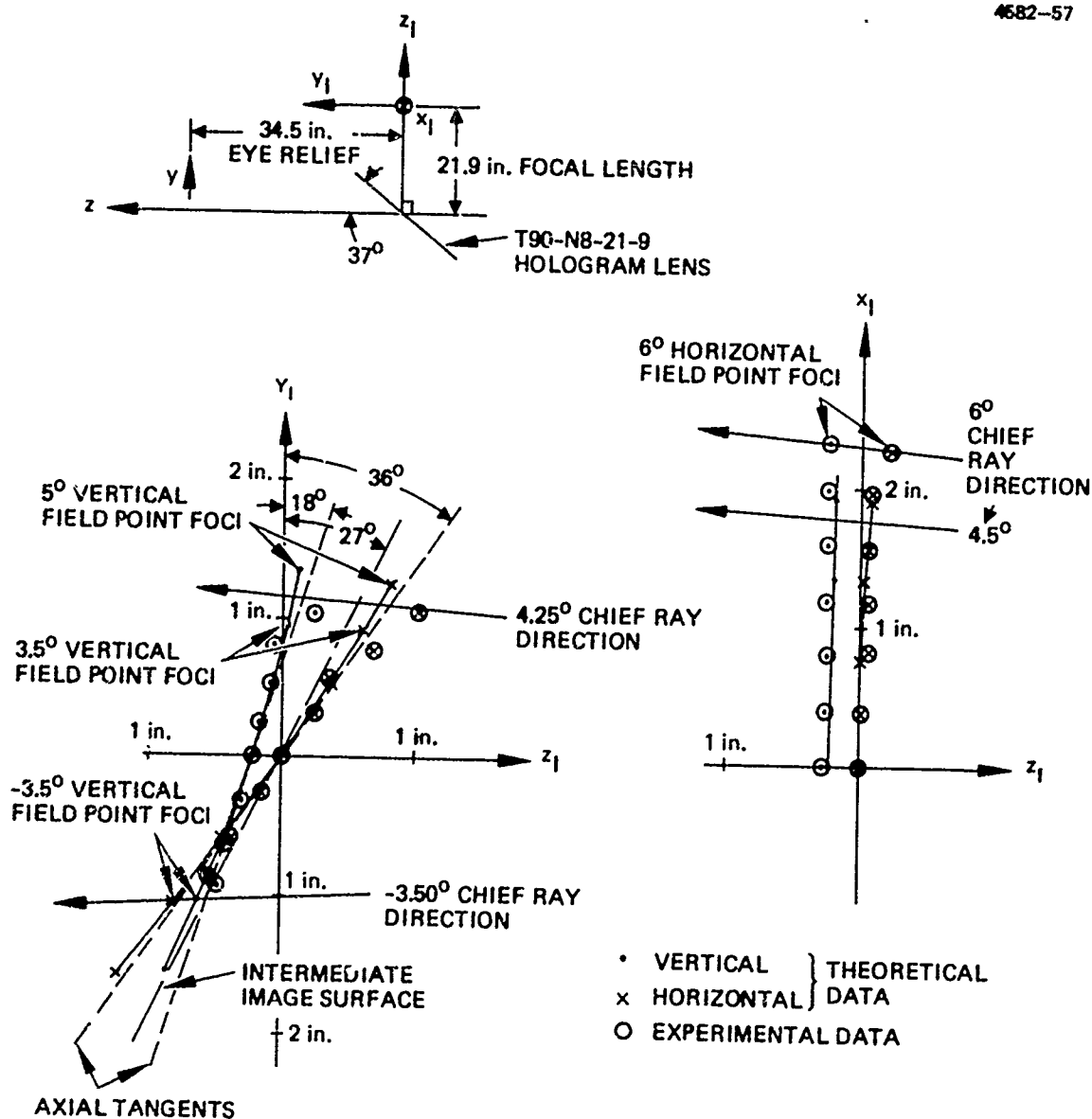
Fig. 40. Vertical and horizontal sections of the spheroidal image
(focal) surfaces of the T90-N8-21.9 hologram lens.
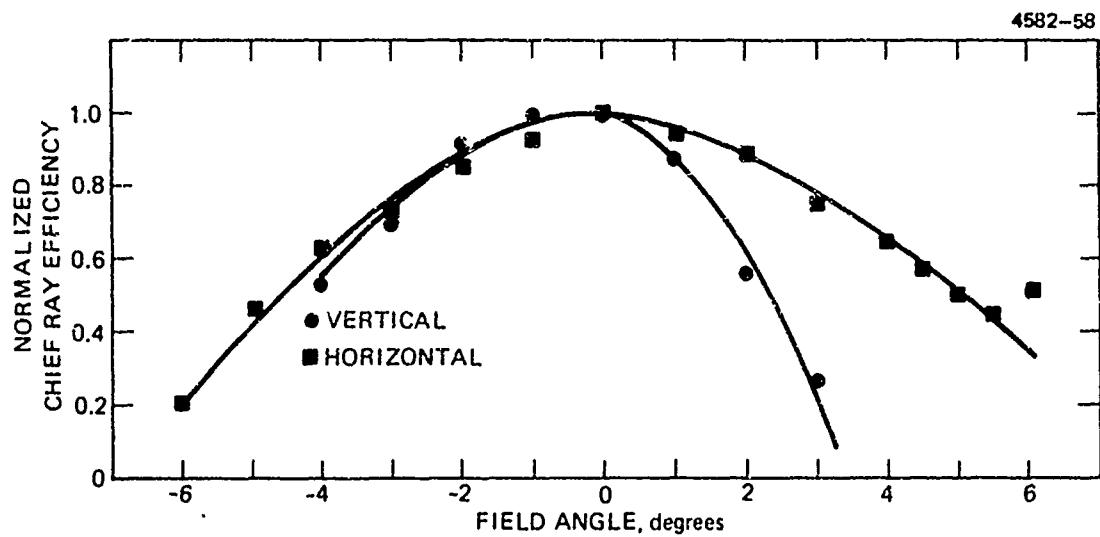
4582–58

Fig. 41.   Chief ray efficiency measured as a function of
vertical and horizontal field angles.

REFERENCES

1. "Specification of Hologram Lens System," Naval Air
    Development Center, Air Vehicle Technology Depart-
    ment, 20 November 1972.

2. Final Technical Report for period 2 April 1973 -
    1 April 1974, Contract N62269-73-C-0388, "Holographic
    Lens for Pilot's Head-Up Display," prepared for
    Naval Air Development Center, Warminster, PA 18974,
    by Hughes Research Laboratories, Malibu, CA 90265,
    D.H. Close, A. Au, and A. Graube, August 1974.

3. Final Technical Report for period 1 July 1974 - 31
    October 1974, Contract N62269-74-C-0642, "Holographic
    Lens for Pilot's Head-Up Display," prepared for Naval
    Air Development Center, Warminster, PA 18974, by
    Hughes Research Laboratories, Malibu, CA 90265,
    D.H. Close, A. Au, and A. Graube, 1 April 1975.

4. G.E. Moss, "Wide-Angle Holographic Lens for a Display
    System," J. Opt. Soc. Am. 64, 552A. April 1974.

5. R.J. Collier, C.B. Burckhardt, and A.H. Lin, Optical
    Holography (Academic Press, New York, 1971).

6. A. Graube, Opt. Comm. 8, 251-253 (1973).

7. M. Chang, Appl. Opt. 10, 2550-2551 (1971).

8. J.E. Jolley, Photographic Science and Engineering 14,
    169-177, (1970).

9. W.S. Colburn, R.G. Zech, and L.M. Ralston, "Holographic
    Optical Elements," Harris Electro-Optics Center of
    Radiation, Technical Report AFAL-TR-72-409 (1973).

10. W.S. Colburn and B.J. Chang, "Design and Fabrication
    of Hologram Optical Elements," Final Technical
    Report AFAL-TR-74-281, Environmental Research Inti-
    tution of Michigan (1975).

11. T.P. Sosnowski and H. Kogelnik, Appl. Optics 9, 2186-
    2187 (1970).

12. D.H. Close and A. Graube, "Material for Holographic
    Optical Elements," Technical Report AFML-TR-73-267,
    Hughes Research Laboratories (1973).

Preceding page blank

13.   R.D. Anwyl, Eastman Kodak Company, private communication.

14.   Test Procedures for Contract N62269-75-C-0299, "Holographic Lens for Pilot's Head-Up Display," prepared for Naval Air Development Center, Warminster, PA 18974, by Hughes Research Laboratories, Malibu, CA 90265, A. Au, October 1975.

15.   A. Graube, Appl. Opt. $\underline{13}$, 2942-2946 (1974).